IONIC LIQUIDS AND A COMMERCIAL ANIONIC SURFACTANT IN DEMULSIFYING CRUDE OIL IN WATER EMULSION

by

Nahid Hassanshahi

B.Sc., Shiraz University, 2015
M.Sc., Shiraz University, 2017

THESIS SUBMITTED IN PARTIAL FULFILLMENT OF
THE REQUIREMENTS FOR THE DEGREE OF
DOCTOR OF PHILOSOPHY
IN
NATURAL RESOURCES AND ENVIRONMENTAL STUDIES

UNIVERSITY OF NORTHERN BRITISH COLUMBIA

December 2022

ABSTRACT

Crude oily wastewaters generate widely in industries and marine oil spill operations. Crude oily wastewaters contain stable oil in water emulsion (O/W), and their treatment has been challenging. Crude oil has toxic compounds for humans and the environment, and effective treatment requires meeting environmental regulations. This dissertation aimed to investigate effective and environmentally friendly demulsifiers (commercial anionic surfactant and ionic liquids) in demulsifying stable O/W emulsions. Firstly, the O/W emulsification process by ultrasonic homogenization was conducted to optimize the processing parameters and determine the required energy to generate stable emulsion, which is applicable for enhancing crude oil demulsification. The optimum condition to generate stable emulsion was at a power level of 76–80 W, sonication time of 16 min, water salinity of 15 g/L NaCl, and pH of 8.3, which required 60−70 kJ energy. Secondly, the commercial anionic surfactant showed high efficiency (99%) in demulsifying O/W emulsion at the concentration of 900 mg/L in a short shaking time (15 min) at room temperature (25 °C). It could reduce the total extractable petroleum hydrocarbons in the separated water to <10 mg/L without gravity separation and achieve promising demulsification performance at high salinity (36 g/L) and various fresh and weathered oil concentrations. Thirdly, ionic liquid with hydroxyl functional groups on the side chains effectively demulsified O/W emulsion (92%) stabilized by natural emulsifiers (e.g., asphaltenes) at a low concentration (25 mg/L) and room temperature without settling. Hence, the hydroxyl functional group is a suitable substitution for the alkyl group on the ionic liquids side chains to reduce ionic liquid toxicity. It was also found that its potency was highly affected by the emulsion type (stabilized by natural emulsifiers+Tween 20), in which demulsification efficiency reached 61% at the ionic liquid concentration of 50 mg/L and the demulsification

temperature of 50 °C at 90 min gravity separation settling time. This indicated the synergistic interaction of natural emulsifiers and Tween 20 and the formation of thicker film at the oil-water interface, which affected the ionic liquid performance. Finally, comparing the performance of three ammonium-based ionic liquids with a distinct side chain (alkyl, ester, and amide) in demulsifying O/W emulsion, it was found that ionic liquid's side chain and hydrophilicity greatly influenced their performance in the demulsifying O/W emulsion. Substitution of the hydrophobic alkyl group with the hydrophilic amide or ester groups to reduce ionic liquid toxicity improved the ionic liquid potency in the demulsifying emulsion. Ionic liquid with the amide group on the side chain resulted in the highest demulsification efficiency (94%) compared to ionic liquids with the ester (91%) and alkyl (88%) groups at the ionic liquid concentration of 25 mg/L and settling time of 15 min at room temperature, indicating the superiority of the amide group in the demulsifying O/W emulsion.

CO-AUTHORSHIP

I was the principal investigator of this dissertation, including designing studies and experiments, acquiring data, analyzing data, and writing all the chapters. I wrote the manuscripts and was responsible for incorporating comments and feedback in the revised manuscripts. Dr. Jianbing Li supervised this study and experiments and contributed to the experimental design, data analysis, and revision of the manuscripts. He is included in authorship on all resulting publications. Dr. Guangji Hu and Dr. Kenneth Lee helped review and improve the manuscripts and were included in some of my publications.

Publication and authorships from this dissertation (Published or prepared for submission)

Hassanshahi, N., Hu, G., Li, J. (2020). Application of ionic liquids for chemical demulsification: A review. *Molecules*, *25*(21), 4915. DOI: https://doi.org/10.3390/molecules25214915. (Chapter 2)

Hassanshahi, N.; Hu, G.; Lee, K.; Li, J. (2022). Effect of ultrasonic homogenization on crude oil-water emulsion stability. *Journal of Environmental Science and Health, Part A*. (Chapter 3)

Hassanshahi, N., Hu, G., Li, J. (2022). Investigation of dioctyl sodium sulfosuccinate in demulsifying crude oil in water emulsions. *ACS Omega, 7*(37), 33397–33407. DOI: https://doi.org/10.1021/acsomega.2c04022. (Chapter 4)

Hassanshahi, N., Li, J. (2022). New ammonium-based ionic liquid with hydroxyl functional groups in the side chains in demulsifying oil in water emulsion. Prepared for submission. (Chapter 5)

Hassanshahi, N., Li, J., Lee, K. (2022). Study on ammonium-based ionic liquids with a different side chain in demulsifying crude oil in water emulsion. Prepared for submission. (Chapter 6)

TABLE OF CONTENTS

LIST OF TABLES

LIST OF FIGURES

List of Schemes

GLOSSARY

ACs	Activated carbons
ACS	American chemical society
AMPS/AA-TE	The quaternized octadecyl amine diethoxylate with tetraethylene glycol with copolymers of 2-acrylamido-2-methylpropane sulfonic acid (AMPS) and acrylic acid (AA)
AMPS/AA-OA	The quaternized octadecylamine with copolymers of 2-acrylamido-2-ethylpropane sulfonic acid (AMPS) and acrylic acid (AA)
ANOVA	Analysis of variance
APTAC	(3-Acrylamidopropyl) trimethylammonium chloride
CCD	Central composite design
CI	Creaming index
CLB	Cold lake blend
CMC	Critical micelle concentration
CP $C_6H_{13}COO$	Caprolactam hexanoate
CTAB	1-Hexadecyltrimethylammonium bromide
C_4mim CF_3CO_2	1-butyl-3-methylimidazolium trifluoroacetate
C_6mim Cl	1-hexyl-3-methylimidazolium chloride
C_8mim Cl	1-octyl-3-methylimidazolium chloride
C_{10}mim Cl	1-decyl-3-methylimidazolium chloride
C_{12}mim Cl	1-dodecyl-3-methylimidazolium chloride

C_{14}mim Cl	1-tetradecyl-3-methylimidazolium chloride
C_{16}mim Cl	1-hexadecyl-3-methylimidazolium chloride
C_{16}mim I	1-hexadecyl-3-methylimidazolium iodide
C_{16}mim Br	1-hexadecyl-3-methylimidazolium bromide
C_2mim BF_4	1-ethyl-3-methyl-imidazolium tetrafluoroborate
C_4mim BF_4	1-butyl-3-methylimidazolium tetrafluoroborate
C_8mim BF_4	1-octyl-3-methylimidazolium tetrafluoroborate
C_{10}mim BF_4	1-decyl-3-methylimidazolium tetrafluoroborate
C_{12}mim BF_4	1-dodecyl-3-methylimidazolium tetrafluoroborate
C_2mim TfO	1-ethyl-3-methyl imidazolium trifluoromethanesulfonates
C_8mim OTf	1-methyl-3-octylimidazolium triflate bis(trifluoromethylsulfonil)
C_4mim NTf_2	1-butyl-3-methylimidazolium bis(trifluoromethylsulfonyl)imide
C_8mim NTf_2	1-methyl-3-octylimidazolium bis(trifluoromethylsulfonyl)imide
C_{10}mim NTf_2	1-decyl-3-methylimidazolium bis(trifluoromethylsulfonyl)imide
C_{12}mim NTf_2	1-dodecyl-3-methylimidazolium bis(trifluoromethylsulfonyl)imide
C_{14}mim NTf_2	1-tetradecyl-3-methylimidazolium bis(trifluoromethylsulfonyl)imide
C_4mim PF_6	-butyl-3-methylimidazolium hexafluorophosphate
C_6mim PF_6	1-hexyl-3-methylimidazolium hexafluorophosphate

C_8mim PF_6	1-octyl-3-methylimidazolium hexafluorophosphate
C_{10}mim PF_6	1-decyl-3-methylimidazolium hexafluorophosphate
C_{12}mim PF_6	1-dodecyl-3-methylimidazolium hexafluorophosphate
C_{14}mim PF_6	1-tetradecyl-3-methylimidazolium hexafluorophosphate
C_4py NTf_2	1-butylpyridinium bis(trifluoromethylsulfonyl)imide
C_8Py Cl	1-octylpyridinium chloride
C_{12}Py Cl	1-dodecylpyridinium chloride
Da	Daltons
DE	Demulsification efficiency
DSS	Dioctyl sodium sulfosuccinate
DTAC	Dodecyl trimethylammonium chloride
EDDI	Etherified di-dodecyl imidazolium acetate
EDHI	Etherified di-heptyl imidazolium acetate
EPDIB	Polymer of EDDI
EPH	Extractable petroleum hydrocarbons
EPHIB	Polymer of EDHI
EOR	Enhanced oil recovery
GC-FID	Gas chromatograph with a flame ionization detector

GEB	Reaction of the epoxy ring of glycidyl 4- nonylphenyl ether using ethanol mine, followed by quaternization using bis(2-chloroethyl) ether resulted in corresponding ionic liquid; GEB
HEOD-TS	N,N-bis-hexaoxyethlene octadecylamine tosylate
HLB	Hydrophilic-lipophilic balance
HLD	Hydrophilic-lipophilic deviation
H NMR	Proton nuclear magnetic resonance
IFT	Interfacial tension
METAC	[2-(Methacryloyloxy)ethyl] trimethylammonium chloride
MTEOA $MeOSO_3$	Tris(2-hydroxyethyl) methylammonium methylsulfate
N_{2224} $N(CN)_2$	Triethylbutylammonium dicyanamide
N_{6222} NTf_2	Triethylhexyaammonium bis(trifluoromethylsulfonyl)imides
O-W	Oil-water
O/W	Oil-in-water
O/W/O	Oil in water in oil
PIT	Phase inversion temperature
PIL	Poly ionic liquids
$P_{666,14}$ $N(CN)_2$	Trihexyltetradecylphosphonium dicyanamide
$P_{666,14}$ Phos	Trihexyltetradecylphosphonium bis (2,4,4-trimethylpentyl)phosphinate
$P_{666,14}$ NTf_2	Trihexyltetradecylphosphonium bis(trifluoromethylsulfonyl)imide

$P_{666,14}Cl$	Trihexyltetradecylphosphonium chloride
$P_{666,14}Br$	Trihexyltetradecylphosphonium bromide
R/A	Resins/asphaltenes
RSM	Response surface methodology
RSN	Relative solubility number
RTIL	Room temperature ionic liquid
SANS	Small angle neutron scattering
SDS	Sodium dodecyl sulfate
SEM	Scanning electron microscopy
TEPH	Total extractable petroleum hydrocarbons
TGA	Thermogravimetric analysis
TOMAB	Trioctylmethylammonium bromide
TOMAC	Trioctylmethylammonium chloride
W/O	Water-in-oil
W/O/W	Water in oil in water

ACKNOWLEDGMENT

First of all, I would like to express my gratitude and appreciation to my supervisor Dr. Jianbing Li whose guidance, support, and encouragement have been invaluable throughout this study. Without his help and advice, I would not have been able to complete this research. Also, I would like to thank my supervisory committee members, Dr. Hossein Kazemian, Dr. Ron Thring, and Dr. Natalie Linklater, for their insightful comments, guidance, and discussions. I would like to extend my thanks to Dr. Bill McGill, Dr. Peter Jackson, and Dr. Chris Johnson as my course supervisors in the first year of my Ph.D.

This research was financially supported by the Natural Sciences and Engineering Research Council of Canada and Fisheries and Oceans Canada's Multi-Partner Oil Spill Research Initiative (MPRI). Additional support from the Office of Research and Innovation, UNBC Graduate Teaching Assistantship, Graduate Teaching Excellence Award, and Anna Sorkomova Memorial Bursary are much appreciated.

Special thanks to Charles Bradshaw, Erwin Rehl, and Mya Schouwenburg for their support and professional advice with sample analysis at UNBC Northern Analytical Laboratory Service. I would like to thank Conan Ma working at UNBC Chemstore, for his support with sample delivery and lab material supply. I would also like to thank Dr. Mike Rutherford, Daniela Fisher, Dr. Faran Ali, Dr. George Jones, Teal Randle, and Dr. Chris Jackson for their patience and helpful instructions as the supervisor of my teaching assistant positions at UNBC. I would like to extend my thanks to several UNBC faculty and staff, Dr. Kaila Fadock, Jordan Wilbey, Beth Gentleman, Doug Thompson, and John Orlowsky, who assisted me in sample analysis, lent me their lab supplies or helped me in other ways.

My gratitude extends to Dr. Kenneth Lee, Dr. Guangji Hu and Dr. Fatemeh Azadi for sharing their knowledge, skills, and thoughts. I would also like to extend my gratitude to Gina Marie Donofrio, Kristine Rowswell, and all my friends in Iran and Canada for always being supportive, inspiring, and understanding.

I would like to dedicate this work to my family for their unconditional support and love. Special thanks go to my mother, a strong woman, who is my life angel and role model, and my lovely sister and brother-in-law. They helped me gather the strength to overcome many challenges and hard times during my Ph.D. study. And to my lovely little nephew Aryo Barzan who was a ray of sunshine during the hard times in my Ph.D. study.

Chapter 1

GENERAL INTRODUCTION

Crude oily wastewaters generate widely in oil and gas industries during different processes, including oil production and enhanced oil recovery (Al-Ghouti et al., 2019; Liu et al., 2021b; Zahid et al., 2011). Also, a significant volume of oily wastewater generates in marine oil spill response operations after the collection of spilled oil in the marine environment due to ship accidents and natural seepage. It has been reported that almost 9,000,000 tons of oil have been spilled since 1965 (Motta et al., 2018).

Oily wastewaters mostly contain oil-in-water (O/W) emulsions, which are stabilized by natural emulsifiers (e.g., asphaltenes, resins) in crude oils. Natural emulsifiers create a rigid film through inter- and intra-molecular interactions (e.g., π–π stacking, hydrogen bonds) around emulsified droplets that prevent coalescence and separation (Chen et al., 2018; Farooq et al., 2021; Ma et al., 2021). The stability of O/W emulsion mainly depends on the amount of emulsifiers (e.g., asphaltenes, resins) in crude oils, in which higher emulsifiers lead to the formation of emulsion with higher stability (Dudek et al., 2019; Yudina et al., 2021). Crude oil contains toxic compounds, including benzene, toluene, and polycyclic aromatic hydrocarbons, posing severe risks to human health and the environment (Ruberg et al., 2021). Consequently, strict regulations are being implemented in North America to treat oily wastewater and obtain qualified water with an oil and grease concentration lower than 42 mg/L/day (Shokri and Fard, 2022).

Different oily wastewater treatment processes, including physical, biological, and chemical, have been used (Faisal and Almomani, 2022; Sousa et al., 2022). Gravity separation is a common physical process for oil-water separation; however, it has significant drawbacks

of long settling time, large space requirements, and inefficiency in demulsifying stable emulsion (Han et al., 2019). Other physical treatment processes, including centrifugal separators, gravitational coalescers, electrocoalescers, gas flotation, and filtration, have also been investigated in demulsifying O/W emulsion (Ismail et al., 2020; Kumar et al., 2021; Less and Vilagines, 2012; Mohayeji et al., 2016; Piccioli et al., 2020). However, they have some limitations and disadvantages, which are inefficient and cost-effective in demulsifying stable emulsion in large-scale applications to meet environmental regulations (Abdulredha et al., 2020; Tian et al., 2022). Biological treatment using biodemulsifiers has the advantage of being environmentally friendly (e.g., biodegradability); however, it is susceptible to operational issues (Hadi and Ali, 2022a). In contrast with the physical and biological processes, a chemical process using demulsifiers (i.e., surface-active compounds) to demulsify emulsion has the advantages of an effective, rapid, cheap, and easy-to-operate process that has attracted research attention. The chemical demulsification process includes the diffusion of demulsifier molecules in the emulsion and reaching the oil-water interface, breaking the rigid film around emulsified droplets, and enhancing oil-water separation.

Different demulsifiers (non-ionic and ionic) have been applied to demulsify emulsion and showed various drawbacks due to the complexity of emulsion and industrial restrictions. For example, non-ionic demulsifiers showed poor efficiency in demulsifying heavy crude oil emulsion. They also were ineffective in demulsifying emulsions containing oil droplets smaller than 2 μm (Adilbekova et al., 2015; Zhang et al., 2016; Zhang et al., 2018a). Ionic demulsifiers are cationic and anionic if they have a positive and negative charge, respectively (Sousa et al., 2021). Various cationic demulsifiers were used in previous studies, and they concluded that cationic demulsifiers required a long settling time and could not efficiently reduce the oil

concentration in separated water to meet the environmental regulations (Yonguep et al., 2021; Yuan et al., 2022). Amine-based dendrimers are also considered ionic demulsifiers and have been investigated in the demulsifying emulsion (Wang et al., 2021). However, the synthesis procedure is costly and time-consuming, which has limited their industrial applications (Bi et al., 2020). Other disadvantages of dendrimers are their poor efficiency in demulsifying emulsions with high salinity and low oil concentration (Hao et al., 2016; Kuang et al., 2020a). Previous studies indicated that demulsifying stable emulsion is still challenging and requires further investigation to find an effective demulsifier.

Anionic surfactants have a high surface activity and have been used widely in industries as surfactant flooding because of their low cost and easy-to-use features (Olajire, 2014). However, their applications as a demulsifier in demulsifying emulsions have not been well studied compared to other demulsifiers. Also, there is a growing interest in applying ionic liquids in the demulsification of crude oil emulsion. Ionic liquids are liquid salts with a melting point below 100 °C. Ionic liquids have unique features of non-flammability, thermal stability, and low vapor pressure, which are essential for industrial applications (Nasirpour et al., 2020). Many studies have shown the effective application of ionic liquids in demulsifying crude oil emulsion (Hassanshahi et al., 2020; Masri et al., 2022; Zolfaghari et al., 2018). However, their application in industries has been limited due to their high toxicity (Hadi and Ali, 2022a; Romero et al., 2008). Hence, further investigations on ionic liquids require to find an effective one in demulsifying stable emulsion with less potential risks to the environment.

Based on the literature review (chapter 2), the main objective of this study is to investigate effective environmentally friendly demulsifiers in demulsifying crude O/W emulsions. Thus, the specific objectives are

- Evaluation of ultrasonic homogenization in the generation of stable crude O/W emulsion, which is applicable for enhancing crude oil demulsification. The effect of power, sonication time, salinity, and pH of water and their interaction on the emulsion stability were investigated. The optimum condition of essential parameters and the required energy to generate emulsion with high stability were determined.
- Investigation of an anionic surfactant (dioctyl sodium sulfosuccinate) in demulsifying crude O/W emulsion. Several experimental parameters influencing the demulsification process were investigated, including dioctyl sodium sulfosuccinate concentration, oil concentration, shaking time, salinity, crude oil condition (fresh and weathered), and gravity separation settling time. The effect of the interaction of parameters in the demulsifying emulsion was also investigated, and their optimum condition was determined.
- Investigating new ammonium-based ionic liquid with hydroxyl functional groups in the side chains (tris(2-hydroxyethyl) methylammonium methylsulfate) in demulsifying crude O/W emulsion. The effect of ionic liquid concentration, demulsification temperature, gravity separation settling time, and emulsion type (natural emulsifiers+Tween 20 and natural emulsifiers) on the demulsification efficiency were investigated.
- Investigation of three ammonium-based ionic liquids with a distinct side chain (dodecyl trimethylammonium chloride, [2-(Methacryloyloxy)ethyl] trimethylammonium chloride, (3-Acrylamidopropyl) trimethylammonium chloride) in demulsifying crude O/W emulsion. The effect of crucial parameters,

including ionic liquid concentration, ionic liquid type (i.e., side chain), and gravity separation settling time, were investigated. The optimum condition of parameters in the demulsification process was also determined.

Hence, based on the objectives mentioned above, this dissertation is structured as follows: in chapter 2, the literature was reviewed; in chapter 3, emulsification of O/W using ultrasonic homogenization was developed; in chapters 4−6, the potency of different demulsifiers in demulsifying crude O/W emulsion were investigated, including an anionic surfactant (chapter 4), and different ionic liquids (chapters 5 and 6); in chapter 7, the conclusion of this research and recommendations for future research were provided.

Chapter 2

APPLICATION OF IONIC LIQUIDS FOR CHEMICAL DEMULSIFICATION: A REVIEW[1]

Abstract

In recent years, ionic liquids have received increasing interest as effective demulsifiers due to their characteristics of non-flammability, thermal stability, recyclability, and low vapor pressure. In this study, emulsion formation and types, chemical demulsification system, the application of ionic liquids as a chemical demulsifier, and key factors affecting their performance were comprehensively reviewed. Future challenges and opportunities of ionic liquids application for chemical demulsification were also discussed. The review indicted that the demulsification performance was affected by the type, molecular weight, and concentration of ionic liquids. Moreover, other factors, including the salinity of aqueous phase, temperature, and oil types, could affect the demulsification process. It can be concluded that ionic liquids can be used as a suitable substitute for commercial demulsifiers, but future efforts should be required to develop non-toxic and less expensive ionic liquids with low viscosity, and the demulsification efficiency could be improved through the application of ionic liquids with other methods such as organic solvents.

Keywords: ionic liquids; emulsion; chemical demulsification; interfacial tension

[1] This work has been published as Hassanshahi, N., Hu, G., Li, J. (2020). Application of ionic liquids for chemical demulsification: A review. *Molecules*, *25*(21), 4915. DOI: https://doi.org/10.3390/molecules25214915.

2.1. Introduction

The presence of emulsion in oil or water has undesired consequences for industries and the environment (Langevin et al., 2004). It may result in the corrosion of pumps, pipes, and related facilities. It increases the viscosity of oil, which leads to the increment in pumping and transport costs, and the emulsion also reduces the quality of oil (Thompson et al., 1985). Discharging produced oily wastewater from oil and gas industries and the spill of oil through ship accidents and offshore wells (e.g., Exxon Valdez and Deepwater Horizon) (Beland and Oloomi, 2019; Prabowo and Bae, 2019) into waters cause adverse consequences to the environment, human health, and the economy (Adzigbli and Yuewen, 2018; Kuppusamy et al., 2020; Taleghani and Tyagi, 2017). The oil spill cleanup usually involves the collection of a large volume of oily wastewater for treatment. Strict limitations are regulated for discharging oily wastewater (e.g., based on USEPA, oil and grease discharge limits are 29 mg/L monthly average and 42 mg/L daily maximum) which induce industries to efficiently treat their oily wastewater (Rawlins, 2009). However, the presence of emulsion in oily wastewater essentially requires demulsification for its effective treatment. Several technologies have been used for separating oil and water, such as various physical (e.g., gravitational settling, thermal treatment, membrane separation, flotation, ultrasonic), biological (bioaugmentation, biostimulation), and chemical (e.g., solidifiers, demulsifiers, sorbents) processes (Doshi et al., 2018; Hassanshahian et al., 2014; Ismail et al., 2020; Luo et al., 2019; Martínez-Palou and Aburto, 2015; Mohayeji et al., 2016; Motta et al., 2018; Santos et al., 2017; Saththasivam et al., 2016). Chemical demulsification using various demulsifiers is one of the reliable methods which has been widely used in industries for breaking emulsions (Martínez-Palou and Aburto, 2015; Shehzad et al., 2018).

Many research studies have been conducted for the application of ionic liquids in chemical demulsification processes, and it was reported that ionic liquids are reliable demulsifiers with high stability, even under harsh conditions (high temperature and high salinity) (Balsamo et al., 2017). Ionic liquids are produced by a combination of different organic cations and organic or inorganic anions (Alves et al., 2017). They are associated with unique characteristics such as thermal stability, non-flammability, recyclability, and low vapor pressure (Han and Row, 2010; Kunz and Häckl, 2016; Sun and Armstrong, 2010). These properties make ionic liquids a suitable substitute for organic solvents and commercial demulsifiers (Atta et al., 2016b; Han and Row, 2010). Ionic liquids have been used by different researchers to evaluate their efficiency in demulsification processes, mostly at laboratory scales. There is a need for a comprehensive discussion of the current ionic liquids demulsification method to identify its advantages and limitations. In this study, a review on the application of ionic liquids for demulsification was conducted, and the impacting parameters on the demulsification performance were discussed to identify challenges and opportunities for future applications. This review is organized into a few sections, including emulsion formation mechanisms and types, chemical demulsification system and ionic liquids application, the effects of influential parameters (concentration, cation type, and the structure of ionic liquids, anion types, molecular weight, salinity, temperature, and oil types), as well as challenges and opportunities for future applications.

2.2. Emulsions

2.2.1. Emulsion formation

An emulsion is produced when two or more immiscible liquids mix vigorously together which results in two phases (a dispersed phase and a continuous phase) (Raya et al., 2020; Saad et al., 2019). The phase that has a smaller volume is usually identified as the dispersed phase and the larger one is the continuous phase. If the volume of both phases is the same, other factors would be considered to recognize the dispersed and continuous phases (Goodarzi and Zendehboudi, 2019; Kokal, 2005). Based on the Bancroft rule, a continuous phase would be the phase that emulsifying agents are more soluble in it (Bancroft, 2002). Commonly investigated emulsions have a water phase and an oil phase. Fine solids and surface-active compounds of crude oils, such as saturates, asphaltenes, resins, and aromatics, can act as natural emulsifying agents (Abdulredha et al., 2020; Wong et al., 2019). Under intensive mixing, natural emulsifying agents could adsorb at the oil–water (O-W) interface, creating a rigid interfacial film around dispersed droplets and hindering the coalescence of droplets (Canevari, 1982; Grenoble and Trabelsi, 2018; Lee, 1999). The strong tension between the water and oil phases is called interfacial tension (IFT), and the stronger the IFT, the more stable the emulsion (Kumar and Mandal, 2018).

2.2.2. Emulsion types

According to the nature of the dispersed phase, emulsions are categorized into oil in water (O/W), water in oil (W/O) and multiple (W/O/W or O/W/O) types (Figure 2.1). O/W emulsions occur when oil droplets are the dispersed phase (inner phase) in the continuous water phase (outer phase), which is also called reverse emulsion. W/O emulsions are generated when water droplets are the dispersed phase in the continuous oil phase. Multiple emulsion is a mixture of

W/O and O/W emulsions. O/W/O emulsions are formed when oil droplets are the dispersed phase in water droplets that are dispersed in the continuous oil phase, while W/O/W emulsions are formed vice versa. The occurrence of multiple emulsions is more common in food, cosmetics, pharmaceutics, and wastewater treatment industries (Abullah et al., 2016; Iqbal et al., 2015; Kovács et al., 2016; Muschiolik and Dickinson, 2017). It should be noted that these emulsions are thermodynamically unstable but are kinetically stable. Emulsions are thermodynamically unstable because they are produced from the mixture of two or more immiscible liquids which naturally tend to separate. However, the kinetic stability of emulsions means that emulsions are stable for weeks to years due to the formation of strict films around them by emulsifiers (Capek, 2004; Zolfaghari et al., 2016).

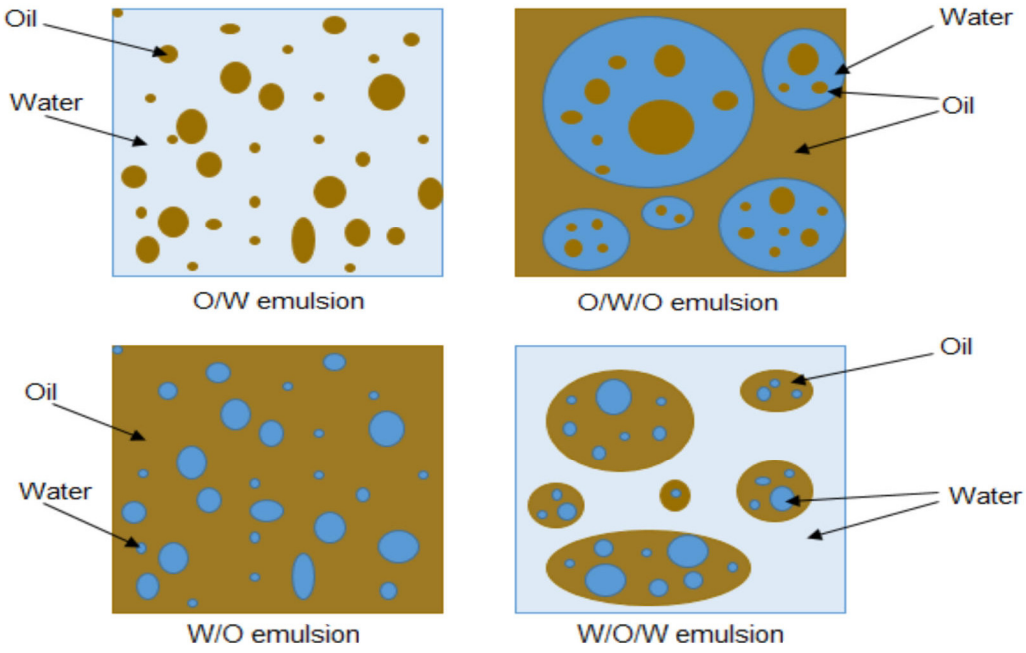

Figure 2.1. Different types of emulsions (Saad et al., 2019).

The aforementioned emulsions can be categorized into stable, metastable, entrained water, and unstable, depending on the time that one phase can be kept dispersed in the other phase (Fingas and Fieldhouse, 2004; Martínez-Palou and Aburto, 2015; Wong et al., 2015). In general, stable W/O emulsions can hold most of the water in the oil phase for more than five days (Fingas et al., 1994). Metastable emulsions are stable within only one to three days, while entrained water and unstable W/O emulsions are not regarded as stable emulsions because both would only remain water in oil for less than one day (Fingas and Fieldhouse, 2004; Raya et al., 2020). Emulsion type is an important factor in selecting demulsifiers which are soluble in the continuous phase and could reach the O-W interface easily (Abullah et al., 2016). The emulsion type depends on the affinity of natural emulsifying agents to the oil (or water) phase. If natural emulsifying agents have a tendency to the oil phase (i.e., hydrophobic natural emulsifying agents), W/O emulsions would form, while the hydrophilic natural emulsifying agents would produce O/W emulsions. The same propensity of natural emulsifying agents to both oil and water phases would lead to the formation of unstable emulsions. The factors determining the affinity of natural emulsifying agents include hydrophilic-lipophilic balance (HLB), hydrophilic–lipophilic deviation (HLD), relative solubility number (RSN), and R ratio (Griffin, 1949; Salager et al., 1979; Winsor, 1954; Wu et al., 2004). Highly affinity of natural emulsifying agents to a lipophilic or a hydrophilic phase leads to the formation of less stable emulsions because natural emulsifying agents tend to stay in a medium rather than migrate to the O-W interface (Borges et al., 2009).

2.3. Ionic liquid demulsification

2.3.1. Chemical demulsification system

Surface-active chemicals (i.e., demulsifiers) are used to destabilize emulsions (Adewunmi and Kamal, 2019; Saad et al., 2019). Some examples of common chemical demulsifiers include sodium dioctyl sulfosuccinate, sodium dodecyl sulfate, and polyethylene oxide (Figure 2.2). The surface activity of demulsifiers should be higher than that of natural emulsifying agents to destabilize the emulsion (Abullah et al., 2016). Surface activity features of demulsifiers can be evaluated by surface tension, electrical conductance, fluorescence, proton nuclear magnetic resonance (H NMR) and small angle neutron scattering (SANS) methods (Sastry et al., 2012). Chemical demulsification is implemented by adding a desired amount of demulsifier to emulsions and mixing them vigorously. After mixing, sufficient time is required to allow Ostwald ripening, flocculation, coalescence, and phase separation (creaming/sedimentation) to occur. Ostwald ripening occurs when a dispersed phase can diffuse easily in a continuous phase to reach together for coalescence. Flocculation is formed when oil or water droplets flock together in a continuous phase while they keep their identity. Coalescence is an irreversible process in which water or oil droplets join together and make bigger droplets. Creaming or sedimentation processes occur based on the density of a dispersed phase (Abdulredha et al., 2020; Moradi et al., 2011). The general chemical demulsification mechanism is shown in Figure 2.3.

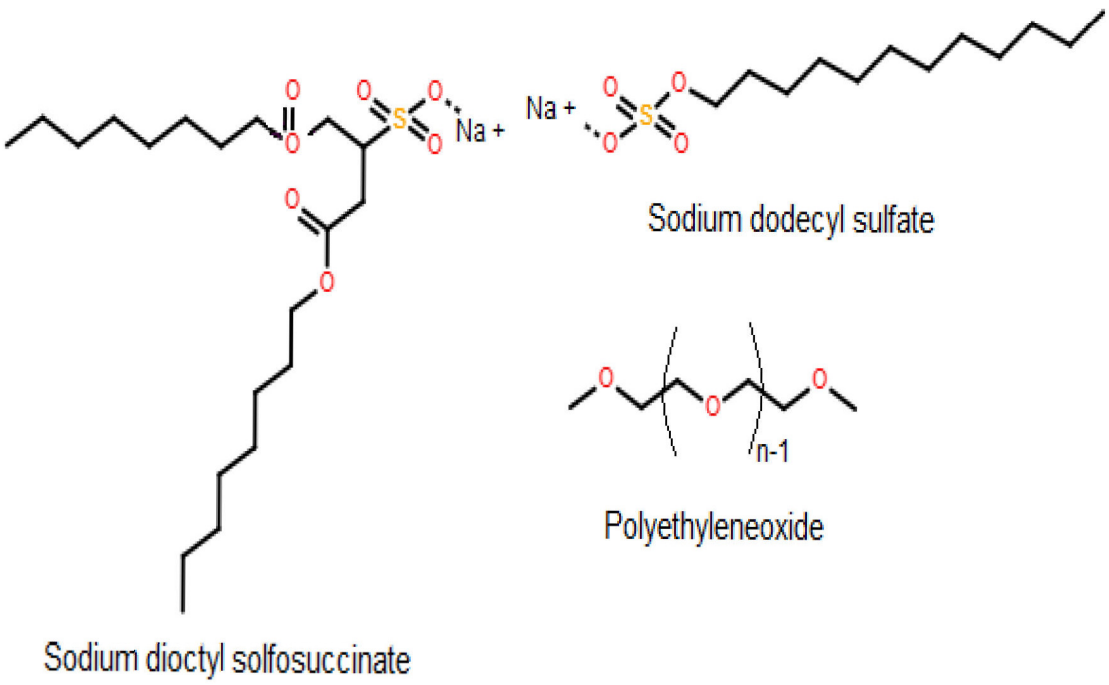

Figure 2.2. Structure of some common demulsifiers.

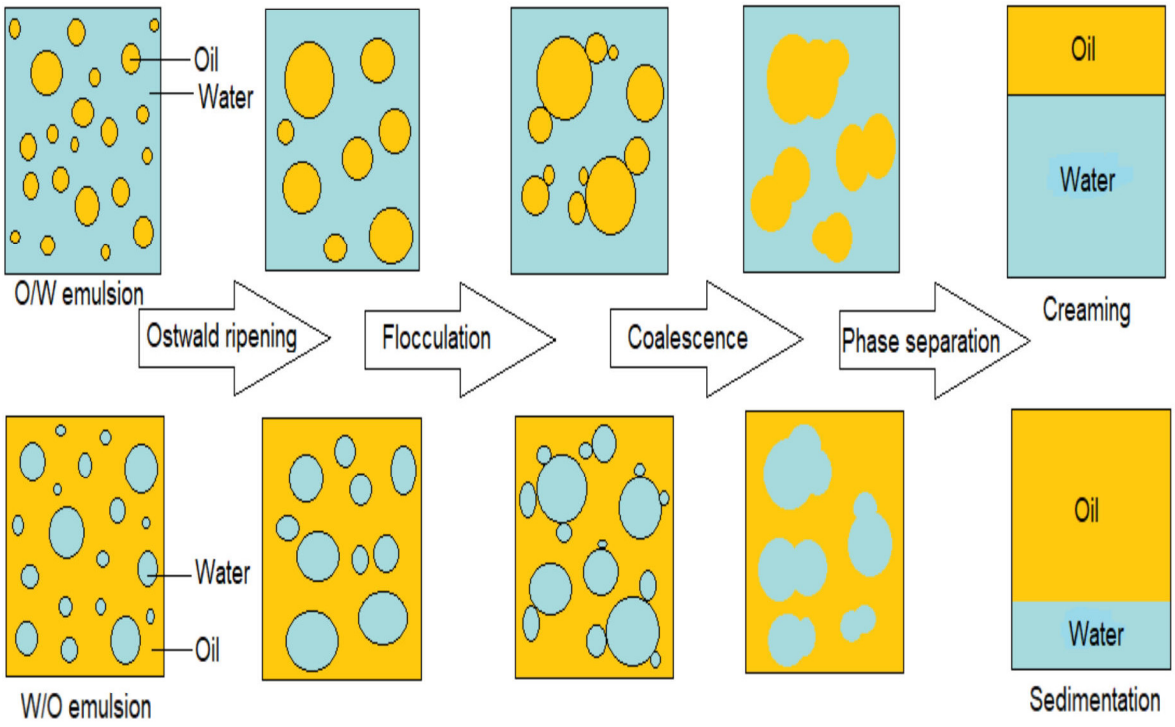

Figure 2.3. Schematic of chemical demulsification mechanism (Abdulredha et al., 2020).

2.3.2. Application of ionic liquids and their characteristics

Ionic liquids were first introduced by Paul Walden in 1914 when he discovered a special chemical-ethyl ammonium nitrate ([$EtNH_3$] [NO_3]) with a melting point of 12 °C (Walden, 1914). Ionic liquids have been widely used in different fields like pharmaceutical, oil and gas, and chemical industries (Bera et al., 2020; Berton et al., 2019; Dharaskar Swapnil, 2012; Kore et al., 2020; Huang et al., 2019; Pernak et al., 2020), such as in pharmaceutical products manufacturing (Chantereau et al., 2020; Chowdhury et al., 2019; Moshikur et al., 2020; Santos and Branco, 2020), viscosity modifiers (Subramanian et al., 2015), desulfurization of liquid fuels (Zhao and Baker, 2015), and liquid-liquid extraction (Chen et al., 2013; Dimitrijevi´et

al., 2020; Florindo et al., 2020). Several types of ionic liquids, such as polymeric ionic liquids (Ardakani et al., 2020; Kammakakam et al., 2020; Patinha et al., 2020), double salt ionic liquids (Pereira et al., 2017), dicationic ionic liquids (Clarke et al., 2020; Guglielmero et al., 2019; Kuhn et al., 2020; Yao et al., 2020), deep eutectic solvents (Abranches et al., 2020; Florindo et al., 2019; Khezeli et al., 2020; Schaeffer et al., 2020), chiral ionic liquids (Gondal et al., 2020), and solvate ionic liquids (Mandai et al., 2014; Schmidt and Schönhoff, 2020), have been synthesized for different aforementioned purposes.

Around ten[18] ionic liquids can be synthesized by combining organic cations and organic or inorganic anions which are non-flammable liquid salts with a melting point below 100 °C (Ratti, 2014; Sun and Armstrong, 2010). Ionic liquids with a melting point below room temperature (~25 °C) are called room temperature ionic liquids (RTIL) (Berthod et al., 2008). Table 2.1 lists some common ionic liquids with their melting points (Zhang et al., 2006). Ionic liquids have lower vapor pressure than conventional volatile organic solvents, and thus present less risk to the environment. They have been applied in many industries as a replacement of conventional volatile organic solvents and significantly reduced the generation volume of hazardous wastes (Ghandi, 2014; Patel and Lee, 2012). Ionic liquids are used successfully in enhanced oil recovery (EOR) processes. Pillai et al. (2018) investigated the effect of C_8mim BF_4, C_{10}mim BF_4, and C_{12}mim BF_4 on EOR and IFT reduction of O-W solution at the temperature of 30 °C. The results indicated that C_8mim BF_4, C_{10}mim BF_4 and C_{12}mim BF_4 reduced IFT to 14.57 mN/m, 4 mN/m, and 2.1 mN/m at the concentration of 12,000 ppm, 5000 ppm, and 2000 ppm, respectively. C_{12}mim BF_4 was applied for EOR which recovered 32.28% of oil additionally in ionic liquid (1.2 × concentration (2000 ppm), 0.5 pore volume), PHPA

polymer (2000 ppm, 0.5 pore volume), and organic alkali triethylamine (1%, 0.5 pore volume) flooding setup (Pillai et al., 2018).

Table 2.1. The melting point of some common ionic liquids (Zhang et al., 2006).

Ionic liquid	Melting point (°C)
C_2mim BF_4	15
C_2mim TfO	–10.15
C_6mim PF_6	–61
C_8mim BF_4	–80
N_{6222} NTf_2	20

The properties of ionic liquids are essential for health and safety concerns in industries. Ionic liquids can remain structurally stable even at high temperatures (e.g., 300 °C), but other conventional surfactants may degrade at those temperatures. Such characteristics make ionic liquids to be unique compared to other demulsifiers (Patel and Lee, 2012). Most researchers prefer to design and synthesize RTIL. RTIL can be achieved by synthesizing nitrogen or phosphorous organic cations with different organic anions, dicyanamide, acetate, trifluoromethylsulfate or inorganic anions, bromide, chloride, tetrafluoroborate, hexafluorophosphate (Berthod et al., 2008). Figure 2.4 shows a few common cations of ionic liquids, including imidazolium, pyridinium, pyrrolidinium, ammonium, and phosphonium. Table 2.2 lists some anions that are used for synthesizing ionic liquids.

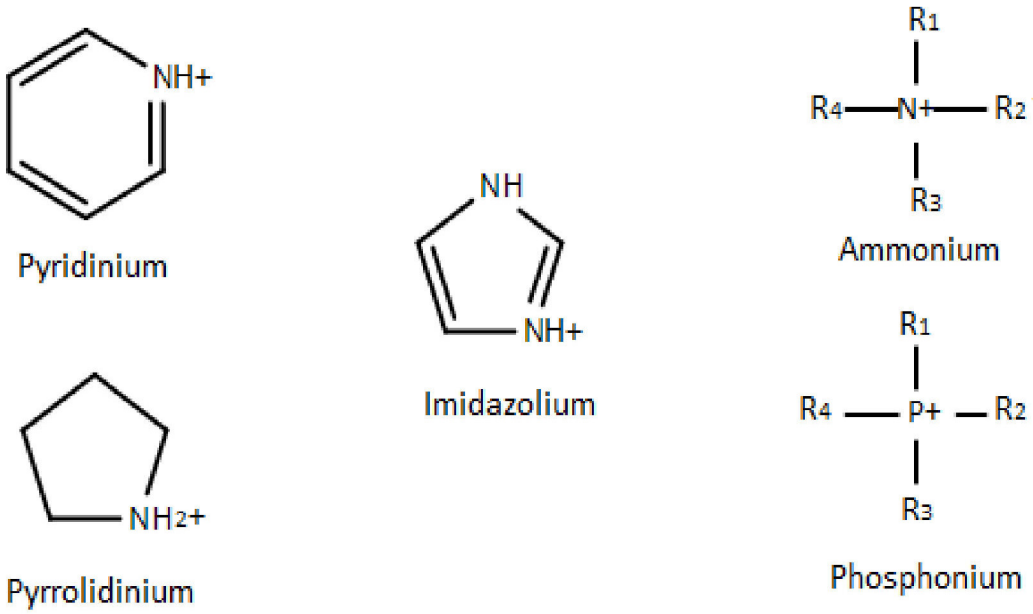

Figure 2.4. Common cations used for synthesizing ionic liquids.

Table 2.2. Different types of anions exist in ionic liquids (Bin Dahbag et al., 2016; Irge, 2016).

Anion	Abbreviation	Types (Organic/Inorganic)
Alkyl sulfate	$R\text{-}O\text{-}SO_3^-$	Organic
Methane sulfonate	$R_3C\text{-}S\text{-}O_3^-$	Organic
Tosylate	$C_7H_7O_3S^-$	Organic
Trifluoroacetate	$CF_3CO_2^-$	Organic
Chloride	Cl^-	Inorganic
Fluoride	F^-	Inorganic
Bromide	Br^-	Inorganic
Iodide	I^-	Inorganic
Tetrachloroaluminate	$AlCl_4^-$	Inorganic
Hexafluorophosphate	PF_6^-	Inorganic
Tetrafluoroborate	BF_4^-	Inorganic
Bis(trifluoromethylsulfonyl) imide	$[(CF_3SO_2)_2N]^-$	Inorganic

Some ionic liquids possess amphiphilic structures which enables them to have an affinity to both water and oil phases (Alves et al., 2017; Martínez-Palou and Aburto, 2015; Shehzad et al., 2018). The amphiphilic character may be in cation or anion part of an ionic liquids structure. Depending on the location of the amphiphilic structure, ionic liquids can be classified into cationic or anionic ionic liquids (Martínez-Palou and Aburto, 2015). Figure 2.5 shows the common structure of ionic liquids and the structure of 1-butyl-3-methylimidazolium chloride.

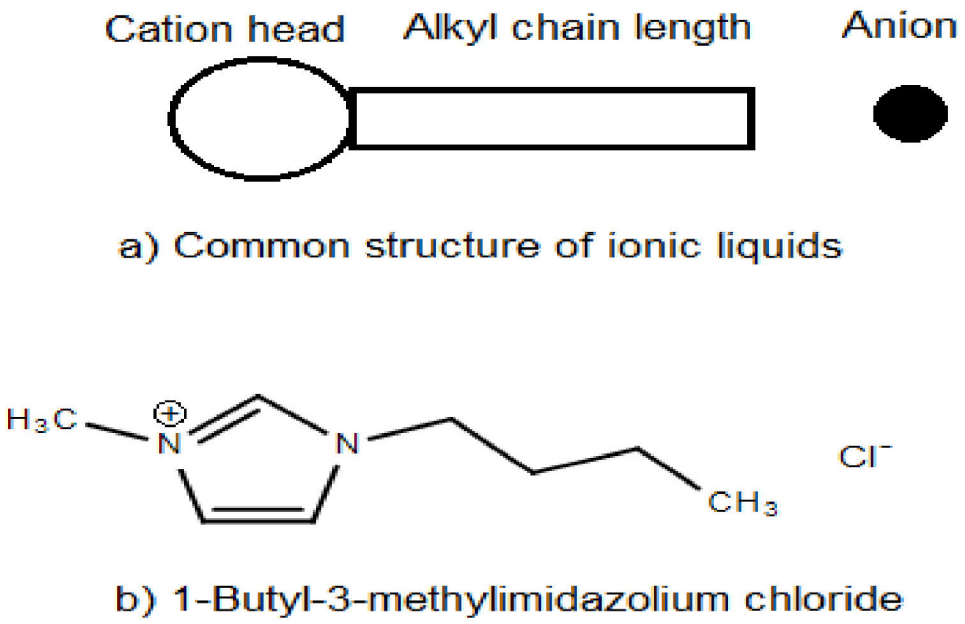

Figure 2.5. Structure of ionic liquids, a) common structure, b) structure of 1-butyl-3-methylimidazolium chloride (Usuki et al., 2017).

The characteristics of ionic liquids such as melting point, thermal stability, and viscosity can be modified by using different combinations of cations and anions to achieve different desirable purposes (Forsyth et al., 2004; Hanamertani et al., 2017). The water solubility (i.e., hydrophobicity and hydrophilicity), viscosity, and melting points of ionic liquids are

dependent on the type, size, and structure of the anions, respectively. Bis(trifluoromethanesulfonyl)amide, bis(pentafluoroethanesulfonyl)amide, and tris(trifluoromethanesulfonyl)methanide are examples of anions that can be used to produce hydrophobic ionic liquids in a combination of cations, such as 1,3-dialkylimidazolium and N-alkylpyridinium, tetraalkylammonium. Tosylate, trifluoroacetate, and dicyanamide are common anions that can be used to produce hydrophilic ionic liquids (Forsyth et al., 2004).

The hydrophobicity (or hydrophilicity) of anions affects the thermal stability of ionic liquids: the more hydrophilic the anions, the less thermally stable the ionic liquid (Cao and Mu, 2014; Irge, 2016; Maton et al., 2013). Ionic liquids with a small anion size tend to have a low viscosity due to the low tendency to participate in hydrogen bonding as well as the diffusive negative charge (Forsyth et al., 2004). The symmetry of anion and cation of ionic liquids affect their melting points: the less symmetry of anions and cations, the lower the melting point of ionic liquids (Irge, 2016; Zhao, 2003). Increasing the cation alkyl chain length (e.g., 3–5 carbon atoms) could result in a decreased melting point of ionic liquids (Forsyth et al., 2004). Nevertheless, increasing the alkyl chain length of ionic liquids could increase the thermal stability, hydrophobicity, and surface-active area of ionic liquids (Bera et al., 2020; Grenoble and Trabelsi, 2018; Yahya et al., 2019).

2.3.3. Demulsification mechanism of ionic liquids

The demulsification mechanism of ionic liquids involves two main steps, including diffusion and adsorption. The diffusion process is the distribution of ionic liquid molecules in the continuous phase before arriving at the O-W interface, while the adsorption process means that the diffused ionic liquid molecules pass through the continuous phase and reach the O-W interface (Hanamertani et al., 2017; Hezave et al., 2013a; Hezave et al., 2013b; Hezave.,

2013c). The ionic liquid molecules then substitute natural emulsifying agents at the interface and change the viscoelastic properties of the interfacial films. This leads to breaking the strong film around O-W droplets and enhancing the coalescence of the dispersed droplets (Canevari, 1982; Grenoble and Trabelsi, 2018; Martínez-Palou and Aburto, 2015).

Recent investigations have found that hydrophobic surface-active ionic liquids can be used for the effective demulsification of W/O emulsions in the oil and gas industries (Atta et al., 2016b; Forsyth et al., 2004). Research conducted by Hazrati et al. (2018) indicated that hydrophobic ionic liquids (e.g., $C_n$mim PF_6) demulsified emulsions better than hydrophilic ionic liquids (e.g., $C_n$mim Cl) (Hazrati et al., 2018). To facilitate the dissolution of ionic liquids in an oil phase, organic solvents such as xylene and methanol can be used along with hydrophobic and hydrophilic ionic liquids, respectively (Abullah et al., 2016). Dichloromethane, chloroform, isopropanol, ethanol, benzene, and toluene can also be used individually or in mixtures to achieve the same purpose (Oropeza et al., 2016). Tian et al. (2019) used C_2mim BF_4 with cyclohexane for enhancing oil recovery from tank bottom oily sludge (a stable emulsion), and they found that more than 95% of total petroleum hydrocarbons recovery can be achieved at 0.1 mL/g of ionic liquid/sludge ratio, a time of 10 min, solvent/sludge of 4:5 mL/g, and a shaking speed of 100 rpm (Tian et al., 2019). Table 2.3 categorizes the common solvents which are used for synthesizing as well as for facilitating the dissolution of ionic liquids in oil phase into three groups, including preferred, usable, and undesirable, based on their physical and chemical properties, toxicity, environmental and safety aspects, operational concerns, and costs (Capello et al., 2007; Slater and Savelski, 2007).

Table 2.3. Guide for solvent selection for synthesizing as well as facilitating the dissolution of ionic liquids in the oil phase (Ghandi, 2014).

Common organic solvents		
Preferred	**Usable**	**Undesirable**
Acetone	Cyclohexane	Pentane
Ethyl acetate	Heptane	Hexane(s)
Water	Toluene	Di isopropyl ether
Ethanol	Methyl cyclohexane	Diethyl ether
Methanol	Isooctane	Dichloromethane
2-propanol	Acetonitrile	Dichloromethane
1-propanol	2-Methyltetrahydrofuran	Chloroform
Isopropylacetate	Tetrahydrofuran	Pyridine
1-butanol	Xylenes	Dioxane
Tert-butyl alcohol	Dimethyl sulfoxide	Dimethoxyethane
	Acetic acid	Benzene
	Ethylene glycol	Carbon tetrachloride
	Methyl Ethyl Ketone	

To evaluate the demulsification efficiency of ionic liquids, bottle test is commonly used in laboratories (Grenoble and Trabelsi, 2018; Martínez-Palou and Aburto, 2015; Shehzad et al., 2018). In a bottle test, an ionic liquid is added dropwise to a graduated settling tube containing emulsions. Then their mixture is shaken for 1–5 min, followed by the measurement of the height of the separated water and oil at different times (Shehzad et al., 2018). The demulsification efficiency is calculated using Equation (2.1) (Santos et al., 2017):

$$DE = \frac{C_i - C_f}{C_i} \times 100 \quad (2.1)$$

where DE is demulsification efficiency, C_i is the initial oil (water) concentration of emulsion, and C_f is the final oil (water) concentration of emulsion.

2.4. Factors affecting ionic liquids demulsification

Many researchers applied different types of ionic liquids to investigate their effects on demulsification processes. Several factors were found to affect the demulsification performance of ionic liquids, and they are described below.

2.4.1. Concentration

The concentration of ionic liquids could affect the demulsification efficiency. Generally, increasing ionic liquid concentration up to reaching micellization would increase the demulsification efficiency. When water at the O-W interface saturates with the hydrophilic parts of an ionic liquid, micellization happens. The concentration of ionic liquids that can initiate micellization is called critical micelle concentration (CMC). The CMC of ionic liquids is identified by measuring the IFT of a solution at different concentrations of ionic liquids: when the IFT is the minimum, the concentration is identified as the CMC (Bin-Dahbag et al., 2014). However, using ionic liquids at concentrations higher than CMC will not lead to any significant change in IFT (Hezave et al., 2013a), and a demulsifier concentration higher than the CMC could lead to adverse effects on a demulsification process because ionic liquid molecules aggregate and become an emulsifier agent (Bin-Dahbag et al., 2014; Biniaz et al., 2016). Moreover, the relationship between IFT reduction and demulsification efficiency is still not well understood (Shehzad et al., 2018). Bin-Dahbag et al. (2014) investigated the effect of tetraalkylammonium sulfate and its concentration (100–1000 ppm) on the efficiency of IFT reduction in saline W/O emulsions (10% and 20% w/w salinity), and they observed that by increasing ionic liquid concentration to CMC (250 ppm), the IFT reduced from 18 to 3.36 mN/m and from 14.5 to 1.65 mN/m for 10% and 20% salinity of solutions, respectively, while increasing ionic liquids concentration above CMC had no significant changes on IFT reduction

(Bin-Dahbag et al., 2014). In a research conducted by Hezave et al. (2013c), the effect of C_{12}mim Cl on IFT reduction in O/W emulsion at different ionic liquid concentrations (0–5000 ppm) and water salinity (10,000–100,000 ppm) was investigated, and they found that by increasing concentration of ionic liquid to CMC (100 ppm), IFT reduced noticeably (from 38.02 to 0.81 mN/m), but no significant change in IFT was observed by increasing the concentration of ionic liquids beyond CMC (Hezave et al., 2013c).

2.4.2. Cation type and structure of ionic liquids

In addition to the applied concentration, the effectiveness of ionic liquids in demulsification processes depends on the cation type and cation alkyl chain length (Sastry et al., 2012; Shehzad et al., 2018). Ionic liquids and their cations must have a high molecular volume (e.g., 1000–1500 $Å^3$) to function effectively as a demulsifier. Larger cation volume (e.g., 900–1400 $Å^3$) increases the polarizability of the cation which leads to higher demulsification efficiency (Flores et al., 2014). Sakthivel et al. (2017) used lactam and imidazolium-based ionic liquids for EOR and IFT reduction, and they evaluated the effectiveness of ionic liquids at the concentration of 5000 ppm under zero and high salinity (100,000 ppm) conditions (Sakthivel et al., 2017). They observed that both ionic liquids performed better at high salinity than zero salinity conditions because of the interaction of ionic liquids and salt ions at the O-W interface, and they demonstrated that the lactam-based ionic liquid was better than the imidazolium-based ionic liquid in IFT reduction and EOR because the former one had more polar moieties in the structure (Sakthivel et al., 2017).

Cation alkyl chain length and its structure (e.g., straight or branched) could change the properties of ionic liquids. Molecular polar-polar interactions between the polar fractions of oil and the polar moieties of ionic liquid would increase by increasing the cation alkyl chain

length (Sakthivel et al., 2017). Saien et al. (2015a, 2015b, 2016) indicated that increasing the alkyl chain length of $C_n$mim Cl ionic liquid from 6 to 16 significantly decreased the IFT of n-butyl acetate-water at 25 °C (Saien et al., 2015a; Saien et al., 2015b; Saien et al., 2016). Ionic liquids with branched and long alkyl chains are more hydrophobic and have lower CMC than those with short and straight alkyl chains (Grenoble and Trabelsi, 2018; Hanamertani et al., 2017; Hezave et al., 2013b). However, it should be noted that a very long alkyl chain might impede ionic liquids to reach the O-W interface of W/O emulsions. Guzman-Lucero et al. (2010) synthesized ionic liquids with different alkyl chain lengths (5–18 carbon atoms) to demulsify W/O emulsions at the ionic liquid concentration of 1000 ppm and the temperature of 80 °C, and they indicated that the ionic liquid with 18 carbon atoms had lower efficiency in demulsification of W/O emulsions than ionic liquids with 12 and 14 carbon atoms (Guzman-Lucero et al., 2010). The surface activity of ionic liquids varies based on their cation types and cation alkyl chain length. Sastry et al. (2012) evaluated the surface activity of ionic liquids with different cation types (methylimidazolium, methylpiperidine, methylpyrrolidine) and alkyl chain length (10,12,14,16,18 carbon atoms) by measuring surface tension and solution conductivity, and they observed that the surface activity of ionic liquids increased by increasing the alkyl chain length. The surface activity of methylimidazolium-based ionic liquids was higher than methylpiperidine and methylpyrrolidine-based ionic liquids with the same carbon alkyl chain (octadecyl) and anion type (chloride) (Sastry et al., 2012).

2.4.3. Anion type of ionic liquids

Investigations indicated that hydrophobicity and hydrophilicity of anions as well as the size of anions are important factors influencing demulsification efficiency (Hazrati et al., 2018; Lemos et al., 2010). Hydrophobic ionic liquids with a large anion size, such as C_8mim PF_6, can reduce the chance of aggregation formation of ionic liquid molecules in a solution, which leads to an enhanced demulsification process and IFT reduction (Lemos et al., 2010). These ionic liquids can obtain a high demulsification efficiency even at low concentrations (Hanamertani et al., 2017; Hazrati et al., 2018; Silva et al., 2013). In other words, anions that have weaker hydration (i.e., high polarizability) would adsorb greatly at the O-W interface, break the strict films around droplets, and enhance the demulsification efficiency. For example, ionic liquids containing bromide anions in their structure performed better than those with chloride anions because bromide has weaker hydration than chloride (Sastry et al., 2012). Saien et al. (2016) compared different halide anions $(I, Br, Cl)^-$ based ionic liquids and found that ionic liquids with bigger anion size ($I^- > Br^- > Cl^-$) were more polarizable and adsorbed better at the O-W interface. Based on the results, C_{16}mim I, C_{16}mim Br, and C_{16}mim Cl reduced IFT from 13.4–14.0 mN/m to 3.7, 3.9, and 4.0 mN/m at the concentration of 2.5×10^{-3} mole/L and the temperature of 25 °C, respectively (Saien et al., 2016). Abdullah and Al-Lohedan (2019) investigated the effect of anion type of GEB-Cl and GEB-TFA ionic liquids on the demulsification efficiency and IFT reduction of sea W/O emulsions (oil: seawater of 50:50, 70:30, 90:10 volume %) at different ionic liquids concentration (250,500,1000 ppm), and they found that increasing concentration to 1000 ppm increased the demulsification efficiency (100%) and reduced the IFT of emulsions from 33.5 mN/m to 8.4 mN/m and 7.2 mN/m for GEB-Cl and GEB-TFA, respectively. Based on their result, the greater hydrophobicity of

trifluoroacetate anion compared to chloride anion led to better IFT reduction by GEB-TFA than GEB-Cl (Abdullah and Al-Lohedan, 2019). Some of the recent studies are summarized in Table 2.4.

Table 2.4. List of application of ionic liquids as demulsifier.

Ionic liquid	Cation type	Anion type	Emulsion type	Dose (ppm)	CMC (ppm)	DE (%)	IFT reduction (%)	Key findings
$C_n$mim NTf_2 n = 10,12, 14	Imidazolium	Bis (trifluoro methyl sulfonyl) imide	SW/O	100–3500	N.A.	93.6–100	77–95	Demulsification experiments were conducted at the temperature of 60 °C. Increasing the dose and alkyl cation chain of hydrophobic ionic liquids improved the demulsification process (100% demulsification) as well as reduced the IFT (95% reduction). Higher hydrophobicity of NTf_2 results in improving demulsification efficiency even with shorter alkyl chain length (e.g., demulsification efficiency was in the range of 93.6–100%). By contrast, for hydrophilic ionic liquid, increasing the dose and alkyl cation chain length of ionic liquid led to aggregation and caused poor demulsification as well as increased IFT.
$C_n$mim PF_6 n = 10,12, 14		Hexafluoro phosphate		500–3500		71.25–86.25	54–81	
$C_n$mim Cl n = 10,12, 14		Chloride		500–3500		76.25–93.75	64–80	

Source: Hazrati et al., 2018

Ionic liquid	Cation type	Anion type	Emulsion type	Dose (ppm)	CMC (ppm)	DE (%)	IFT reduction (%)	Key findings
TOMAC	Ammonium	Chloride	W/O	1000–2000	N.A.	100	N.A.	The efficiency of three ionic liquids (TOMAC, TOMAB, CTAB) with different hydrophobicity and hydrophilicity were evaluated for demulsification of W/O emulsions. Response surface methodology was applied to investigate the effect of temperature (50 °C–80 °C), pH (5–9), and water of aqueous phase (3–10%) on the demulsification efficiency. They observed that increasing ionic liquids concentration to 1039.2 ppm, 1480 ppm, 332.09 ppm for TOMAC, TOMAB, and CTAB, respectively led to the maximum demulsification efficiency (100, 90.29, and 64.9% for TOMAC, TOMAB, and CTAB, respectively). Demulsification efficiency increased at the pH of 7 and the temperature of 80 °C. Increasing water of emulsion (up to 10%) increased the demulsification efficiency of system to 64.88% and 90.29% using hydrophilic TOMAB and CTAB ionic liquids, respectively. Among three ionic liquids, TOMAC had the highest efficiency (100%) because it was more hydrophobic than other ionic liquids.
TOMAB		Bromide		1000–2000	N.A.	64.9		
CTAB		Bromide		300–700	N.A.	90.29		

Source: Biniaz et al., 2016

Ionic liquid	Cation type	Anion type	Emulsion type	Dose (ppm)	CMC (ppm)	DE (%)	IFT reduction (%)	Key findings
Trihexyl tetradecyl phosphonium [Y]	Phosphonium	Chloride	W/O	50–4000	N.A.	71.42–99	N.A.	Experiments were conducted at different temperatures (60 °C and 80 °C) to investigate the efficiency of phosphonium based ionic liquids at different concentration of 50 to 4000 ppm on demulsifying W/O emulsions. Different hydrophobicity of anions led to different demulsification efficiency (e.g., varying from 14.29 to 99%).
		Decanoate				14.29–92.86		
		Dicyanamide				50–99		
AMPS/AA-TE	Oxyethylene ammonium	Sulfonate and carboxylate	W/O	100–500	27×10^{-5} *	8–100	N.A.	Experiments were conducted at the temperature of 65 °C and different water content of emulsions (10, 20, 30, 50%). AMPS/AA-TE poly ionic liquid has oxyethylene in its structure which increased the polarity of AMPS/AA-TE. This led to AMPS/AA-TE having lower CMC than AMPS/AA-OA.
AMPS/AA-OA	Ammonium				53×10^{-5} *	10–100		

Source: Abullah et al., 2016; Adewunmi and Kamal, 2019;

Ionic liquid	Cation type	Anion type	Emulsion type	Dose (ppm)	CMC (ppm)	DE (%)	IFT reduction (%)	Key findings
TOMAC	Ammonium	Chloride	W/O	1500	N.A.	90	N.A.	Experiments were conducted at the temperature of 80 °C. TOMAC removed water from an extra heavy crude oil in less than an hour while two hours were required for trioctylmethyl ammonium ethyl sulfate and trioctylmethyl ammonium methyl sulfate to remove the same amount of water.
Trioctyl methyl ammonium [Y]		Ethyl sulfate					N.A.	
		Methyl sulfate					N.A.	
C_{12} mim NTf_2	Imidazolium	Bis(trifluoro methyl sulfonyl) imide	W/O	5–125	100	N.A.	33.3	Applying ionic liquids with long alkyl chain lengths (12 carbon atoms) was more capable to displace the natural emulsifying agents of the crude oil which resulted in enhancing the IFT reduction (33%). Increasing ionic liquid concentration to CMC (100 ppm) reduced IFT, while no significant change was observed with a concentration more than CMC.

Source: Alves et al., 2017; Oropeza et al., 2016

Ionic liquid	Cation type	Anion type	Emulsion type	Dose (ppm)	CMC (ppm)	DE (%)	IFT reduction (%)	Key findings
HEOD-TS	Ammonium	Tosylate	SW/O	100–500	N.A.	30–100	95–99.5	Demulsification experiments were conducted at 65 °C. Increasing the concentration of hydrophobic HEOD-TS ionic liquid (e.g., from 100 to 500 ppm) for demulsifying SW/O emulsions at different water contents (10, 30, 50%) resulted in demulsifying emulsions completely (100%) as well as decreasing the IFT.
TOMAC	Ammonium	Chloride	W/O	1000 and 1500	N.A.	100	N.A.	Demulsification experiments were conducted at 80 °C using a water bath to remove the water of two extra-heavy crude oils (with a water content of 56 and 60%). Increasing the concentration of ionic liquids from 1000 to 1500 ppm resulted in 100% demulsification efficiency. Ionic liquids with smaller anion sizes have lower anion polarizability which results in the dehydration of extra-heavy crude oils effectively.
Trioctylmethyl ammonium [Y]		Bisulfate						
		Dihydrogen phosphate						

Source: Atta et al., 2016b; Flores et al., 2014

Ionic liquid	Cation type	Anion type	Emulsion type	Dose (ppm)	CMC (ppm)	DE (%)	IFT reduction (%)	Key findings
C_8mim PF_6	Imidazolium	Hexafluoro phosphate	W/O	600–6200	N.A.	54.7–95.6	92	High dosage of ionic liquids resulted in 95.6% and 87.4% of demulsifying W/O emulsions using C_8mim PF_6 and C_8mim BF_4, respectively that were implemented under microwave heating (90 °C) and different water content of emulsions (~ 30 to 50%). C_8mim PF_6 decreased the IFT and separated water from oil more effectively than C_8mim BF_4 (95.6 and 87.4% for C_8mim PF_6 and C_8mim BF_4, respectively). The reason is that C_8mim PF_6 has a bigger anion size and lower solubility in water which prevents the aggregation of ionic liquid in the medium in comparison with C_8mim BF_4.
C_8mim BF_4		Tetrafluoro borate		1000–7200		0–87.4	85	

Source: Lemos et al., 2010

Ionic liquid	Cation type	Anion type	Emulsion type	Dose (ppm)	CMC (ppm)	DE (%)	IFT reduction (%)	Key findings
C_4mim NTf_2	Imidazolium	Bis (trifluoro methyl sulfonyl)imide	SW/O	0.74–8.9 **	N.A.	10	1	Imidazolium and pyridinium-based ionic liquids were used to demulsify W/O emulsion (water content of 40 wt%) at the temperature of 120 °C. There was no significant difference in the demulsification efficiency between the imidazolium and the pyridinium ionic liquids with the same alkyl chain length and anion type. Ionic liquids with longer alkyl chains (e.g., 8 and 12 carbon atoms) were more capable to displace the natural emulsifying agents of the crude oil which resulted in enhancing the demulsification process (74% and 90% for C_8mim NTf_2 and C_{12}mim NTf_2, respectively) as well as IFT reduction. Higher hydrophobicity of NTf_2 results in improving demulsification efficiency (e.g., 74% and 40% for C_8mim NTf_2 and C_8mim OTf, respectively).
C_8mim NTf_2						74	4	
C_{12}mim NTf_2						90	34	
C_8mim OTf		Triflate				~40	N.A.	
C_4py NTf_2	Pyridinium	Bis(trifluoro methyl sulfonyl)imide				10>	N.A.	

Source: Silva et al., 2013

Ionic liquid	Cation type	Anion type	Emulsion type	Dose (ppm)	CMC (ppm)	DE (%)	IFT reduction (%)	Key findings
EDHI	Imidazolium	Acetate	W/O	50–250	N.A.	0–70	N.A.	The demulsification process using imidazolium-based ionic liquids was conducted at 60 °C and different water contents (10, 20, 30%). Increasing ionic liquids concentration from 50 to 250 ppm increased the demulsification efficiency to 70, 85, 100, and 100 for EDHI, EPHIB, EDDI, and EDPIB, respectively at different experimental conditions. Using 4-(trifluoromethoxy)phenylborate anion increased the hydrophobicity of EPHIB compared to EDHI which resulted in enhancing the demulsification process (e.g., demulsification efficiency increased from 70 to 85%). Based on the results, the efficiency of polymeric ionic liquids was better than that of their monomeric ionic liquids.
EPHIB		4-(trifluoro methoxy) phenylborate				10–85		
EDDI		Acetate				70–100		
EPDIB		4-(trifluoro methoxy) phenylborate				85–100		

Source: Ezzat et al., 2018

Ionic liquid	Cation type	Anion type	Emulsion type	Dose (ppm)	CMC (ppm)	DE (%)	IFT reduction (%)	Key findings
$P_{666,14}(CN)_2$	Phosphonium	Dicyanamide	O/W	***	N.A.	100	N.A.	In this research, different ionic liquids with hydrophobic cations and hydrophilic anions were used to demulsify O/W emulsions at room temperature. $P_{666,14}[N(CN)_2]$ had a high surface-active area and removed oil from the water completely. However, stable emulsions still existed in the systems that $P_{666,14}$[Phos], $P_{666,14}[NTf_2]$ and $N_{2224}[N(CN)_2]$ were used because the surface active area would not achieve in too hydrophobic ($P_{666,14}$[Phos], $P_{666,14}[NTf_2]$) and too hydrophilic ($N_{2224}[N(CN)_2]$) ionic liquids. Halogenide ionic liquids, $P_{666,14}$[Cl] and $P_{666,14}$[Br] separated oil from water in a very short time (20 min) compared to non-halogenide ionic liquid $P_{666,14}[N(CN)_2]$ (24 h).
$P_{666,14}$ Phos		Bis(2,4,4-trimethyl pentyl) phosphinate				0		
$P_{666,14}NTf_2$		Bis(trifluoro methyl sulfonyl) imide				0		
$P_{666,14}$ Cl		Chloride				>90		
$P_{666,14}$ Br		Bromide						
$N_{2224}N(CN)_2$	Ammonium	Dicyanamide				0		

Source: Li et al., 2016

Ionic liquid	Cation type	Anion type	Emulsion type	Dose (ppm)	CMC (ppm)	DE (%)	IFT reduction (%)	Key findings
C_8mim Cl	Imidazolium	Chloride	W/O	100–10000	1000	N.A.	3–73	In this research, imidazolium and pyridinium based ionic liquids were used at different concentration (100–1000 ppm) and different temperatures (20 °C to 60 °C) to evaluate their efficiency on IFT reduction. Pyridinium cation is more hydrophobic than imidazolium cation, therefore pyridinium based ionic liquids can remain at the O-W interface better than imidazolium based ionic liquids, which enable them to reduce the IFT of crude oil-distilled water effectively at lower CMC.
C_{12}mim Cl					2000		6–84	
C_8Py Cl	Pyridinium				N.A.		4–45	
C_{12}Py Cl					500		7–93	

Source: Hezave et al., 2013b

Note: DE: Demulsification efficiency. SW: Saline water. N.A.: Not available. [Y]: Refer to anion type. * Mole/Liter. ** μmole/gram of emulsion. *** Mole ratio of ionic liquid:sodium dodecylbenzenesulfonate is 1.

2.4.4. Molecular weight

The molecular weight of ionic liquids could affect their molecules' movability and diffusion through a continuous phase (Ghandi, 2014; Grenoble and Trabelsi, 2018). Demulsifiers with a molecular weight > 10,000 Daltons (Da) are known as high molecular weight demulsifiers. These demulsifiers have low diffusion ability and require a relatively long time to function (Peña et al., 2005). However, high molecular weight demulsifiers were reported capable of flocculating small water droplets in the continuous oil phase and destabilizing them (Hao et al., 2016; Peña et al., 2005). Low molecular weight demulsifiers (i.e., <3000 Da) diffuse quickly in a continuous phase, and they possess high interfacial activity which can easily absorb onto the O-W interface and weaken the rigid films around droplets (Grenoble and Trabelsi, 2018; Hao et al., 2016; Peña et al., 2005). However, a high dosage of low molecular weight demulsifiers may be required for successful demulsification. Wu et al. (2003) evaluated the effect of 52 nonionic demulsifiers on the demulsification of W/O emulsions at the temperature of 80 °C, and they observed that commercial demulsifiers from four families (Span, Brij, Tween, and Igepol) were ineffective at low applied concentrations (300–400 ppm). They concluded that using demulsifiers with a molecular weight between 7500 to 15,000 Da could lead to a higher demulsification efficiency than using a demulsifier with a molecular weight of 4000 Da (Wu et al., 2003). Commonly used demulsifying ionic liquids usually have a molecular weight of < 1000 Da (Abdullah et al., 2017; Adewunmi and Kamal, 2019; Balsamo et al., 2017; Silva et al., 2013). Balsamo et al. (2017) in their research investigated the effect of TOMAC and C_8mim PF_6 ionic liquids on the demulsification efficiency at different concentrations (2.5×10^{-3}, 1.2×10^{-2} and 2.9×10^{-2} mole/L), and their results indicated that TOMAC separated the water from the oil effectively (74%) at the

concentration of 2.9×10^{-2} mole/L because it was more hydrophobic and had a higher molecular weight (404 Da) than C_8mim PF_6 (340 Da) (Balsamo et al., 2017).

2.4.5. Salinity

The presence of salt in the water phase can help to improve the demulsification performance of ionic liquids by two means. First, salt anions in the solution (e.g., Cl^-) can reduce the electrical repulsions between positive homonymous charges of ionic liquids at the O-W interface. This enables ionic liquids to saturate the interface completely, leading to the reduction of IFT and thus enhancement of the demulsification process (Atta et al., 2016b; Hezave et al., 2013a; Hezave et al., 2013b; Hezave et al., 2013c). Second, the cations of salts (e.g., Na^+) have a smaller molecule size and a higher surface charge density than the cations of ionic liquids. Therefore, cations of salts tend to adsorb the water and induce the molecules of the ionic liquid to accumulate at the O-W interface (Hanamertani et al., 2017). This phenomenon is known as salting out which enhances the demulsification process and IFT reduction (Borges et al., 2009). For example, Bin-Dahbag et al. (2014) found that salinity (10% w/w) contributed to the reduction of IFT noticeably by improving the distribution of ionic liquid molecules at the oil-brine interfaces (Bin-Dahbag et al., 2014).

Salinity has more significant effects on imidazolium-based ionic liquids than on pyridinium-based ionic liquids. Imidazolium cation is more hydrophilic than pyridinium cation, which leads to better adsorption of imidazolium-based ionic liquids onto the water film at the O-W interface. The presence of salt anions in the water reduces the repulsions among imidazolium cations and results in better saturation of ionic liquids at the interface. However, as pyridinium cations are more hydrophobic than imidazolium cations, they tend to immerse to the oil phase where the anions of water have less effect on them. To confirm this, Hezave et

al. (2013b; 2013c) used pyridinium and imidazolium-based ionic liquids to investigate their efficiency on IFT reduction of W/O emulsions with and without salt ions in the water, and they found that the IFT and CMC of ionic liquids for emulsions containing salt ions (~100,000 ppm) reduced noticeably, while no research has indicated that conventional surfactants are effective to reduce IFT at high salinity (Hezave et al., 2013b; Hezave et al., 2013c). They also indicated that the CMC of C_{12}mim Cl reduced from 2000 ppm to 100 ppm in the presence of salt ions, while that of C_{12}Py Cl reduced from 500 ppm to 250 ppm (Hezave et al., 2013b). Sakthivel et al. (2017) investigated the effect of salinity on reducing IFT of O-W using CP $C_6H_{13}COO$ ionic liquid, and they observed that the IFT of solution reduced from 39 to 15 mN/m and 10 mN/m at distilled water and saline water (100,000 ppm) conditions, respectively. They also concluded that the selected ionic liquid was stable and effective in high salinity compared to the other conventional surfactants such as sodium dodecyl sulfate (Sakthivel et al., 2017).

Salinity would also affect the duration of the demulsification process when using ionic liquids. Borges et al. (2009) found that salinity influenced the demulsification process by reducing the O-W separation time (Borges et al., 2009). Adewunmi and Kamal (2019) indicated that, when using three types of ionic liquids (trihexyltetradecylphosphonium chloride, trihexyltetradecylphosphonium decanoate, trihexyltetradecylphosphonium dicyanamide) at 80 °C, the demulsification time of W/O emulsions reduced from 10 to 5 min when saline W/O substituted distilled W/O (Adewunmi and Kamal, 2019). In contrast, Lemos et al. (2010) observed that increasing the salinity of the aqueous phase from 0 to 50,000 ppm reduced the demulsification efficiency of C_8mim PF_6 from 54.7% to 27.1%, but no salinity-caused effect was observed for the demulsification process with the use of C_8mim BF_4 (Lemos et al., 2010).

2.4.6. Temperature

Temperature can affect the physical properties of emulsion such as viscosity. The viscosity of a continuous phase reduces at high temperatures (e.g., 70 °C) (Hezave et al., 2013c), which facilitates the dissolution of ionic liquids in the continuous phase (Biniaz et al., 2016; Kokal, 2005; Saad et al., 2019). The temperature should be increased up to the phase inversion temperature (PIT), at which emulsion alteration occurs (e.g., W/O turns into O/W) (Shinoda, 1967). A temperature higher than PIT enables the saturation of O-W interface by ionic liquid molecules and facilitates the distribution of ionic liquid molecules in the continuous phase (Hanamertani et al., 2017; Hezave et al., 2013a). Hezave et al. (2013a; 2013c) found that by increasing the temperature of W/O emulsion higher than the PIT (e.g., 20 °C in their research), the IFT of the emulsion increased due to the distribution of C_{12}mim Cl in the continuous oil phase (Hezave et al., 2013a; Hezave et al., 2013c). However, Bin-Dahbag et al. (2014) indicated that increasing the temperature from 22 °C to 90 °C had a negligible effect on the IFT reduction using tetraalkylammonium sulfate as a demulsifier (Bin-Dahbag et al., 2014).

Increasing the temperature of an emulsion can significantly reduce its viscosity. However, it is difficult to differentiate the demulsification enhancement effects brought by reduced viscosity and by ionic liquids (Balsamo et al., 2017). Balsamo et al. (2017) investigated the effect of temperature (30, 45, and 60 °C) on the demulsification process using TOMAC and C_8mim PF_6, and they concluded that by increasing temperature from 30 °C to 45 °C, the demulsification efficiency increased for samples containing the two ionic liquids. However, increasing the temperature to 60 °C resulted in a high demulsification efficiency for all the samples (with and without ionic liquids), and the reason was that a great reduction in the

viscosity of the oil phase occurred at the temperature of 60 °C, which facilitated the coalescence of water droplets for increased settling (Balsamo et al., 2017).

2.4.7. Oil types

Since the physiochemical properties of oil (e.g., density, viscosity, and natural emulsifying agents) vary greatly from field to field (Adilbekova et al., 2015; Canevari, 1982), the demulsification performance of the same ionic liquid on emulsions containing different types of oil might not be consistent (Guzman-Lucero et al., 2010). Crude oil is categorized into different groups based on API rating, including light, medium, heavy, and ultra-heavy. Guzman-Lucero et al. (2010) investigated the demulsification efficiency of different ionic liquids for medium, heavy, and ultra-heavy crude oils, and they observed that all of the ionic liquids effectively destabilized emulsions of medium crude oil, but their efficiency was reduced for the ultra-heavy crude oil. A high amount of natural emulsifying agents in the ultra-heavy crude oil could lead to the production of highly stable emulsions and the increment of oil viscosity, which would reduce the diffusion of ionic liquids. Ionic liquids with imidazolium, pyridinium, and ammonium cations with long alkyl chain lengths would be suitable for demulsifying heavy crude oils (Guzman-Lucero et al., 2010). Similar results were obtained from the application of trioctylmethyl ammonium ethyl sulfate for demulsifying heavy and ultra-heavy crude oils, and a lower demulsification efficiency (50%) was observed for ultra-heavy crude oil than for heavy crude oil (70%) when 1500 ppm of trioctylmethyl ammonium ethyl sulfate was applied (Oropeza et al., 2016). However, no significant changes were observed when TOMAC was used for medium, heavy, and ultra-heavy crude oils, and around 95% demulsification efficiency was achieved for all types of crude oils at an ionic liquid concentration of 1500 ppm and a treatment time of 6 h (Oropeza et al., 2016).

2.5. Challenges and opportunities

In this review, the application of ionic liquids in demulsification processes and the influential factors are discussed. Along with the advantages of ionic liquids, there are still some challenges and opportunities regarding their demulsification applications.

2.5.1. Toxicity of ionic liquids

Generally, the toxicity of ionic liquids is some order of magnitude lower than conventional solvents such as acetone and methanol (Gathergood et al., 2004). However, not all ionic liquids are environmentally friendly (Zhou et al., 2018). Toxicity of ionic liquids mainly depends on the cation type (e.g., imidazolium) and the cation alkyl chain length (e.g., >10 carbon atoms) (Gathergood et al., 2004; Gathergood et al., 2006). Romero et al. (2008) examined the toxicity of imidazolium-based ionic liquids with different alkyl chain lengths (1–8 carbon atoms), and they observed that the toxicity of ionic liquids increased by increasing the alkyl chain length while anion type had less effect on the toxicity of ionic liquids (Romero et al., 2008). It is reported that some of the ionic liquids containing fluoride and/or chloride ($[BF_4]^-$, $[PF_6]^-$) might generate hydrofluoric acid and/or hydrochloric acid in the presence of water (Bera et al., 2020; Dharaskar Swapnil, 2012; Shehzad et al., 2018;). The hydrolysis stability of anion should be high to prevent the formation of hydrofluoric acid and hydrochloric acid. Quijano et al. (2011) investigated the amount of the remained fluoride anion in the aqueous phase and evaluated its toxicity to microorganisms. They applied C_4mim PF_6 and C_4mim NTf_2 ionic liquids at the concentration of 5 and 25% (volume/volume) in the mineral salt aqueous phase at a pH of 7 and the temperature of 25 °C. Their results indicated that fluoride anion in the aqueous phase was at a very low concentration (0.73 to 2.98 ppm) which did not change the pH of the mineral salt aqueous phase and was not toxic for microorganisms, and they also claimed that any

changes in experimental conditions such as lower pH and higher temperatures (more than 25 °C) might have effects on the toxicity of fluoride anion (Quijano et al., 2011). Consequently, the toxicity of ionic liquids should be taken into consideration in their application for demulsification (Dharaskar Swapnil, 2012).

Bio-based ionic liquids (e.g., fatty acid ionic liquids) are considered biodegradable ionic liquids with less or without significant toxicity (Gundolf et al., 2019; Hijo et al., 2020). They are made of natural-derived compounds, and their physical properties can be changed by manipulating their anion alkyl chain length. Longer anion alkyl chain length of fatty acid ionic liquids results in lower viscosity, density, water solubility (C_{18}-stearate ionic liquids are not soluble in water), and corrosiveness as well as higher thermal stability (Mezzetta et al., 2019; Sernaglia et al., 2020; Wang et al., 2019). Investigations indicated that the presence of a hydroxyl group in the imidazolium cation part of fatty acid ionic liquids increased their thermal stability (Mezzetta et al., 2019). Biodegradability and toxicity of fatty acid ionic liquids are proportional to their physical properties (e.g., kinematic viscosity and water solubility) with linear relationships. Increased kinematic viscosity and water solubility would increase the biodegradability of fatty acid ionic liquids. Also, the toxicity of fatty acid ionic liquids decreased slightly by increasing the kinematic viscosity (Oulego et al., 2019). Also, fatty acid ionic liquids are non-fluoride-based hydrophobic ionic liquids, which can prevent the formation of acids in aqueous solutions.

Fatty acid ionic liquids were used successfully in various industries for different purposes, such as pharmaceutical (Mondal et al., 2016), biorefining processes (Huet et al., 2020), solvents and co-solvents (Duan et al., 2020; Hulsbosch et al., 2016; Zhang et al., 2019), dissolution and levulination of cellulose (Becherini et al., 2019), formation of aqueous biphasic

systems (Pereira et al., 2019), CO_2 capture (Kirchhecke and Esposito, 2016; Silva et al., 2020), catalyst (Szepi´nski et al., 2020), lubricant additives (Khan et al., 2019), plant protection products (Turguła et al., 2020), and extraction agents (Patsos et al., 2019). Therefore, the demulsification potential of bio-based ionic liquids, as well as their human health effects, are worthy of further investigation in future.

2.5.2. Viscosity of ionic liquids

Ionic liquids often have high viscosity which is undesired for their diffusion in a continuous phase. The viscosity of ionic liquids depends on the types of cations and anions. Selecting some types of anions (e.g., dicyanamide or bis(trifluoromethylsulfonyl)imide) in synthesizing ionic liquids can significantly reduce their viscosity (Shirota and Castner, 2005). However, these anions may not be effective for a variety of applications. Ionic liquids can be used with solvents (e.g., ethanol, methanol, and xylene) to reduce their viscosity. Research was conducted by Li et al. (2007) to evaluate the effect of different solvents (e.g., chloroform, acetonitrile, dichloromethane) on the properties of ionic liquids (C_4mim PF_6, C_4mim BF_4, C_4mim CF_3CO_2) such as viscosity, and the results indicated that mixing ionic liquids in solvents noticeably reduced their viscosity. For example, the viscosity of C_4mim PF_6 was reduced by 64% (from 261 mPa s to 92.9 mPa s) with the addition of 0.2 mole fraction of acetonitrile (Li et al., 2007). Different solvents were reported to be applied with ionic liquids in many demulsification processes to increase the solubility of ionic liquids in the oil phase. Xylene, methanol, 2-propanol, and ethanol are some of the solvents that were used to facilitate the dissolution of ionic liquids in the oil phase (Abdullah and Al-Lohedan, 2019; Adewunmi and Kamal, 2019; Biniaz et al., 2016; Ezzat et al., 2018). It was reported that solvents with high dielectric constant (e.g., acetone, acetonitrile) can have a better effect in reducing the

viscosity of ionic liquids than solvents with low dielectric constant (e.g., chloroform). Solvents with high dielectric constant have good miscibility with ionic liquids which can effectively reduce the electrostatic attraction between ions of ionic liquids and thus lower the viscosity (Li et al., 2007). Therefore, the combination of ionic liquids with different solvents may be required before chemical demulsification to reduce the viscosity of ionic liquids. However, this might increase the costs of the entire demulsification treatment.

2.5.3. Recovery of ionic liquids

Although many commercial ionic liquids are available at a low cost, some of the best performers are still expensive for large-scale applications compared to other commercial demulsifiers. Recovery and reuse of ionic liquids without compromising the demulsification efficiency becomes essential for their field-scale application because this can greatly reduce the cost (Bera et al., 2020; Zhou et al., 2018). There are many different methods to recover ionic liquids, such as liquid-liquid extraction, distillation, adsorption, crystallization, force field separation, and membrane processes (Abu-Eishah, 2011; Bera et al., 2020; Zhou et al., 2018). The purity of ionic liquids is another important factor which should be considered in recycling or synthesizing ionic liquids. On one hand, impurities may lead to the production of unintentional by-products in the demulsification system; on the other hand, the impurities can change the expected characteristics of ionic liquids (Dharaskar Swapnil, 2012). Among the aforementioned recovery methods, adsorption by activated carbons (ACs) is one of the common methods to separate ionic liquids from water streams. Lemus et al. (2012) evaluated the efficiency of ACs with different structures in removing and recovering several imidazolium-based ionic liquids (e.g., C_8mim PF_6) from aqueous solution at the temperature of 34.85 °C, and their results indicated that most of the applying commercial ACs could

separate at least 340 $mg_{C8mim\ PF6}/g_{ACs}$ from aqueous solution. The exhausted ACs could be regenerated using acetone extraction because the volatility and solvent capacity of acetone is high, and C_8mim PF_6 was recovered from regenerating acetone by atmospheric distillation at the temperature of 59.85 °C as characterized by H NMR spectroscopy. Based on their H NMR results, there was no difference in the properties of the fresh and the recovered C_8mim PF_6, which indicated the successful recovery of C_8mim PF_6 (Lemus et al., 2012).

2.5.4. Combination of ionic liquids with nanoparticles

Recent investigations demonstrated that the presence of nanoparticles with ionic liquids or other demulsifiers in a system could enhance the interfacial properties and the demulsification process. The enhancement may be because demulsifier molecules adsorb on the surface of nanoparticles and create large particles which push them to move towards the O-W interface and break the interfacial film (Hassan et al., 2019; Saien and Hashemi, 2018). Another method was reported to coat ionic liquids onto the surface of nanoparticles to achieve promising results (Atta et al., 2017; Mi et al., 2020). Atta et al. (2017) in their research investigated the effect of 1-allyl-3-methylimidazolium oleate (AMO) coated magnetic nanoparticles (Fe_3O_4) at different concentrations (magnetic to oil ratio 1:10, 1:20, 1:25, 1:50) to remove oil from water, and found that 90% of the oil was removed from the water at the lowest concentration of magnetic nanoparticles capped with AMO (1:50). The magnetic nanoparticles were recycled for five times with a less reduction in their efficiency (efficiency reduced from 90% to 80% in the fifth cycle), and they concluded that magnetic nanoparticles can remove oil from water selectively without collecting water. These magnetic nanoparticles are easy to synthesize, cheap and reusable which could be applied in industrial scales (Atta et

al., 2017). Therefore, more efforts are needed to investigate the combinational demulsification effect of nanoparticles and ionic liquids to develop their applications in field-scales.

2.5.5. Poly ionic liquids

Synthesizing poly ionic liquids (PILs) has recently attracted research attention in oil field-related practices (e.g., EOR). PILs are polyelectrolytes consisting of a polymeric backbone and an ionic liquid. In comparison with ionic liquids, PILs possess high activity at low concentrations as well as they are stable at high salinity and temperature (Abdullah et al., 2017; Bera et al., 2020; Ezzat et al., 2018). Ezzat et al. (2018) used ionic liquids and PILs based on 1,3-dialkylimidazolium to evaluate their efficiency in demulsification of W/O emulsions at different concentrations (50, 100, 250 ppm) and water contents (10%, 20%, 30%) at the temperature of 60 °C. Based on their results, PILs demulsified W/O emulsions better than their monomeric ionic liquids under the same experimental conditions (e.g., demulsification efficiency was 90% versus 70% at the concentration of 50 ppm and water content of 30% for EPDIB and EDDI, respectively) (Ezzat et al., 2018). However, more investigations of PILs for demulsification under harsh environmental conditions are desired.

2.6. Summary

This review summarizes the recent advances in the application of ionic liquids as chemical demulsifiers for oil and water separation. Ionic liquids are promising demulsifiers, especially for applying under harsh environmental conditions characterized by high salinity and temperature as well as high viscosity (e.g., ultra-heavy crude oils). The main characteristics of ionic liquids that have attracted researchers' attention are their thermal stability, non-flammability, recyclability, low vapor pressure, and low toxicity. Factors affecting their

demulsification efficiency include ionic liquids types and concentrations, molecular weight, salinity, temperature, and types of oil in emulsions. The demulsification efficiency would be enhanced by selecting appropriate ionic liquids and dosage for specific types of emulsions as well as identifying optimal treatment conditions. Along with the advantages of ionic liquids, there are still some limitations which require further investigations to make them suitable for a wide application.

Chapter 3

EFFECT OF ULTRASONIC HOMOGENIZATION ON CRUDE OIL EMULSION STABILITY[1]

Abstract

This research aims to evaluate the effect of ultrasonic processing parameters (power and sonication time), emulsion characteristics (water salinity and pH) and their interaction on oil-in-water emulsion stability. Response surface methodology was used to design experimental runs, in which the parameters were investigated at five levels. Emulsion stability was evaluated by measuring creaming index, emulsion turbidity and microscopic image analysis. The effect of crude oil condition (fresh and weathered) on the emulsion stability was also investigated at the optimum sonication parameters and emulsion characteristics. The optimum condition was found at a power level of 76–80 W, sonication time of 16 mins, water salinity of 15 g/L NaCl, and pH of 8.3. Increasing sonication time beyond the optimum value had an adverse effect on the emulsion stability. High water salinity (> 20 g/L NaCl) and pH (> 9) decreased the emulsion stability. These adverse effects intensified at higher power levels (> 80–87 W) and longer sonication times (> 16 mins). The interaction of parameters showed that the required energy to generate a stable emulsion was within 60−70 kJ. Emulsions with fresh crude oil were more stable than those generated with weathered oil.

Keywords: Crude oil in water; emulsion; stability; ultrasonic; creaming index; turbidity difference.

[1] This work has been published as Hassanshahi, N., Hu, G., Lee, K., Li, J. (2022). Effect of ultrasonic homogenization on crude oil emulsion stability. *Journal of Environmental Science and Health, Part A*.

3.1. Introduction

Increasing crude oil production, transportation, and storage activities would lead to increased environmental risk due to oil spills and leaks on land and sea (Rongsayamanont et al., 2020). For example, oil leakage was detected in about 35% of underground storage tank systems in the United States and Canada (Gitipour et al., 2015). The leaking oil can pollute the source groundwater and pose severe health risks to the residents in communities (Gu et al., 2020). Crude oil is a complex mixture containing toxic compounds like monocyclic and polycyclic aromatic hydrocarbons, known as carcinogenic, teratogenic, and mutagenic toxic substances (Logeshwaran et al., 2018). Therefore, it is necessary to remediate oil-contaminated soil and groundwater for risk minimization. Among available technologies, emulsion washing is an effective technology to remedy oil-contaminated soil (Liu et al., 2021a).

The emulsion contains water, oil, salt, surfactant, and co-solvents. The emulsion is generated by vigorously mixing these components that create two phases: a dispersed phase and a continuous phase (i.e., bulk phase). Oil-in-water (O/W) and water-in-oil (W/O) are the common types of emulsion (McClements and Jafari, 2018; Ravera et al., 2020). Small size distribution of the dispersed phase, high stability, and high solubilization capacity of emulsion bring about high oil removal efficiency in contaminated soils. Mechanisms to recover oil from contaminant soils by emulsion washing are mobilization (i.e., by decreasing the interfacial tension) and enhanced solubilization (i.e., incorporating contaminants into the micelles). Emulsion with smaller dispersed droplets (i.e., higher stability) has a larger surface area which penetrates deeply into the porous media and results in higher efficiency of soil remediation (Pekdemir et al., 2005).

Generation of stable emulsion with smaller dispersed droplets size is challenging and may require additives like mixtures of surfactants, co-solvents, and salts (Rongsayamanont et al., 2020). Previous research used different surfactants to reduce the interfacial tension between oil and water and generate emulsions with smaller dispersed droplet sizes (Sousa et al., 2021; Taha et al., 2020). However, environmental risks associated with high surfactant concentrations and the cost of surfactants have limited their applications (Liu et al., 2021a; Sartomo et al., 2020). Therefore, it is required to investigate the effects of different physicochemical methods on the emulsification process and not merely rely on surfactants.

Among available devices (e.g., high shear mixers (Koh et al., 2014) and high-pressure homogenizers (Fernandez-Avila and Trujillo, 2016)) to generate emulsion, ultrasonic-based processes have advantages such as good emulsion stability, small droplet size, narrow droplet size distribution, and easy to operate and clean (Modarres-Gheisari et al., 2019; Taha et al., 2020). Ultrasonication generates emulsion by acoustic cavitation, in which ultrasound waves pass through a liquid and cause a mechanical vibration in the liquid. This creates pressure fluctuations in the liquid and results in the generation and growth of air bubbles (Li et al., 2013). Air bubbles oscillate and collapse in the liquid, which leads to physical effects, including extreme shear forces, shock waves, micro-jets, turbulence, and high temperature and pressure within a very short time (Hu et al., 2014; Hu et al., 2016). Such physical effects in the liquid lead to stable emulsion formation (Ashokkumar, 2011; Taha et al., 2020). Figure 3.1 shows a schematic diagram of generating stable O/W emulsion using a probe-type ultrasonic device.

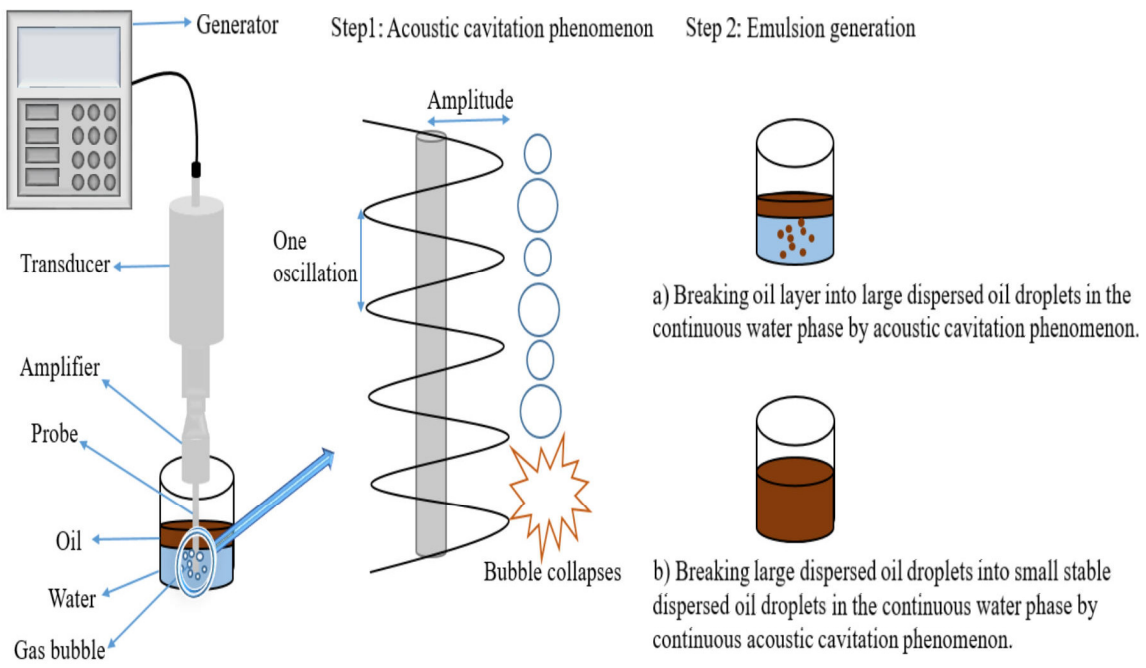

Figure 3.1. Generation of stable O/W emulsion by an ultrasonic probe (Taha et al., 2020).

Ultrasonic processing parameters (e.g., frequency, power, sonication time) and emulsion characteristics (e.g., salinity, pH, temperature) play a vital role in generating a stable emulsion (Cabrera-Trujillo et al., 2016; Daaou and Bendedouch, 2012; Kumar and Mahto, 2017; Liang et al., 2018; Pan et al., 2012; Zhou et al., 2021). However, the significance level of parameters and interactions among parameters on emulsion stability have not been studied yet. The experimental design of ultrasonic processing parameters and emulsion characteristics has not been applied to investigate their significance and interactions with emulsion stability. For future research projects, statistical analysis of these parameters is required to account for the results scientifically (Sousa et al., 2021). This is very important because the generation of stable emulsion requires energy. Empirical correlations of parameters on emulsion stability are required to determine the energy needed for emulsion generation (Sartomo et al., 2020).

In this study, a low-frequency ultrasonic device (20 kHz) was used to evaluate ultrasound-assisted emulsification for the generation of stable crude O/W emulsion without external surfactant and optimization of processing parameters for generating stable emulsion. Effects of ultrasonic processing parameters (power and sonication time), emulsion characteristics (water salinity and pH), and crude oil condition (fresh and weathered) on O/W emulsion stability were investigated. The effect of crude oil condition was considered because crude oil properties change over time in contact with the atmosphere, affecting the emulsion stability. Fresh crude oil is crude oil in which the properties have not changed, while the weathered one is crude oil whose properties have changed in contact with the atmosphere. The interaction of parameters on emulsion stability was investigated, and the required energy to generate a stable emulsion was determined. Statistical analysis of these parameters was also conducted to determine the significance of each parameter on emulsion stability. Emulsion stability was evaluated by various measures, including dispersed droplet size (Aslan and Dogan, 2018) based on microscopic images, emulsion turbidity (Rostami et al., 2018) and creaming index (CI) (Liang et al., 2018).

3.2. Materials and methods

3.2.1. Materials

Cold Lake Blend (CLB) crude oil was provided by Multi-Partner Research Initiative (MPRI) in Canada. CLB crude oil was selected to generate O/W emulsion because it is a major unconventional product produced in Canada that may be exported to overseas markets. Thus, it is important to generate emulsions for environmental studies evaluating various mitigation strategies. The crude oil was placed in a fume hood to obtain weathered oil by reaching a 15% mass loss (15% CLB). Table 3.1 lists the physicochemical properties of the fresh and 15%

weathered CLB crude oil. The weathered CLB was sticky with a high dynamic viscosity of 12682.0 mPa.s (at 25°C). Sodium chloride (NaCl, ≥99.0%), sodium hydroxide (NaOH, ≥97.0%), and Tween 20 emulsifier (≥40%) were purchased from Sigma-Aldrich company. The chemicals were American Chemical Society (ACS) reagent grade and were used without further purification. Ultrapure water used in this research was produced by a water purification system (Milli-Q Advantage A10).

Table 3.1. Physicochemical properties of fresh and 15% weathered CLB crude oil.

Parameter	Value	
	Fresh	15% Weathered
API gravity	20.86	12.76
Dynamic viscosity at 25°C (mPa.s)	237.8	12682.0
Density at 25 °C (g/cm^3)	0.926	0.978
Water content (µg/g)	410	302
Saturates (%wt.)	45.4	46
Aromatics (%wt.)	12.0	4.8
Resins (%wt.)	24.4	28.9
Asphaltenes (%wt.)	20.0	18.2

3.2.2. Emulsification process

The CLB O/W emulsion (fresh and weathered) was prepared by mixing 0.1 g of CLB and 100 mL of ultrapure water in a glass beaker (volume = 250 mL) at room temperature (~ 25°C) using a Q700 Sonicator (Qsonica, 20 kHz, solid titanium probe diameter = 12.7 mm, USA). The Sonicator probe was submerged in the middle of a 100 mL sample. Before starting ultrasonic processing, a Kimwipes tissue (Kimtech Science^{TM}) was wetted with 0.1 mL of Tween 20 (a non-toxic and non-ionic detergent) and then was used to wet the glass beaker and Sonicator probe (Sartomo et al., 2020). The sample was sonicated at a constant frequency of 20 kHz and pulse condition of 20:20 seconds (On/Off). Sodium hydroxide solution (0.1N) was

used to adjust the pH of water, which was measured using a Mettler Toledo FG2 portable pH meter.

3.2.3. Experimental design

Based on previous research, several influential ultrasonic processing parameters and emulsion characteristics on the stability of O/W emulsion were selected (Costa et al., 2018; Hashtjin and Abbasi, 2015; Khorshid et al., 2021). Table 3.2 lists different parameters and considered ranges. These ranges were selected based on ambient environmental conditions, pre-tests, and previous studies (Abbas et al., 2014; Consoli et al., 2017). Experiments were designed using response surface methodology (RSM) (Design Expert, Version 12.0, Stat-Ease Inc.) to investigate the effects of ultrasonic processing parameters (power and sonication time) and emulsion characteristics (water salinity and pH) on emulsion stability. The generated power and energy in the emulsion by ultrasound device at different amplitudes and sonication times were recorded. The central composite design (CCD) of RSM was used, a full factorial design that evaluates parameters at five levels. Experimental data from CCD were analyzed using Equation (3.1) (Azadi et al., 2021; Hassanshahi and Karimi-Jashni, 2018).

$$Y = \beta_0 + \sum_{i=1}^{k} \beta_i X_i + \sum_{i=1}^{k} \beta_{ii} X_i^2 + \sum_{i<j} \sum_{j} \beta_{ij} X_i X_j \quad (3.1)$$

Where Y is the predicted response, β_0 is a constant, β_i represents the linear effect of X_i variable, β_{ii} represents the effect of the second-order variable X_i, and β_{ij} represents the effect of the linear interaction between parameters X_i and X_j. Analysis of variance (ANOVA) was performed to determine the significance of the effects of parameters and the developed model.

The effect of crude oil conditions (fresh and weathered) was also investigated on the stability of O/W emulsion at the optimum condition of ultrasonic processing parameters and emulsion characteristics based on RSM results.

Table 3.2. Levels of independent parameters in the emulsification process by ultrasonic

Independent parameter	Unit	Coded levels				
		–α	–1	0	1	α
Amplitude	%	52	64	76	88	100
Sonication time	mins	9	12	15	18	21
Water salinity	g/L	0	10	20	30	40
pH of water	–	7	8	9	10	11

3.2.4. Emulsion stability

Emulsion stability was evaluated by measuring the CI of emulsion and emulsion turbidity and taking microscopic images after 24 hours for quantification of oil droplets' size. These methods are described below.

To measure CI of emulsion, 10 mL of CLB O/W emulsion (fresh and weathered) was transferred into 10 mL of the graduated cylinder and sealed with parafilm laboratory film and stored at room temperature (~ 25°C) for 24 hours. Emulsion stability was characterized by calculating CI using Equation (3.2) (Liang et al., 2018).

$$CI = ({}^{hs}/_{he}) \times 100 \quad (3.2)$$

Where h_s is the height of the stable emulsion layer and h_e is the total initial height of the emulsion. The higher CI, the higher the emulsion stability.

Emulsion turbidity is a function of dispersed oil concentration, oil droplets size, and distribution. Small droplet size and narrow droplet size distribution increase emulsion stability,

which is directly proportional to turbidity (Aslan and Dogan, 2018; Linke and Drusch, 2016; Modarres-Gheisari et al., 2019). In this study, emulsion stability was determined by measuring emulsion turbidity immediately after emulsion preparation (T_0) and after 24 hours (T_{24h}) at room temperature (~ 25°C) by UV-Vis Spectrophotometers 8100 (Orion^{TM} AquaMate UV-Vis spectrophotometer, Perkin Elmer). The aliquot of CLB O/W emulsion was diluted at a ratio of 1:50 with ultrapure water. The sample was taken at a 3.5 mL quartz Suprasil cell with a 1.0 cm path length and polytetrafluoroethylene lid. Absorbance was measured at 220 to 1000 nm wavelengths to determine the maximum absorbance wavelength (λ_{max}). Ultrapure water was used as a blank control. The CLB O/W emulsion turbidity (τ) was calculated using Equation (3.3) at λ_{max} (Reddy and Fogler, 1981; Shinoda and Uchimura, 2018).

$$\tau = {\ln\left(\frac{I_0}{I}\right)}\Big/{l} \tag{3.3}$$

Where I_0, I, and l are the intensity of incident light, the intensity of transmitted light, and scattering path length (cm), respectively.

The morphology of CLB O/W emulsion at T_0 and T_{24h} was observed, and the images were captured using a compound microscope (Fisher Scientific) with a 200X objective magnification. The images were analyzed by SeBaView software (version 4.7) to determine the average size of dispersed oil droplets.

3.3. Results and discussions

3.3.1. Maximum absorbance wavelength at UV-Vis spectrophotometry

UV-Vis absorbance of diluted CLB O/W emulsion (1:50 dilution ratio) was measured from 220 nm to 1000 nm to obtain the maximum absorbance wavelength (λ_{max}). As shown in Figure

3.2, the maximum absorbance was at the wavelength of 235 nm, and this wavelength was considered for emulsion turbidity calculations.

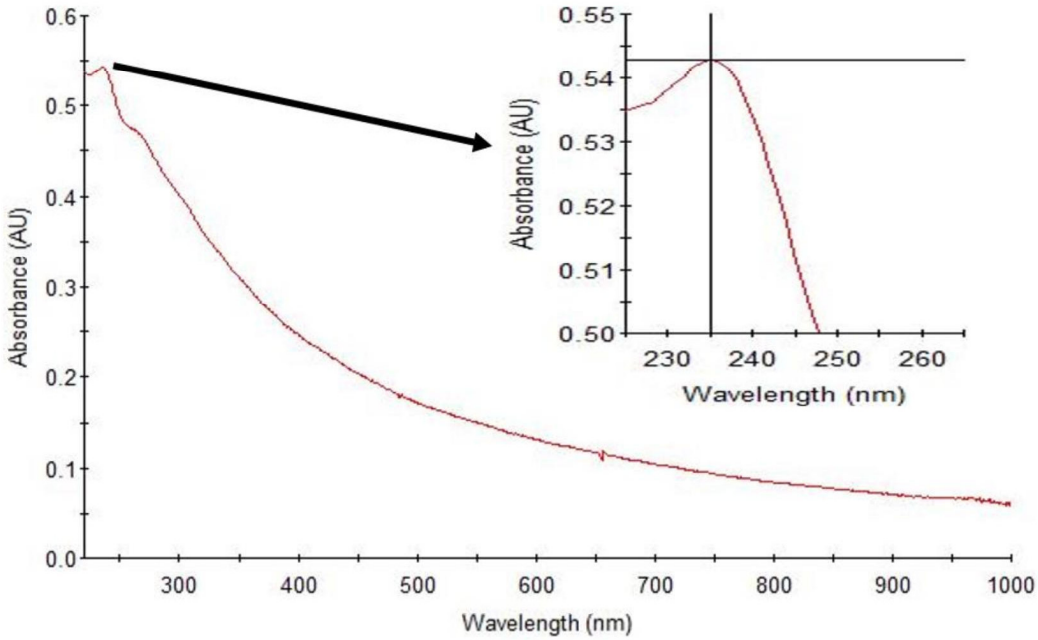

Figure 3.2. UV-Vis spectra of diluted CLB O/W emulsion (1:50 dilution ratio) at room temperature (~ 25 °C).

3.3.2. Crude O/W emulsification process and the regression model

Table 3.3 shows the designed experiments for the weathered CLB O/W emulsification process and the obtained results. The optimum condition of the emulsification process was determined by RSM software based on the experimental results and the developed quadratic model.

Table 3.3. Central composite design for emulsification process and the obtained results.

Run	Independent parameters				Results					
	Amplitude (%)	Sonication time (mins)	Water salinity (g/L)	pH of water	Temperature (°C)	Power (W)	Energy (J)	Emulsion turbidity at T_0 (cm^{-1})	Emulsion turbidity at T_{24h} (cm^{-1})	Emulsion turbidity difference (%)
1	52	15	20	9	58	58–62	47,022	5.32	4.77	10.49
2	64	12	30	8	62	68–75	46,632	9.64	4.87	49.48
3	64	12	30	10	60	68–75	45,995	19.73	9.29	52.9
4	64	12	10	8	61	68–75	46,071	13.31	11.48	13.75
5	64	12	10	10	62	68–75	45,832	13.56	10.58	21.97
6	64	18	10	8	63	68–75	67,220	12.01	11.00	8.4
7	64	18	10	10	62	68–75	68,172	18.34	15.69	14.44
8	64	18	30	8	63	68–75	68,609	21.80	16.76	23.08
9	64	18	30	10	64	68–75	67,966	23.89	17.53	26.63
10	76	9	20	9	59	80–87	39,920	9.88	5.97	39.54
11	76	15	0	9	66	80–87	64,914	13.23	11.32	14.44
12	76	15	40	9	63	80–87	64,978	24.36	22.62	7.67
13	76	15	20	9	66	80–87	64,542	15.36	15.25	0.69
14	76	15	20	9	65	80–87	64,967	27.79	27.24	1.99
15	76	15	20	9	66	80–87	64,914	17.12	16.91	1.23
16	76	15	20	9	66	80–87	65,029	19.75	19.41	1.75
17	76	15	20	9	67	80–87	65,492	24.71	23.90	3.4
18	76	15	20	7	66	80–87	63,998	16.94	14.01	17.29
19	76	15	20	11	65	80–87	65,353	18.70	16.78	10.28
20	76	21	20	9	66	80–87	87,643	24.56	20.38	17.01
21	88	12	10	8	67	90–96	58,317	24.00	21.48	10.50
22	88	12	10	10	68	90–96	58,826	27.08	21.26	21.48

Table 3.3. (Continued)

Run	Independent parameters				Results					
	Amplitude (%)	Sonication time (mins)	Water salinity (g/L)	pH of water	Temperature (°C)	Power (W)	Energy (J)	Emulsion turbidity at T_0 (cm^{-1})	Emulsion turbidity at T_{24h} (cm^{-1})	Emulsion turbidity difference (%)
23	88	12	30	8	68	90–96	59,275	33.39	27.52	17.60
24	88	12	30	10	66	90–96	59,309	26.38	15.06	31.20
25	88	18	10	8	68	90–96	86,834	24.60	19.80	19.51
26	88	18	10	10	69	90–96	87,670	28.03	21.88	21.93
27	88	18	30	8	70	90–96	87,712	20.78	17.83	14.16
28	88	18	30	10	67	90–96	87,328	24.56	16.89	43
29	100	15	20	9	70	106–112	82,218	18.43	18.38	0.24

The following quadratic model was established by RSM based on the obtained results to determine the weathered CLB O/W emulsion turbidity difference:

$$Y = +1052.53 - 4.94X_1 - 35.05X_2 - 0.78X_3 - 136.49X_4 + 0.15X_1X_2 - 0.30X_1X_3 + 0.19X_1X_4 - 0.79X_2X_3 + 0.15X_2X_4 + 1.53X_3X_4 + 0.0091X_1^2 + 0.75X_2^2 + 7.57X_3^2 + 6.75X_4^2 \quad (3.4)$$

Where Y, X_1, X_2, X_3, X_4 represent weathered CLB O/W emulsion turbidity difference (cm^{-1}), amplitude (%), sonication time (mins), water salinity (g/L NaCl), and pH, respectively. X_1, X_2, X_3, and X_4 are in the range of [52–100%], [9–21 mins], [0–40 g/L NaCl], and [7–11], respectively.

According to the ANOVA analysis shown in Table A1 in Appendix A, the model F-value (16.98) and p-value (0.0001) indicated that the model was significant and could describe the weathered CLB O/W emulsion turbidity difference well. Based on ANOVA analysis (Table A1), X_1, X_2, X_3, X_4, X_1X_2, X_1X_3, X_2^2, X_3^2, X_4^2 were significant parameters in the established model to predict weathered CLB O/W emulsion turbidity difference. The R^2 value of 0.94 (Table A2 in Appendix A) proved that the quadratic model accurately predicted the experimental data.

3.3.3. Effect of different parameters on crude O/W emulsion stability

3.3.3.1. Power

The amplitude of the ultrasonic device for emulsion generation directly affects the temperature, power, and energy produced in the solution (Taha et al., 2020). Table 3.3 lists the effect of different amplitudes (52% to 100%) on the generated temperature (58°C to 70°C), power (58 W to 112 W), and energy (39,920 J to 87,715 J) by the ultrasonic device in the

weathered CLB O/W emulsion. Increasing power from 58–62 W to 80–87 W led to the reduction of weathered CLB O/W emulsion turbidity, a difference from 10.49% to the average of 1.8%, respectively (e.g., increased O/W emulsion stability). The reason is that increasing the power increased the generated energy, which resulted in the high generation of bubbles in the solution. This caused high bubbles collision incidents followed by the generation of high shear forces and increment of temperature (from 58°C to 66°C) in the solution that facilitated oil disruption and formed stable O/W emulsion. However, increasing power from 80–87 W to 106–112 W had an insignificant effect on the weathered CLB O/W emulsion turbidity difference (reduced from 1.8% to 0.24%). As explained, increasing temperature due to the generation of high energy in the emulsion facilitated the dissolution of crude oil in the water. Studying emulsion generation at lower temperatures and investigating the emulsion stability is suggested for future studies. Figure 3.3a shows the CI of weathered CLB O/W emulsion generated at different power (68–75 W and 90–96 W) and constant sonication time of 18 mins, water salinity of 30 g/L NaCl and pH of 10. CI of weathered CLB O/W emulsion generated by the power of 90–96 W was lower than that one generated by the power of 68–75 W. This proved that dispersed crude oil droplets in weathered CLB O/W emulsion generated by the power of 90–96 W were less stable than those generated by the power of 68–75 W.

The average dispersed oil droplet size of weathered CLB O/W emulsion at T_0 and T_{24h} at different ultrasonic processing parameters and emulsion characteristics were determined from the analysis of microscopic images. As listed in Table 3.4, by increasing the power above 58–62 W, the average dispersed oil droplets size was reduced to a narrow size range (<10 μm). This reduced the chance of crude oil droplets coalescence and creaming process; hence the emulsion stability increased significantly.

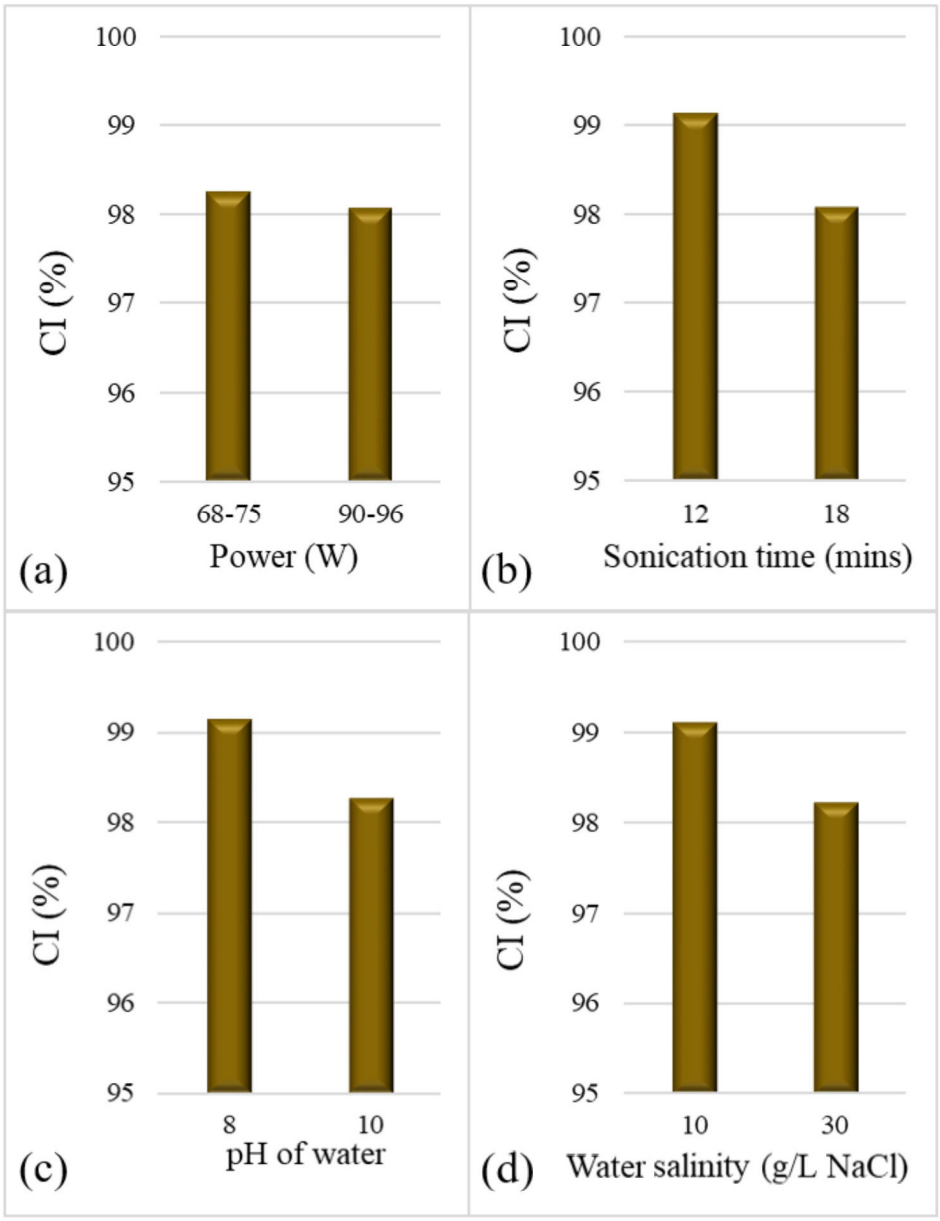

Figure 3.3. Effect of different parameters on CI of weathered CLB O/W emulsion after 24 hours settling a) power (W) at sonication time of 18 mins, water salinity of 30 g/L NaCl and pH of 10, b) sonication time (mins) at the power of 90–96 W, water salinity of 30 g/L NaCl and pH of 10, c) pH of water at the power of 68–75 W, sonication time of 12 mins and water salinity of 30 g/L NaCl, d) water salinity (g/L NaCl) at the power of 90–96 W, sonication time of 18 mins and pH of 8.

Table 3.4. The average dispersed oil droplets size of weathered CLB O/W emulsion at T_0 and T_{24h} based on the microscopic images.

Parameters	Values	Average dispersed droplet size at T_0 (µm)	Average dispersed droplet size at T_{24h} (µm)	Description
Power (W)	58–62	13.40	9.11	Sonication time of 15 mins, pH of 9, and water salinity of 20 g/L NaCl
	80–87	5.91	4.08	
	106–112	6.48	6.31	
Sonication time (mins)	9	13.13	8.81	Power of 80–87 W, pH of 9, and water salinity of 20 g/L NaCl
	15	5.58	4.56	
	21	9.83	5.69	
pH of water	7	13.43	5.81	Power of 80–87 W, sonication time of 15 mins, and water salinity of 20 g/L NaCl
	9	5.96	5.38	
	11	8.40	4.93	
Water salinity (g/L NaCl)	0	10.96	10.11	Power of 80–87 W, sonication time of 15 mins, and pH of 9
	20	6.28	4.46	
	40	11.01	8.80	

3.3.3.2. Sonication time

Increasing sonication time raises the level of generated energy and temperature in a solution, thus enhancing the disruption and dissolution of oil droplets in water (Shahavi et al., 2019). As listed in Table 3.3, increasing sonication time from 9 to 15 mins increased the generated energy from 39,920 to 64,542 J and temperature from 59 to 66°C, respectively. This facilitated the disruption of sticky weathered CLB oil in water and the formation of a stable emulsion with limited change in emulsion turbidity (approximately 1.8%). However, increasing sonication time from 15 to 21 mins led to over-processing, increasing the emulsion turbidity difference from 1.8% to 17%. This may be attributed to the increase in energy from a longer sonication time, which led to the collision of dispersed fine crude oil droplets and the formation of bigger ones. Figure 3.3b shows the effect of sonication time (12 and 18 mins) on the CI of weathered CLB O/W emulsion generated at the power of 90–96 W, water salinity of 30 g/L NaCl, and pH of 10. As shown, a lower CI (less stable crude O/W emulsion) was obtained with a longer sonication time (18 mins).

The above results were visually observed and verified by the analysis of microscopic images of the weathered CLB O/W emulsion (Figure 3.4). By comparing Figures 3.4a with 3.4b, it is evident that 9 mins of sonication were insufficient in reducing the average dispersed oil droplets size to less than 10 μm (13.13 μm) compared to 15 mins of sonication time (5.58 μm). Figure 3.4c shows the coalescence of tiny crude oil droplets (indicated by blue arrows) and the formation of bigger ones as a consequence of extending sonication time.

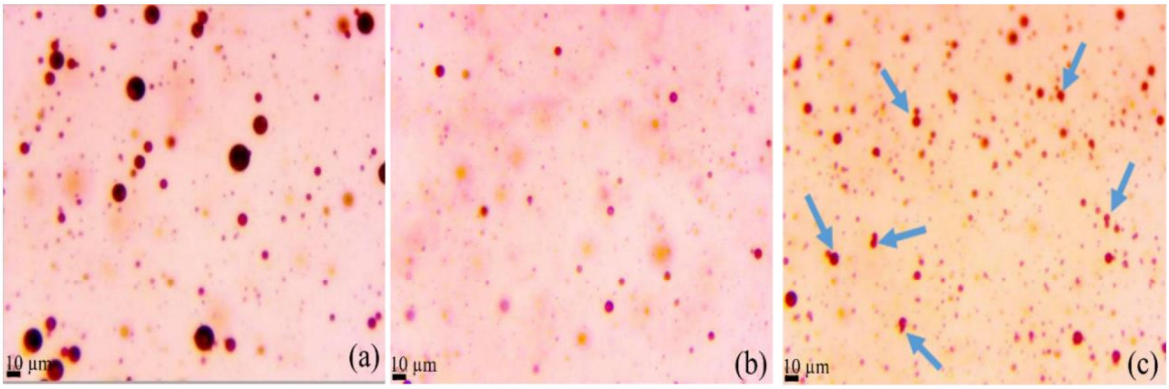

Figure 3.4. Microscopic images of weathered CLB O/W emulsion at T_0 at a constant power of 80–87 W, pH of 9, water salinity of 20 g/L, and different sonication times a) 9 mins, b) 15 mins, c) 21 mins.

3.3.3.3. pH of water

The stability of crude O/W emulsion generated by natural emulsifying agents of crude oils (e.g., asphaltenes) largely depends on the water phase's pH (Hutin et al., 2016). As listed in Table 3.3, by changing the water phase's pH from neutral (7) to moderate basic (9), the emulsion turbidity difference reduced from 17.27% to an average of 1.8%. At the basic pH (e.g., 9), the presence of hydroxide ions (OH^-) in the water phase brings about the ionization of polar groups of natural emulsifying agents of crude oil (e.g., asphaltenes). This leads to an increment of electrostatic repulsive interaction between dispersed oil droplets and then the prevention of their coalescence. However, increasing the pH of the water phase to more than 9 (e.g., 10 and 11) increased the emulsion turbidity difference and reduced emulsion stability. One of the possible reasons is that asphaltenes compounds of crude oils (the main compound in the generation of stable crude O/W emulsion) may form a weak film around dispersed crude oil droplets within the water phase under high basic pH conditions, which reduces crude O/W

emulsion stability (Abdulredha et al., 2020). Monitoring weathered CLB O/W emulsion and calculation of CI also indicated that when the pH of the water phase increased from 8 to 10, a lower CI was obtained (Figure 3.3c). As shown in Table 3.4, at pH 7 and 11, the average dispersed oil droplets size was higher than when the pH was 9, reducing the emulsion stability.

3.3.3.4. Water salinity

Salinity affects O/W emulsion stability. The results indicated that the presence of salt in the water phase (20 g/L of NaCl) significantly enhanced the emulsion stability (0.69% emulsion turbidity difference) in comparison to the control (0 g/L of NaCl), which was reflected by a 14.44% emulsion turbidity difference. Salinity in the water phase may reduce the interfacial tension between the oil and water phases. This facilitates the reduction of oil droplets' size in the water phase and generates stable emulsion (Kumar and Mahto, 2017). However, by increasing water salinity above 20 g/L NaCl (comparing runs #2, 4:#5, 3; #6, 8; #7, 9; #12, 13; #21, 23, #22, 24, and #26, 28), the emulsion turbidity difference increased, and the emulsion stability decreased. In the case of crude O/W emulsion, natural emulsifying agents of crude oil have more affinity to the water phase (i.e., hydrophilic phase). By decreasing the hydrophilicity of emulsion (increasing water salinity), dispersed crude oil droplets have a higher probability of colliding and coalescing, decreasing emulsion stability (Fortuny et al., 2007). Electrostatic interactions between ionic compounds of weathered CLB oil (e.g., asphaltenes) and NaCl molecules may result in the formation of bigger crude oil droplets and enhancement of the creaming process. Figure 3.3d shows that the CI of weathered CLB O/W emulsion is reduced by increasing water salinity from 10 g/L to 30 g/L NaCl due to electrostatic interactions among ionic molecules in the emulsion.

The effect of water salinity on the stability of weathered CLB O/W emulsion was also justified by the average dispersed oil droplets in the emulsion (Table 3.4). Smaller oil droplets size (6.28 μm) was generated when the water salinity was 20 g/L NaCl compared to when there was no salt in the water (10.96 μm). This illustrates the importance of the presence of salt in the water phase in the generation of stable O/W emulsion with smaller dispersed droplets size.

3.3.3.5. Interaction of parameters

The effect of the interaction of different ultrasonic processing parameters (power and sonication time) and emulsion characteristics (water salinity and pH) on weathered CLB O/W emulsion turbidity differences were evaluated. As shown in Figure 3.5a, increasing power and sonication time simultaneously led to the generation of high input energy in the emulsion and the generation of less stable O/W emulsion due to the coalescence of dispersed oil droplets. At low power (68-75 W) and high sonication time (18 min) (run #6), the emulsion turbidity difference was 8.4. At high power (90-96 W) and low sonication time (12 min) (run #21), the emulsion turbidity difference was 10.5. Similar relations were achieved by comparing runs #7 with #22 and #9 with #24. The results showed that applying lower power at a higher sonication time brings higher emulsion stability than higher power at a low sonication time. Emulsion characteristics (water salinity and pH) also significantly affected the performance of power in the generation of stable weathered CLB O/W emulsion. At higher water salinity (30 g/L NaCl), high power of 90–96 W (amplitude 88%) was required to reduce the emulsion turbidity difference, while at higher pH (10), the emulsion was less stable where this power had no notable effect on emulsion turbidity difference (Figures 3.5b, and 3.5c). Figures 3.5d and 3.5e show the relationship between sonication time with pH and salinity of water phase on weathered CLB O/W emulsion stability, respectively. Based on Figure 3.5d, at high pH of

water, dispersed crude oil droplets were generated weakly, and increasing sonication time had less effect on the generation of stable weathered CLB O/W emulsion. Figure 3.5e shows that over-processing sonication time (> 16 mins) reduced the emulsion stability at both 10 g/L and 30 g/L NaCl water salinity. Extending sonication time led ionic molecules in the water phase to attach and enhance the creaming process rather than dispersing them. Figure 3.5f shows the importance of pH and salinity of the water phase simultaneously on weathered CLB O/W emulsion stability. High water salinity (30 g/L NaCl) and high basic pH of water (10) significantly affected weathered CLB O/W emulsion stability. This effect was extreme at higher power (e.g., >80 W). The reason was that the created turbulence by the generated energy in the emulsion unites in strong electrostatic interactions among ionic molecules and facilitates the coalescence of weak dispersed crude oil droplets.

By considering the interaction of different parameters on emulsion stability, it was determined that the required energy to generate a stable emulsion was within 60−70 kJ (Figure 3.6). Experimental results showed that generating energy lower and higher than this range in the emulsion reduced the stability. Lower energy was insufficient to disrupt crude oil in the water phase, while higher energy led to the coalescence of dispersed crude oil droplets and the formation of bigger ones.

The optimum condition for different independent parameters was determined by the numerical optimization method of RSM based on the obtained results and the developed quadratic model. This method aimed to minimize the emulsion turbidity difference by considering the practical in-range value for each independent parameter. The optimum range suggested by RSM for power (amplitude), sonication time, water salinity, and pH were 76–80 W (70%), 16 mins, 15 g/L NaCl, and 8.3, respectively. This optimum condition was considered

for investigating the effect of crude oil conditions (fresh and weathered) on crude O/W emulsion stability.

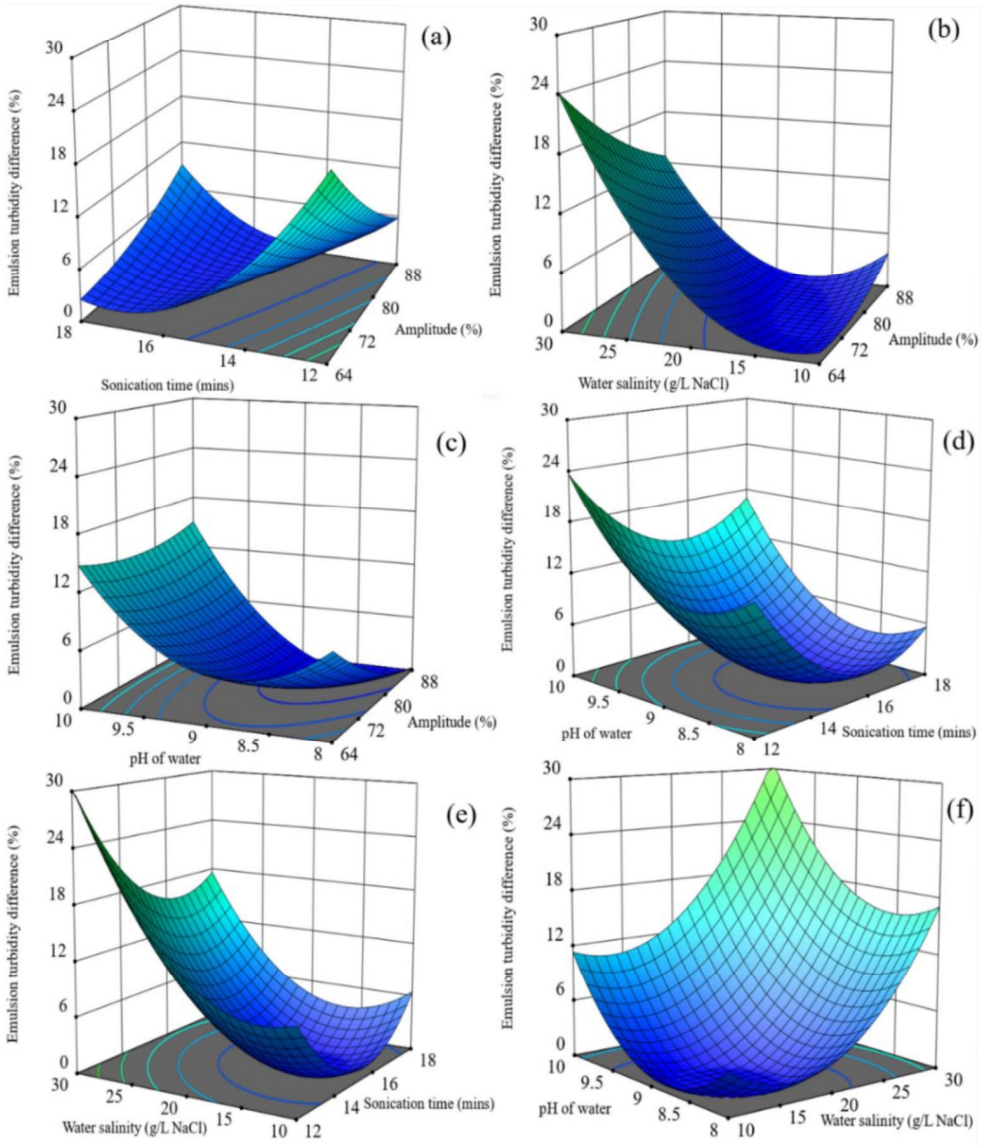

Figure 3.5. Effect of interaction of independent parameters on weathered CLB O/W emulsion turbidity difference a) power (amplitude)-sonication time at water salinity of 20 g/L NaCl, pH of 9, b) power (amplitude)-water salinity at sonication time of 15 mins and pH of 9, c) power (amplitude)-pH of water at sonication time of 15 mins and water salinity of 20 g/L NaCl, d) sonication time-pH of water at the power of 80–87 W and water salinity of 20 g/L NaCl, e) sonication time-water salinity at the power of 80–87 W and pH of 9, f) water salinity-pH of water at the power of 80–87 W, sonication time of 15 mins.

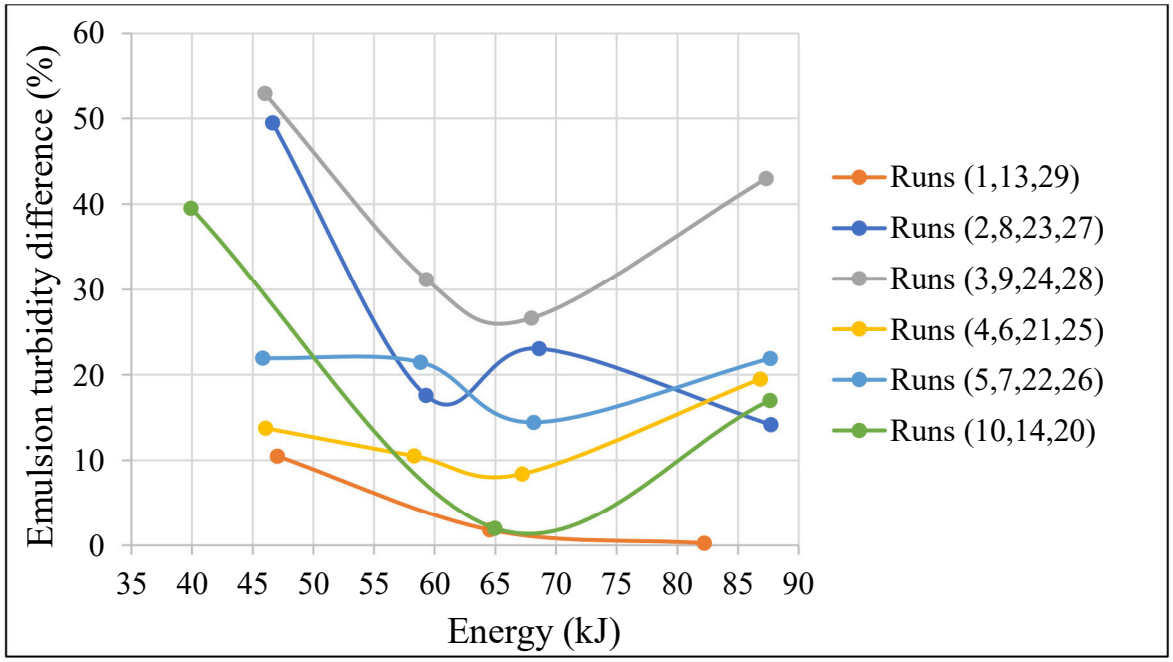

Figure 3.6. Effect of generated energy in the emulsion at different experimental conditions on emulsion turbidity difference.

3.3.3.6. CLB crude oil condition (fresh and weathered)

To determine the effect of CLB crude oil condition (fresh and weathered) on crude O/W emulsion stability, experiments were conducted at the optimum conditions suggested by RSM software. About 0.1 g of fresh or weathered CLB oil was sonicated in 100 mL of water (salinity of 15 g/L NaCl and pH of 8.3) at the power of 76–80 W and sonication time of 16 mins. The generated fresh CLB O/W emulsion was more stable (emulsion turbidity difference 1.5%) than the weathered CLB O/W emulsion (emulsion turbidity difference 2.68%). Lower CI was observed for the weathered CLB O/W emulsion than the fresh one (Figure 3.7). Weathered CLB oil was more viscous and stickier than fresh CLB crude oil, which hampered its dissolution in the water phase. The generated energy in the solution at the first 9 mins

sonication time was used to disrupt weathered CLB oil in the water and then break them into small dispersed crude oil droplets. However, fresh CLB crude oil was disrupted in the water after 4 mins sonication time. Therefore, the remaining energy was used to break dispersed crude oil droplets into smaller sizes and distribute them homogeneously. Another possible reason is that the amount of asphaltenes compound, the main compound of crude oil in the generation of the stable emulsion, was lower in the weathered CLB crude oil than in a fresh one, Table 3.1. This is also clear based on the oil droplet size distribution histogram of fresh and weathered CLB oil at T_{24} (Figure 3.8). Based on the oil droplet size distribution histogram, the average dispersed oil droplet size at T_{24} for fresh and weathered O/W emulsion were 3.74 µm and 5.71 µm, respectively.

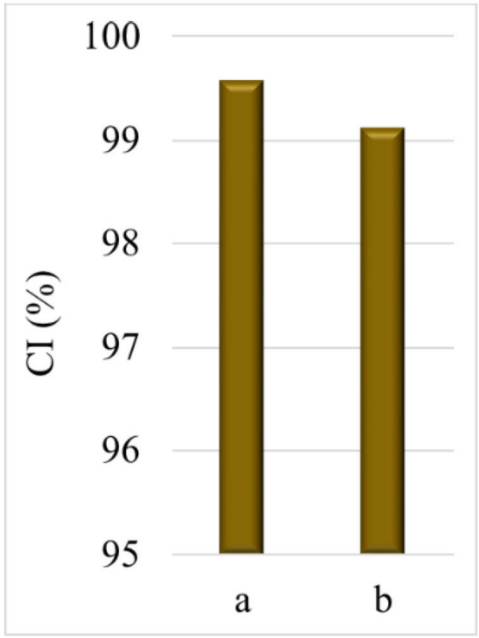

Figure 3.7. Effect of fresh and weathered CLB O/W emulsion generated at a constant power of 76–80 W, sonication time of 16 mins, pH of 8.3, and water salinity of 15 g/L NaCl on CI after 24 hours settling a) fresh CLB, b) weathered CLB.

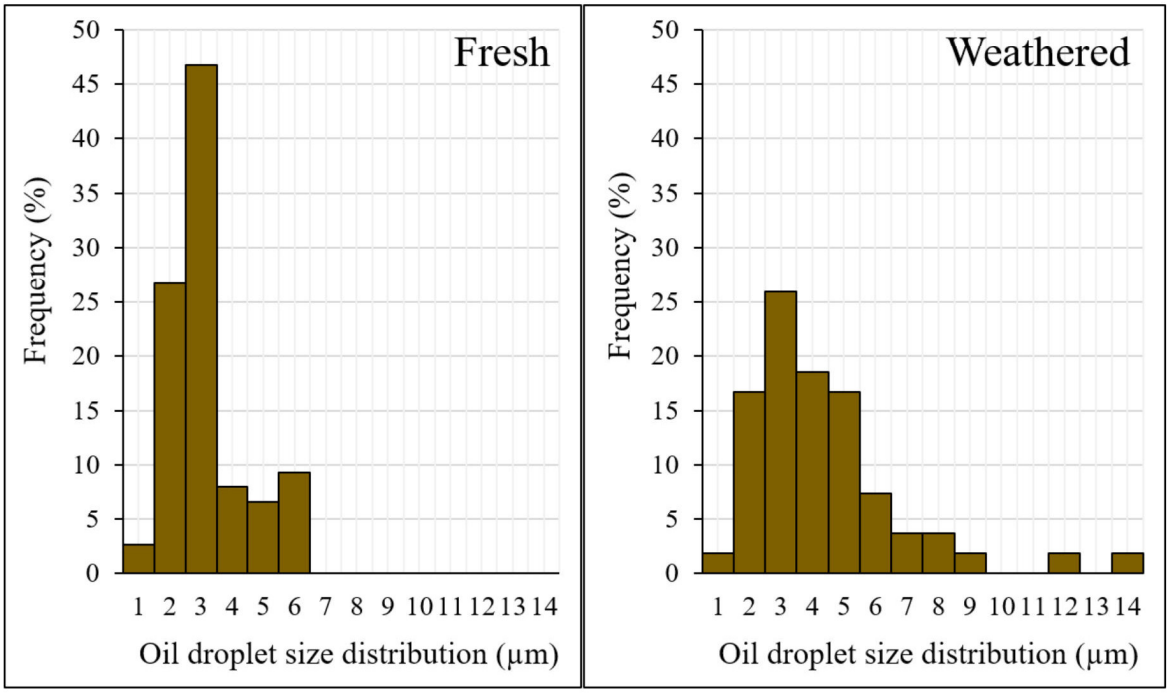

Figure 3.8. Oil droplet size distribution of CLB crude O/W emulsion at T_{24h} at a constant power of 76–80 W, sonication time of 16 mins, pH of 8.3, and water salinity of 15 g/L NaCl.

3.4. Summary

This study investigated the effect of ultrasonic processing parameters (power and sonication time) and emulsion characteristics (water salinity and pH) and their interactions on crude O/W emulsion stability. The optimal condition was determined to be a power level of 76–80 W, sonication time of 16 mins, water salinity of 15 g/L NaCl, and pH of 8.3. Increasing power beyond the optimal value and over-processing conditions (> 16 mins) had insignificant and adverse effects on crude O/W emulsion stability. The presence of salt in the water phase (NaCl salt) improved crude O/W emulsion stability while increasing salinity concentration by more than 20 g/L reduced emulsion stability significantly due to electrostatic interaction between molecules. Low to moderate basic pH of the water phase (8 and 9) led to the generation of

stable crude O/W emulsion compared to neutral pH (7). However, emulsion stability was noticeably reduced at high pH levels (10 and 11) due to a weak film forming around the dispersed crude oil droplets in the crude O/W emulsion.

The interaction of parameters showed that increasing power and sonication time simultaneously reduced crude O/W emulsion stability. At high pH (10 and 11) and salinity levels (> 20 g/L NaCl), emulsion stability was reduced notably; under these conditions increasing power and sonication time did not generate a stable crude O/W emulsion. Based on the interaction of parameters, the required energy to generate a stable emulsion was within 60−70 kJ. The effect of CLB crude oil condition (fresh and weathered) was evaluated at the optimum condition of parameters on crude O/W emulsion stability. The results indicated that the fresh CLB crude O/W emulsion was more stable. Fresh CLB crude oil was less viscous and sticky than the weathered CLB crude oil, which facilitated its disruption and dissolution in the water phase; hence smaller oil droplets (4.41 μm) were distributed homogeneously in the water phase that increased crude O/W emulsion stability. Fresh crude oil has a higher asphaltenes compound than the weathered one, which is the main compound in generating a stable emulsion. This research demonstrated a practical approach to generating stable crude O/W emulsions without the addition of external surfactants for different scientific applications and environmental practices.

Chapter 4

INVESTIGATION OF DIOCTYL SODIUM SULFOSUCCINATE IN DEMULSIFYING CRUDE OIL IN WATER EMULSIONS[1]

Abstract

This research investigated the performance of dioctyl sodium sulfosuccinate (DSS), a double-chain anionic surfactant, in breaking crude oil-in-water emulsions. The response surface methodology was used to consider the effect of the DSS concentration, oil concentration, and shaking time on demulsification efficiency and obtain optimum demulsification conditions. Further single-factor experiments were conducted to investigate the effects of salinity, crude oil conditions (fresh and weathered), and gravity separation settling time. The results showed that DSS efficiently demulsified stable emulsions under different oil concentrations (500−3000 mg/L) within 15 min shaking time. Increasing the DSS concentration to 900 mg/L (critical micelle concentration) increased the demulsification efficiency to 99%. DSS not only improved the demulsification efficiency but also did not impede the demulsifier interfacial adsorption at the oil−water interface due to the presence of the double-chain structure. The low molecular weight enables the homogeneous distribution of DSS molecules in the emulsion, leading to a high demulsification efficiency within 15 min. Analysis of variance results indicated the importance of considering the interaction of oil concentration and shaking time in demulsification. DSS could reduce the total extractable petroleum hydrocarbons in the separated water to <10 mg/L without gravity separation and could achieve promising demulsification performance at high salinity (36 g/L) and various concentrations of fresh and weathered oil. The demulsification mechanism was explained by

[1] This work has been published as Hassanshahi, N., Hu, G., Li, J. (2022). Investigation of dioctyl sodium sulfosuccinate in demulsifying crude oil in water emulsions. *ACS Omega, 7*(37), 33397–33407. DOI: https://doi.org/10.1021/acsomega.2c04022.

analyzing the microscopic images and the transmittance of the emulsion. DSS could be an efficient double-chain anionic surfactant in demulsifying stable oil-in-water emulsions.

Graphical Abstract

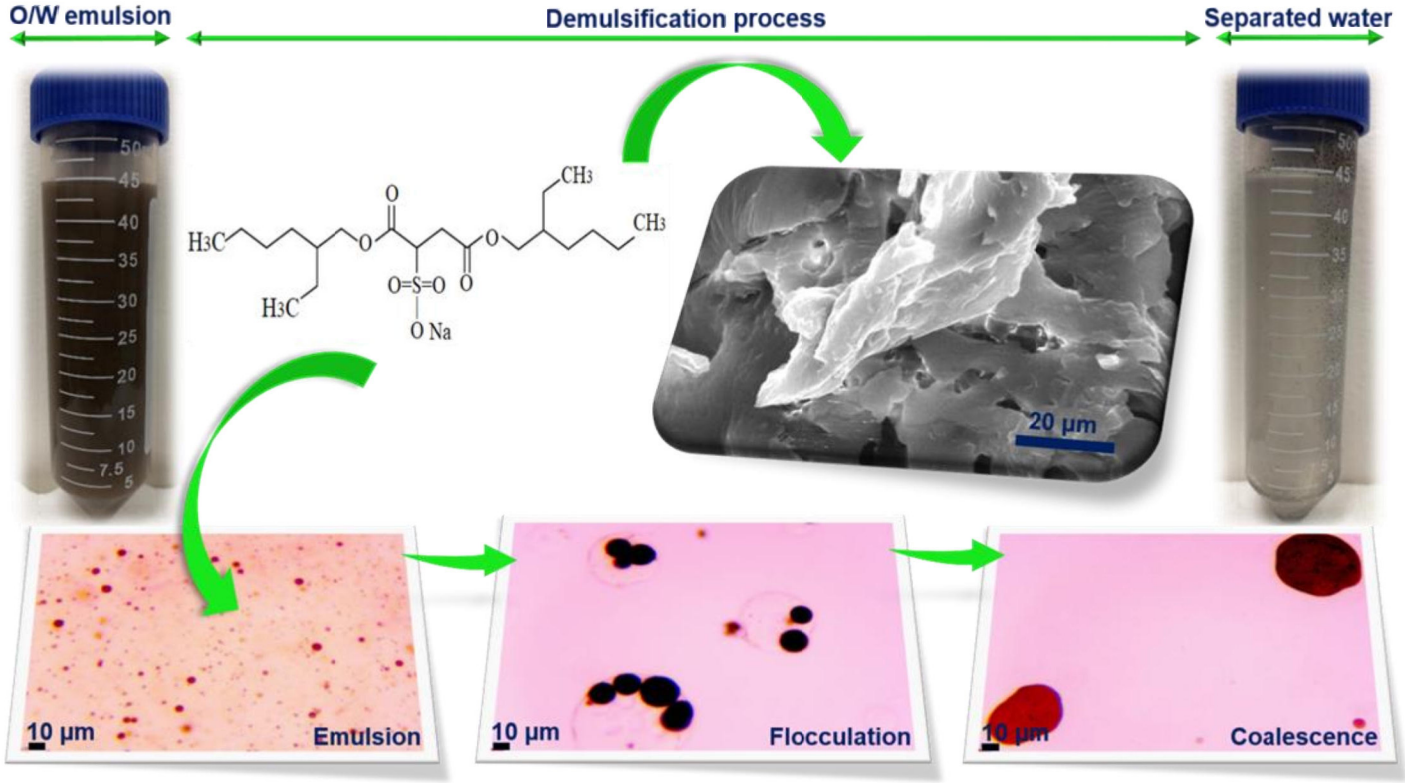

4.1. Introduction

A large volume of oily wastewater can be generated from various industrial processes, including oil exploration, enhanced oil recovery, pipeline transportation, and marine oil spill response operation (Abdulredha et al., 2020; Al-Ghouti et al., 2019; Liu et al., 2019; Varjani et al., 2020). In general, oily wastewater contains tiny oil droplets with sizes varying from about 0.5 μm in diameter to greater than 200 μm, which are categorized as dispersed oil (>10 μm) and emulsified oil (0.1−10 μm) (Stewart, 2009). Natural emulsifying agents in crude oil (e.g., resins and asphaltenes) stabilize emulsified oil droplets and form oil-in-water (O/W) emulsions by creating a rigid film around oil droplets (Goodarzi and Zendehboudi, 2019; Zembyla et al., 2020). The amount of natural emulsifying agents varies with the crude oil type (e.g., light and heavy) and conditions (fresh and weathered) that changes over time after being released into the marine environment. The stability of O/W emulsions mainly depends on the amount of resins and asphaltenes in crude oils and their ratios. A lower resin/asphaltene (R/A) ratio leads to higher emulsion stability (Dudek et al., 2019; Yudina et al., 2021). Oily wastewater contains toxic materials (e.g., benzene, toluene, and polycyclic aromatic compounds), which can pose severe risks to the aquatic environment if discharged without proper treatment (Adetunji and Olaniran, 2021; Al-Ghouti et al., 2019). Strict regulations are being implemented in North America to limit the discharge of oil and grease in oily wastewater to a monthly average of 29 mg/L and a daily maximum of 42 mg/L (Shokri and Fard, 2022).

Different oily wastewater treatment processes have been used, including gravity separation, biological treatment, plate coalescence, gas flotation, and filtration. Their efficiency depends on the oil droplet size distribution in wastewater (Ismail et al., 2020; Mohayeji et al., 2016; Piccioli et al., 2020). As the oil droplet size decreases (<10 μm), the

emulsion stability increases and reduces the efficiency of the treatment processes (Dickhout et al., 2017; Lu et al., 2021; Stewart, 2009). Long settling time, large space requirement, poor efficiency, and fouling are some of the main limitations in demulsifying stable O/W emulsions (Han et al., 2019; Lusinier et al., 2019; Piccioli et al., 2020; Tawalbeh et al., 2018). An efficient treatment process is required to break stable O/W emulsions and enhance oil−water separation to meet environmental regulations.

Chemical demulsification has attracted research attention to demulsify stable emulsions because it is a rapid, cost-effective, and easy-to-operate process (Yang et al., 2020). Chemical demulsifiers (e.g., ethylcellulose and block polyethers) are surface-active agents (i.e., surfactants) that adsorb at the oil−water interface, reducing the interfacial tension between oil and water phases and break rigid films around oil droplets (Peng et al., 2012; Wang et al., 2021). This process can be combined with gravity separation to demulsify stable emulsions effectively and speed up oil−water separation (Hazrati et al., 2018). Parameters that affect the chemical demulsification process include the type and concentration of the demulsifier, the type and concentration of oil, temperature, shaking time, settling time, and salinity (Hassanshahi et al., 2020; Ma et al., 2022; Yonguep et al., 2022).

Different demulsifiers (nonionic and ionic) have been applied in demulsification; however, they have some limitations due to the complexity of the emulsion and industrial restrictions. Nonionic demulsifiers are mainly based on nonionic polyether and are not very effective at demulsifying O/W emulsion containing tiny emulsified oil droplets (≤2 μm) (Zhang et al., 2016; Zhang et al., 2018a). They are also ineffective at demulsifying heavy crude oil emulsions, where only a 51.95% demulsification efficiency was achieved at high temperatures (e.g., 80 °C) (Adilbekova et al., 2015). Ionic demulsifiers contain a positive or negative charge

known as cationic or anionic demulsifiers, respectively (Sousa et al., 2021). Cationic demulsifiers are mainly quaternary ammonium salts that can reduce electrostatic repulsion among oil droplets, neutralize the negative charge on the surface of oil droplets, and thus enhance their coalescence (Yuan et al., 2022). Yonguep et al. investigated the effect of two cationic demulsifiers (cetyl-trimethylammonium bromide and trimethyl-tetradecylammonium chloride) on the demulsification of O/W emulsions, and the results showed that more than 80% demulsification efficiency was achieved with 10 h of settling (Yonguep and Chowdhury, 2021). This long settling time restricts cationic demulsifier application in industries like offshore oilfields where the space of offshore platforms is limited (Duan et al., 2019). Another research compared the efficiency of different cationic demulsifiers and found that the most effective cationic demulsifier reduced the oil concentration in water to 93 mg/L (Yuan et al., 2022). This oil concentration in separated water is still too high to discharge into the environment. Dendrimer-based demulsifiers are macromolecules consisting of highly branched polymers emanating from a central core with numerous terminal groups surrounding this core (Hao et al., 2016; Wang et al., 2021). They can be synthesized as ionic demulsifiers and used for O/W demulsification (Wang et al., 2021). Synthesis of dendrimer-based demulsifiers is a lengthy and costly process that limits their industrial applications (Bi et al., 2020). In addition, dendrimer-based demulsifiers showed poor efficiency in demulsifying O/W emulsions at low oil concentrations (e.g., 3000 mg/L), and thus they are not applicable in the oil and gas industry, where the oil concentration in wastewater is often lower than 10,000 mg/L (Hao et al., 2016; Zhang et al., 2018a). Also, it has been reported that dendrimer-based demulsifiers have poor demulsification efficiency when the salinity of the water phase is high (Kuang et al., 2020a). Oily wastewater with high salinity, such as those generated from marine

oil spill response operations, would require the application of a salinity-resistant demulsifier (Kuang et al., 2020a; Wang et al., 2021).

Anionic surfactants mainly contain fatty acid sodium salt compounds with alkyl sulfonates, and they have been widely used in surfactant flooding for enhanced oil recovery because of their low cost and easy-to-use features (Khandoozi et al., 2022). Anionic surfactants have a high surface activity that can efficiently recover residual oil from oil wells by reducing the interfacial tension between oil and water (Olajire, 2014). However, the demulsification application of anionic surfactants has not been well studied as compared to other types of demulsifiers (e.g., cationic and nonionic). A study showed the poor efficiency of sodium dodecyl sulfate (SDS), an anionic surfactant, in the demulsification of water-in-oil emulsions. The inefficiency of SDS was due to its water solubility, which is not suitable for demulsifying emulsions where the continuous phase is oil (Kang et al., 2018). Also, SDS only has one alkyl chain in the structure, which might reduce its homogenous distribution in the emulsion and reduce the adsorption capacity of its molecules at the oil−water interface (Yan et al., 2020; Zhang et al., 2014). An anionic surfactant with a double-chain structure is expected to improve the demulsification performance. Such a surfactant would be effective at demulsifying highly saline stable emulsions without requiring a long settling time, as previously reported demulsifiers (e.g., dendrimers, nonionic, and cationic) showed poor efficiency (Kuang et al., 2020a; Yonguep and Chowdhury, 2021; Zhang et al., 2016). In this study, dioctyl sodium sulfosuccinate (DSS) with a double-chain structure is used for chemical demulsification. As a biodegradable anionic surfactant, DSS has a high adsorption capacity at the oil−water interface, which is beneficial for the demulsification process (Techtmann et al., 2017; Yan et al., 2020). It is expected that the DSS can overcome the drawbacks of single-chain anionic

surfactants reported in previous research and the drawbacks of previously reported demulsifier-impeding interfacial adsorption. The response surface methodology (RSM) is used to design experiments and investigate the effect of DSS concentration, oil concentration, shaking time, and their interactions on the demulsification process. Under the optimum conditions, the effects of salinity, crude oil conditions, and settling time are also investigated. The demulsification mechanism of DSS is also explained based on the obtained results.

4.2. Materials and methods

4.2.1. Materials

Cold Lake Blend (CLB) heavy crude oil was obtained from Canada's Multi-Partner Research Initiative (MPRI). DSS (96%) was purchased from Fisher Scientific Company, Canada. Its structure is shown in Figure 4.1. Required salts to make synthetic ocean water were magnesium chloride hexahydrate ($MgCl_2.6H_2O$, 99.4%), calcium chloride anhydrous ($CaCl_2$, ≥ 96.0%), sodium bicarbonate ($NaHCO_3$, 100.1%), sodium sulfate anhydrous (Na_2SO_4, 99.5%), sodium hydroxide (NaOH, ≥ 97.0%), which were purchased from Fisher Scientific, and strontium chloride hexahydrate ($SrCl_2.6H_2O$, 99.0%), potassium chloride (KCl, 99.0–100.5%), potassium bromide (KBr, ≥ 99.0%), boric acid (H_3BO_3, ≥ 99.5%), sodium fluoride (NaF, ≥ 99.0%), sodium chloride (NaCl, ≥ 99.0%), which were purchased from Sigma-Aldrich, Canada. The chemicals were American Chemical Society (ACS) reagent grade and were used without further purification. Anhydrous silica gel (75–150 µm, 30 Å pore size, Davisil Grade 923), sodium sulfate (granular anhydrous), hexane, and dichloromethane (high-performance liquid chromatography grade) were purchased from Sigma-Aldrich, Canada. Anhydrous silica gel and sodium sulfate (granular anhydrous) were dried at 200–250 °C for 24 h. Ultrapure water was produced by a water purification system (Milli-Q Advantage A10).

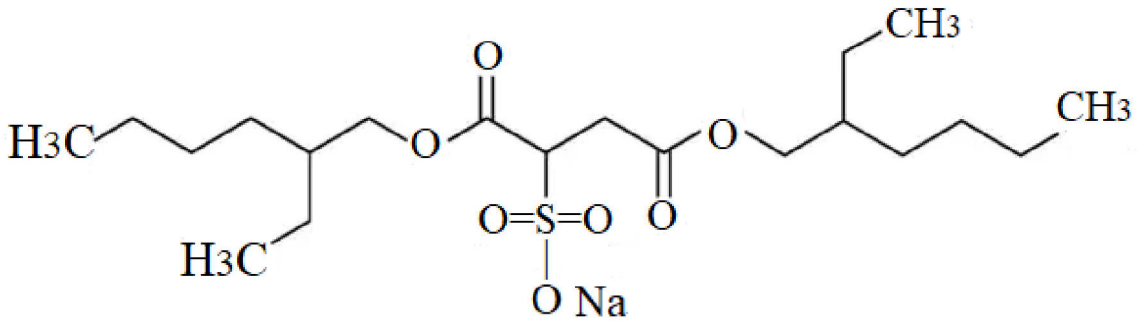

Figure 4.1. Schematic structure of DSS

4.2.2. Methods

4.2.2.1. CLB crude oil weathering process

Fresh CLB crude oil (7 g) was placed in a fume hood and the cumulative mass loss was monitored for 7 days. As shown in Figure 4.2, the cumulative CLB mass loss was 15% after 3 days, and after that, it was insignificant. Thus, CLB crude oil with 15% weathering (i.e., weathered CLB crude oil) was used to prepare O/W emulsions in this research. Table 4.1 lists the physicochemical properties of fresh and weathered CLB crude oil.

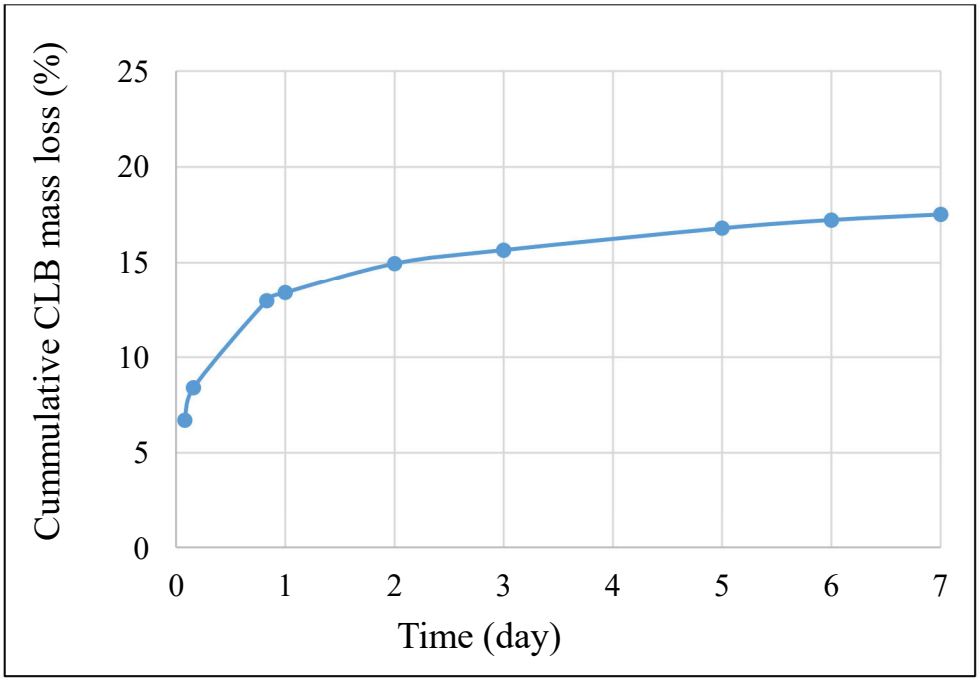

Figure 4.2. Cumulative CLB mass loss at different times.

Table 4.1. Physicochemical properties of fresh and weathered CLB crude oil.

Parameter	Value	
	Fresh	Weathered
API gravity	20.86	12.76
Dynamic viscosity at 25 °C (mPa.s)	237.8	12682.0
Density at 25 °C (g/cm^3)	0.926	0.978
Water content (%wt.)	0.041	0.030
Saturates (%wt.)	45.4	46
Aromatics (%wt.)	12.0	4.8
Resins (%wt.)	24.4	28.9
Asphaltenes (%wt.)	20.0	18.2
Ratio of resins/asphaltenes	1.22	1.59

4.2.2.2. Synthesis of ocean water

The ocean water was synthesized by following the ASTM D1141 method (ASTM, 2013). The chemical composition of the synthetic ocean water is listed in Table 4.2. Sodium

hydroxide solution (0.1 N) was used to adjust the pH of synthetic ocean water to 8.2 before starting each experiment. A Mettler Toledo FG2 portable pH meter was used to measure the pH.

Table 4.2. The chemical concentration of synthetic ocean water.

Compound	Concentration (g/L)
NaCl	24.53
$MgCl_2$	5.20
Na_2SO_4	4.09
$CaCl_2$	1.16
KCl	0.695
$NaHCO_3$	0.201
KBr	0.101
H_3BO_3	0.027
$SrCl_2$	0.025
NaF	0.003

4.2.2.3. Demulsifier characterization

The water solubility of DSS was evaluated by dissolving 1 g of DSS in 99 g of Milli-Q water following the previous research method (Yuan et al., 2022). The morphology and thermal stability of pure DSS were investigated by scanning electron microscopy (SEM) (Philips XL30) and thermogravimetric analysis (TGA) (TA instruments Discovery TGA), respectively. TGA analysis was conducted under a nitrogen atmosphere from room temperature (28 °C) to 600 °C at a heating rate of 20 °C/min.

4.2.2.4. O/W emulsion preparation

The crude CLB O/W emulsion was prepared by using a Q700 Sonicator (Qsonica, 20 kHz, solid titanium probe diameter = 12.7 mm, USA) following the method based on our previous research (Hassanshahi et al., 2022). A given amount of CLB crude oil was poured on the

surface of 100 mL synthetic ocean water according to the desired oil concentration (500–3000 mg/L), and then the sonicator probe was submerged in the middle of the sample. The Q700 Sonicator sonicated the sample to make a stable emulsion. Sonication was conducted at an amplitude of 70% (power of 76–80 W) for 16 min at a 20:20 second On/Off pulse. When the pulse was on, the probe passed ultrasound waves through the sample and generated high shear forces and shock waves in the sample, leading to stable emulsion formation. The On/Off pulse was used to prevent the increase of the emulsion temperature. There was no significant sign of emulsion breaking after 24 h.

4.2.2.5. Demulsification process

The demulsification process was conducted in a batch system. About 45 mL of O/W emulsion was added to a 50 mL centrifugal tube. A given amount of pure DSS was added to the emulsion at the desired demulsifier concentration, and the mixture was shaken at 100 rpm on a Talboy 3500 Orbital Shaker for different shaking times. Then the solution was subjected to gravity separation at room temperature (~ 25 °C) for 45 min to allow oil−water separation. Gravity separation of the emulsion (45 mL) without adding a demulsifier was considered as a control experiment. The transmittance value of separated water was measured at different shaking times (Kuang et al., 2020a; Zhang et al., 2018a). Measurements were conducted at a wavelength of 235 nm using UV-Vis Spectrophotometer 8100 (OrionTM AquaMate UV-Vis spectrophotometer, Perkin Elmer). After mixing the demulsifier and emulsion, the size and shape of the oil droplets in water were monitored using a compound microscope (Fisher Scientific AX800) with a 200× objective magnification (Yuan et al., 2022). The images were captured by a digital camera (Fisher Scientific C-Mount Digital Camera) and analyzed using SeBaView software (version 4.7).

4.2.2.6. Experimental design

Important experimental parameters on demulsification efficiency, including demulsifier concentration, oil concentration, and shaking time, were selected based on previous studies (Hao et al., 2016; Hassanshahi et al., 2020; Sun et al., 2020). Table 4.3 lists the parameters and their levels. Design Expert (version 12.0.11.0, Stat-Ease, Inc.) was used to design experiments. RSM was used to evaluate the effect of each independent parameter and their interactions and identify the optimum conditions for the demulsification process. Central composite design (CCD) as a comprehensive design of RSM was used in this study. For each independent numeric parameter, five levels (coded with ±1, ±α, 0) were considered in CCD. Experimental data from CCD were fitted using Equation (4.1) (Hassanshahi and Karimi-Jashni, 2018).

$$Y = \beta_0 + \sum_{i=1}^{k} \beta_i X_i + \sum_{i=1}^{k} \beta_{ii} X_i^2 + \sum_{i<j} \sum_j \beta_{ij} X_i X_j, \quad (4.1)$$

where Y represents the predicted response, β_0 is a constant coefficient, β_i is the linear effect of X_i variable, β_{ii} is the second-order effect of variable X_i, and β_{ij} is the effect of the linear interaction between parameters X_i and X_j. Analysis of variance (ANOVA) was performed to determine the significance of the parameters.

Table 4.3. Experimental parameters and levels in RSM.

Parameter	Unit	Coded levels				
		–α	–1	0	+1	+α
DSS concentration	mg/L	300	500	800	1100	1300
Weathered CLB oil concentration	mg/L	500	1000	1750	2500	3000
Shaking time	min	8	10	13	16	18

Further single-factor experiments were conducted at the optimum conditions suggested by RSM to investigate the effect of salinity (0 and 36 g/L) and crude oil conditions (fresh and weathered) on DSS performance. The effect of settling time of gravity separation on the demulsification efficiency was investigated to determine when the demulsification process reaches equilibrium. Single-factor experiments were repeated three times, and the average was reported.

4.2.2.7. Analysis of total extractable petroleum hydrocarbons in water and emulsion

Total extractable petroleum hydrocarbons (TEPH) that remained in separated water were extracted following the liquid−liquid extraction method using hexane/ dichloromethane (1:1 vol.) in the British Columbia laboratory manual (British Columbia laboratory manual, 2017). This was conducted by taking 40 mL of sample from separated water and mixing it with 2 mL of the solvent in a 50 mL vial (solvent: sample volume ratio was 1:20). The mixture of the solvent and sample was shaken on an orbital shaker for 30 min at 70 rpm. After that, the solvent and water were allowed to separate, and then the solvent was passed through activated anhydrous sodium sulfate and silica gel to remove moisture and polar organic compounds. Then, 1 mL of the fresh solvent was poured to elute the sodium sulfate and silica gel. The whole extraction was collected in a gas chromatography vial. Then, a portion of that was taken for analysis of TEPH using an Agilent 6890 gas chromatograph with a flame ionization detector (GC–FID). The hydrocarbons mixtures were grouped in (nC_{10}–nC_{19}), (nC_{19}–nC_{32}), and (nC_{32}–nC_{50}). Decane (nC_{10}), nonadecane (nC_{19}), eicosane (nC_{20}), dotriacontane (nC_{32}), tetriacontane (nC_{34}), and pentacontane (nC_{50}) were used as the external standards. A ZB-1HT INFERNO capillary column (Phenomenex) with a length of 30 m, an inner diameter of 0.32 mm, and a film thickness of 0.25 μm was used. The carrier gas was helium at a rate of 1.6

mL/min. TEPH extract (1 μL) was injected into the system, and a split ratio of 10:1 was used for each run. During analysis, the injector and detector temperatures were kept at 290 and 320 °C, respectively. The initial temperature of the oven was at 130 °C, then increased to 310 and 340 °C at 20 and 5 °C/min, respectively, and held at 340 °C for 8 min. The procedures to determine TEPH in the emulsion were the same as that for the measurement of TEPH in separated water.

Demulsification efficiency (DE) was calculated using Equation (4.2) (Fard et al., 2016).

$$DE = \frac{C_i - C_f}{C_i} \times 100 \quad (4.2)$$

Where C_i and C_f are the initial and final TEPH concentrations in the emulsion and the separated water, respectively.

4.3. Results and discussion

4.3.1. Characterization of DSS

The water solubility test of DSS showed that DSS was a water-soluble demulsifier that dissolved in the water completely. The morphological structure of DSS was determined by SEM analysis. As shown in Figure 4.3a, DSS has a flaky and thin structure involving different macropores, which are responsible for its lightweight. Thermal stability is one of the characteristics of demulsifiers that plays a crucial role in their applications in industries. The TGA result of DSS is shown in Figure 4.3b. The initial 2.5% weight loss of DSS is due to water evaporation. DSS remained thermally stable up to around 250 °C as a result of the higher decomposition temperature of dioctyl sulfosuccinate as the anion in the chemical structure. DSS decomposed and significantly lost weight at a temperature >250 °C. Based on the TGA

curve, it is concluded that DSS is relatively thermally stable and can be used in a wide range of applications (e.g., where the oily wastewater temperature is high).

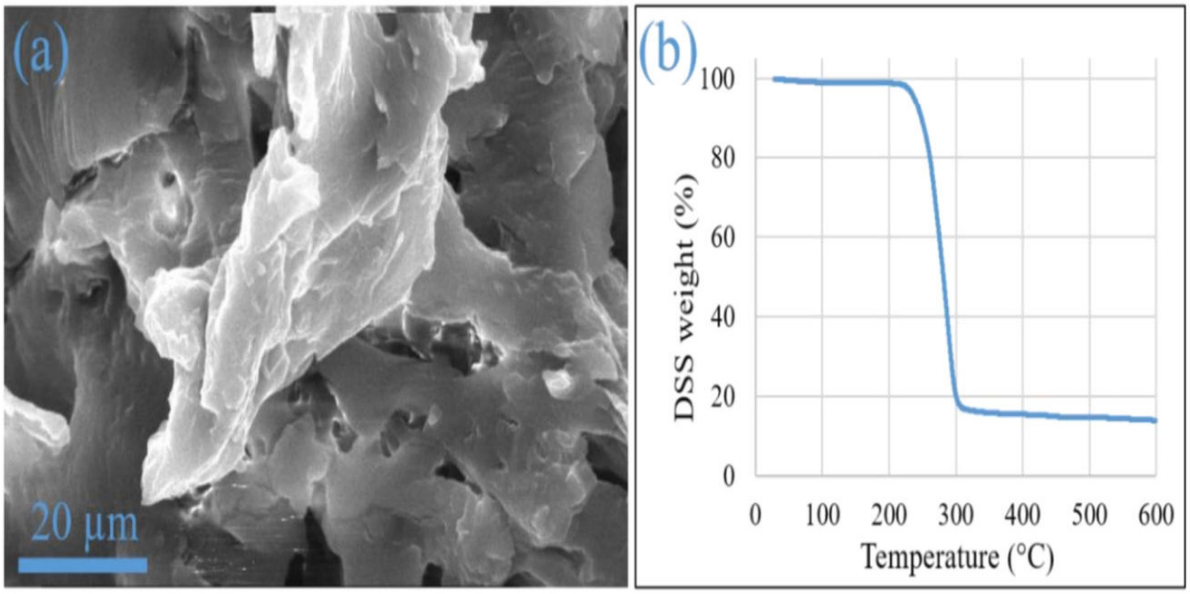

Figure 4.3. Characterization of DSS a) SEM image and b) the TGA curve (heating rate: 20 °C/min, under a nitrogen atmosphere).

4.3.2. Demulsification results

4.3.2.1. RSM experimental results

Considering DSS concentration, oil concentration, and shaking time as experimental parameters, 20 experiments were designed by CCD design. Table 4.4 shows the parameters and the experimental results.

Table 4.4. CCD matrix in the DSS demulsification process and the obtained results.

Run	Experimental parameters			EPH in separated water			
	DSS concentration (mg/L)	Weathered CLB oil concentration (mg/L)	Shaking time (min)	TEPH (C_{10}–C_{50}) concentration (mg/L)	EPH (C_{10}–C_{19}) fraction (%)	EPH (C_{19}–C_{32}) fraction (%)	EPH (C_{32}–C_{50}) fraction (%)
1	300	1750	13	519.2	36.3	51.3	12.4
2	500	1000	10	233.7	35.9	52.7	11.4
3	500	1000	16	66.6	37.8	52.1	10.1
4	500	2500	10	54.2	41.1	46.0	12.9
5	500	2500	16	62.9	38.6	51.0	10.4
6	800	500	13	2.3	98.8	1.2	ND[1]
7	800	3000	13	22.5	46.3	53.7	ND
8	800	1750	8	26.7	49.9	50.1	ND
9	800	1750	13	2.0	62.0	38.0	ND
10	800	1750	13	3.4	84.9	15.1	ND
11	800	1750	13	16.8	47.2	52.8	ND
12	800	1750	13	14.3	51.0	49.0	ND
13	800	1750	13	35.6	50.3	49.7	ND
14	800	1750	13	37.4	43.9	56.1	ND
15	800	1750	18	13.3	50.8	49.2	ND
16	1100	1000	10	25.1	53.5	46.5	ND
17	1100	1000	16	6.4	68.5	31.5	ND
18	1100	2500	10	5.3	78.4	21.6	ND
19	1100	2500	16	8.6	70.5	29.5	ND
20	1300	1750	13	7.5	17.0	83.0	ND

[1] ND: Not detected

A quadratic model was developed for the demulsification process, as shown below:

$$DE = -204.37 + 0.34X_1 + 0.08X_2 + 7.68X_3 - 4\times10^{-5}X_1X_2 - 3.50\times10^{-3}X_2X_3 - 1.36\times10^{-4}X_1^2 \quad (4.3)$$

Where DE is the demulsification efficiency (%), X_1 represents the DSS concentration (mg/L), X_2 represents the oil concentration (mg/L), and X_3 represents the shaking time (min). The ranges of experimental parameters are listed in Table 4.3.

ANOVA was used to confirm the adequacy of the model and the importance of the effect of each independent parameter, and the results are shown in Table B1. ANOVA showed that the developed quadratic model was significant (F-value: 12.40, P-value: 0.0001) in determining the demulsification efficiency. X_1, X_2, X_1X_2, X_2X_3, and X_1^2 were significant parameters (P-values < 0.05) in this model to predict demulsification efficiency. Model summary statistics for the generated quadratic model by RSM are listed in Table B2.

4.3.2.1.1. DSS concentration

Based on ANOVA, the DSS concentration was one of the critical parameters in the demulsification process (F-value: 34.83, P-value < 0.0001). Demulsification efficiency reached around 70% (Figure 4.4a), and the TEPH in the separated water was reduced to <70 mg/L (Table 4.4) when the DSS concentration was 500 mg/L (except for run #2). DSS is a low molecular weight demulsifier (444.56 Da), and a low molecular weight demulsifier often requires a high concentration to effectively demulsify an O/W emulsion (Hassanshahi et al., 2020). However, it is readily biodegradable and less toxic than high-molecular-weight demulsifiers with complex structures that may be effective at a lower concentration. Additional

merits of DSS over other demulsifiers are its availablity, physicochemical stability and easy-to-use feature. As shown in Figure 4.4a, increasing the DSS concentration to 900 mg/L increased demulsification efficiency, and beyond this concentration, the improvement in demulsification efficiency was insignificant. It can be concluded that the critical micelle concentration (CMC) of DSS for O/W demulsification is 900 mg/L (Lyu et al., 2020; Zhang et al., 2022). As listed in Table 4.4, increasing DSS concentration from 300 mg/L to 1300 mg/L reduced TEPH in separated water to <10 mg/L. This high demulsification efficiency of DSS may be because the double-chain structure facilitated the homogenous distribution of DSS in the emulsion. Also, the double-chain structure did not impede DSS interfacial adsorption at the oil−water interface as opposed to the double-chain cationic demulsifier, the efficiency of which was reduced notably due to interfacial adsorption restriction (Zolfaghari et al., 2018).

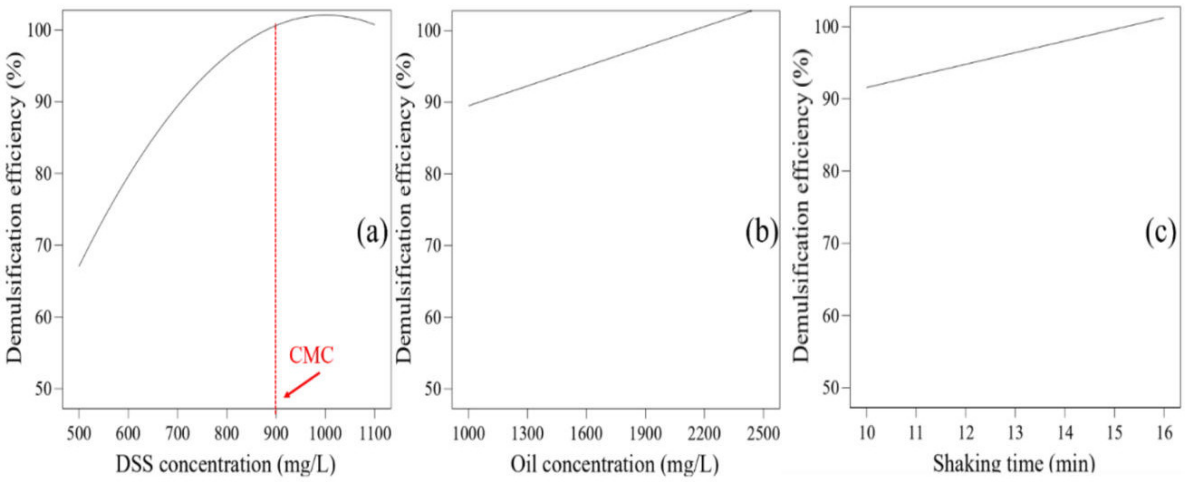

Figure 4.4. Predicted effect of a single parameter on demulsification efficiency, a) oil concentration: 1750 mg/L, shaking time: 13 min; b) DSS concentration: 800 mg/L, shaking time: 13 min; and c) DSS concentration: 800 mg/L, oil concentration: 1750 mg/L.

4.3.2.1.2. Oil concentration

Oil concentration is one of the essential parameters for evaluating demulsification performance. The ANOVA results suggest that oil concentration significantly affected the demulsification efficiency (P-value: 0.03). The effect of oil concentration on demulsification efficiency is shown in Figure 4.4b. DSS efficiently demulsified emulsions containing different oil concentrations (demulsification efficiency ≥90%). By increasing oil concentration, higher demulsification efficiencies were achieved. The reason is the high probability of collision of emulsified oil droplets and the formation of bigger ones at high oil concentrations compared to lower ones. Results of the same experimental conditions (experimental runs #2 and #4 in Table 4.4) showed that increasing the oil concentration in the emulsion from 1000 to 2500 mg/L helped in coalescence and then settling of oil droplets which resulted in a significant reduction of TEPH from 233.7 to 54.2 mg/L, respectively. At low oil concentrations (e.g., 500 mg/L), tiny emulsified oil droplets are far away from each other, and thus the chance of their coalescence is low. These persistent emulsified oil droplets required a higher DSS concentration (800 mg/L) to demulsify them (Table 4.4). This concentration is still lower than the CMC, which reduced the TEPH in the separated water to 2.3 mg/L. The significant reduction in TEPH indicated that the demulsification efficiency of DSS was not affected by the initial oil concentration. This is an advantage of DSS over other demulsifiers (e.g., dendrimers), which have low efficiency for emulsions with low oil concentrations (Hao et al., 2016). DSS is widely applicable to various oil concentrations in emulsions, even when the oil concentration is as low as 500 mg/L.

4.3.2.1.3. Shaking time

Sufficient shaking time is required for DSS dissolution and dispersion in the emulsion to reach the oil−water interface. The effect of shaking time on demulsification efficiency was investigated (Figure 4.4c). The required shaking time to demulsify the crude O/W emulsion by DSS was low (<16 min), which made DSS a suitable demulsifier for industrial applications. DSS was a water-soluble demulsifier with a low molecular weight (< 3000 Da), which brought about the quick diffusion of the demulsifier in the continuous water phase (Hassanshahi et al., 2020). Table 4.4 shows the remaining TEPH in the water and their fractions at different shaking times. The high interfacial activity and adsorption capacity of DSS because of two long tails in its structure caused it to weaken and then break the rigid film at the oil−water interface within a low shaking time (<16 min). It is worth noting that the solid form of DSS was used in this study and this did not affect the demulsifier efficiency (98%). Hence, applying pure solid DSS rather than dissolving it in an organic solvent, a common method for applying demulsifiers that are in the solid form, can reduce the toxicity of the demulsification system and the generation volume of hazardous liquid wastes.

4.3.2.1.4. Interaction of parameters

The effect of the interaction of different experimental parameters on the efficiency of the demulsification process was investigated. As shown in Figure 4.5a, at a high oil concentration in emulsion (e.g., 2500 mg/L), a lower DSS concentration (500 mg/L) could achieve a high demulsification efficiency (~80%). A higher DSS concentration was required to achieve similar results when the oil concentration was low. The effect of the interaction of the DSS concentration and shaking time on demulsification efficiency is shown in Figure 4.5b. It was found that increasing shaking time led to higher demulsification efficiency at lower DSS

concentrations, and this was due to sufficient time for dissolution and dispersion of DSS in the emulsion to reach the oil−water interface and break the rigid film. Figure 4.5c indicates that when oil concentration was high, a lower shaking time (10 min) was sufficient to achieve high demulsification efficiency because many oil droplets in the emulsion at high oil concentration coalesced quickly and increased the demulsification efficiency. It is crucial to consider the effect of the interaction of parameters on demulsification efficiency, which may bring benefits of applying demulsifiers at lower concentrations.

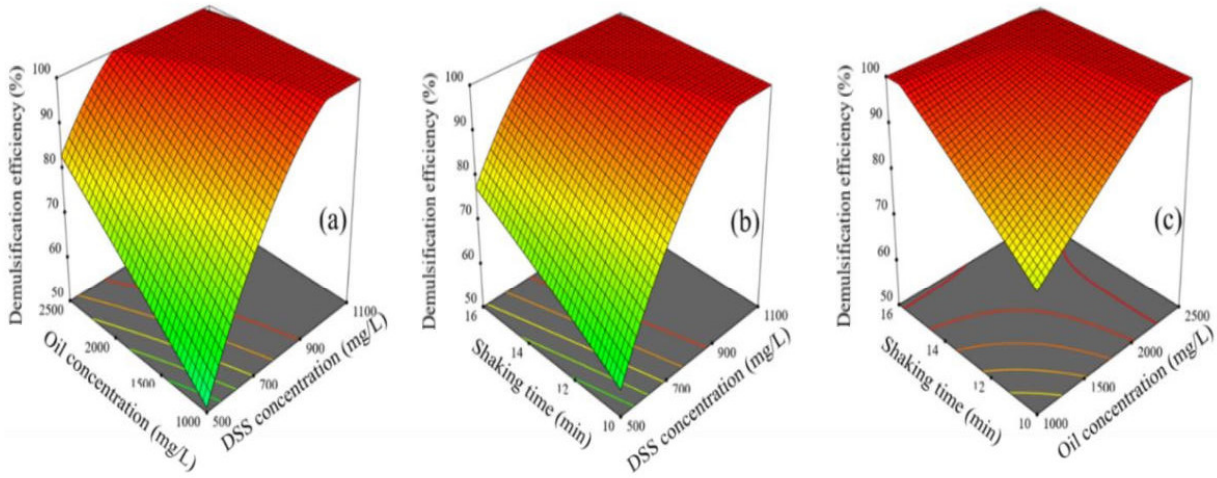

Figure 4.5. Effect of interactions of different parameters on demulsification efficiency at a) a shaking time of 13 min, b) oil concentration of 1750 mg/L, and c) DSS concentration of 800 mg/L.

The optimum conditions of different parameters for achieving maximum demulsification were obtained (Table 4.4), and it was at the oil concentration of 1000 mg/L, a DSS concentration of 900 mg/L, and a shaking time of 15 min, respectively. The effects of salinity, gravity separation settling time, and crude oil conditions on demulsification efficiency were then investigated under these optimum conditions.

4.3.2.2. Single-factor experimental results

4.3.2.2.1. Salinity

Figure 4.6a illustrates the effect of the presence of salts in the water phase on the demulsification efficiency. Asphaltenes are crude oil's polar fraction with a negative surface charge in aqueous solutions where pH is above 4 (Ezzat et al., 2021). Asphaltenes create a rigid film around the emulsified oil droplets in the water and form droplets with a negative surface charge. Also, DSS is an anionic demulsifier, in which the molecules have a negative surface charge. Without salts in the water, repulsive electrical force among the DSS molecules and asphaltenes reduced the number of DSS molecules present at the oil−water interface. This phenomenon led to low demulsification efficiency by DSS (around 63%). However, salts in the water increased the DSS performance significantly and reduced TEPH in separated water notably (Table 4.5). This is a merit of DSS over other demulsifiers such as dendrimers, whose efficiency was highly reduced in highly saline emulsions (Kuang et al., 2020a). Salt cations in the water phase (e.g., Na^{+}, Mg^{2+}, Ca^{2+}) neutralized the repulsive electrical force among the DSS molecules and emulsified oil droplets, facilitating the DSS molecules to reach and saturate the oil−water interface (Ezzat et al., 2021). Hence, it is concluded that for an anionic demulsifier in a demulsifying O/W emulsion, the combination of destabilization of the rigid film around emulsified oil droplets due to the high surface activity of the demulsifier and the electrostatic force among molecules in the emulsion brings about the highest demulsification efficiency.

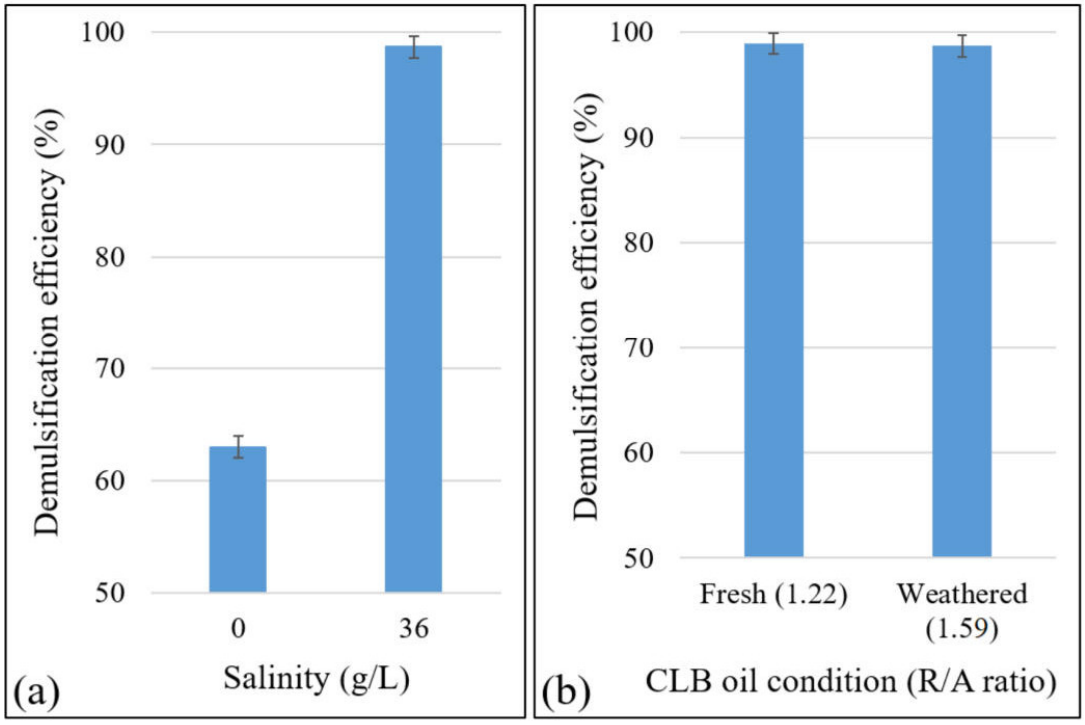

Figure 4.6. Effect of a) salinity and b) CLB oil condition (R/A ratio) on demulsification efficiency.

Table 4.5. Effect of salinity, CLB crude oil conditions, and settling time on demulsification process[1].

Run	Experimental parameters			EPH in separated water			
	Salinity (g/L)	CLB oil condition	Settling time (min)	TEPH (C_{10}-C_{50}) concentration (mg/L)	EPH (C_{10}-C_{19}) fraction (%)	EPH (C_{19}-C_{32}) fraction (%)	EPH (C_{32}-C_{50}) fraction (%)
1	0	Weathered	45	111.5	29.6	55.9	14.5
2	36	Weathered	45	3.9	56.4	28.6	15.0
3	36	Weathered	30	8.1	75.8	12.5	11.7
4	36	Weathered	15	2.7	36.4	12.7	50.9
5	36	Weathered	0	7.8	18.6	10.1	71.3
6	36	Fresh	45	3.1	67.5	17.1	15.4

[1]DSS concentration of 900 mg/L, oil concentration of 1000 mg/L, shaking time of 15 min, and shaking speed of 100 rpm.

4.3.2.2.2. CLB oil condition (R/A ratio)

Natural emulsifying agents (e.g., resins and asphaltenes) of crude oils vary greatly (Adilbekova et al., 2015). The physicochemical composition of crude oils affects the emulsion stability, affecting demulsifier efficiency (Guzmán-Lucero et al., 2010). The performance of DSS in demulsifying emulsions containing different natural emulsifying amounts was investigated using different crude oil conditions (Figure 4.6b). DSS was effective at demulsifying both fresh and weathered emulsions (different R/A ratios) which proved that DSS performance was not affected by the physicochemical composition of crude oils. The R/A ratio determines the stability of the emulsion, where a lower ratio increases emulsion stability (Ramirez-Corredores, 2017). Fresh CLB had a lower R/A ratio (1.22) than the weathered one (1.59), as listed in Table 4.1, and thus had higher emulsion stability. This is also supported by the emulsified oil droplets size distribution in the emulsion generated by fresh and weathered CLB (Figure 4.7). The average oil droplets size for the fresh and weathered CLB emulsions were 4.6 and 6.1 μm, respectively. Based on the oil droplets' size distribution and their average size, and TEPH remaining in separated water (Table 4.5), it can be concluded that DSS can effectively demulsify O/W emulsion, where the average size of oil droplets is <10 μm. This is another advantage of DSS over nonionic demulsifiers, which showed poor efficiency in demulsifying heavy crude oil emulsions containing emulsified oil droplets (<10 μm) (Adilbekova et al., 2015; Zhang et al., 2016).

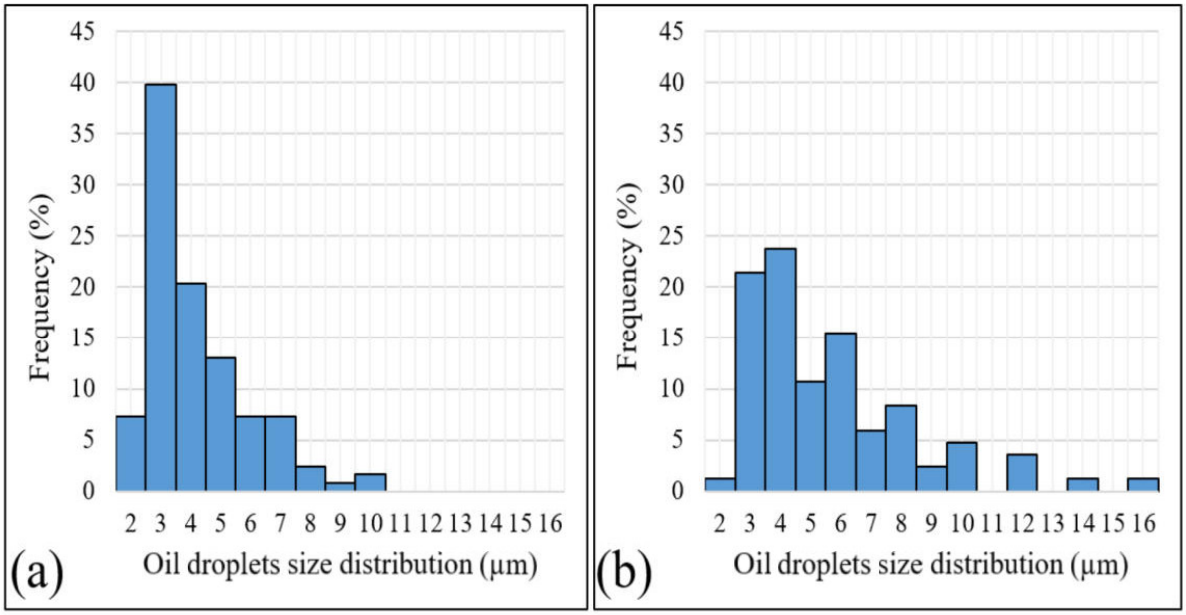

Figure 4.7. Oil droplets size distribution in the generated O/W emulsion a) fresh CLB O/W emulsion, b) weathered CLB O/W emulsion.

4.3.2.2.3. Settling time

The settling time of gravity separation is one of the critical parameters in the demulsification process, which affects the processing time and settling tank size (Chong et al., 2016). After 15 min of shaking time, different gravity separation settling times (0, 15, 30, and 45 min) were considered to settle the oil droplets in water. The effect of settling time on demulsification efficiency is shown in Figure 4.8, and the TEPH remaining in the water and their fractions at different settling times are listed in Table 4.5. As shown, the application of a demulsifier significantly broke the O/W emulsion and promoted the separation of oil from water, and thus the gravity separation settling time had an insignificant effect on further oil/water separation. The demulsification efficiency was higher than 96% for all settling times. The remaining TEPH in separated water was lower than 10 mg/L for all investigated settling

times (0, 15, 30, and 45 min). The results indicated that DSS efficiently demulsified the O/W emulsion without the need for a long settling time under gravity separation, thus reducing the demulsification process time significantly. This is quite a remarkable result over other demulsifiers (e.g., cationic), which have been reported to require a long settling time (e.g., 10 hours) to achieve desirable results (Yonguep and Chowdhury, 2021). As no settling time is required for DSS demulsification, it is an efficient demulsifier for application in oil and gas industries and offshore oil spill response operations.

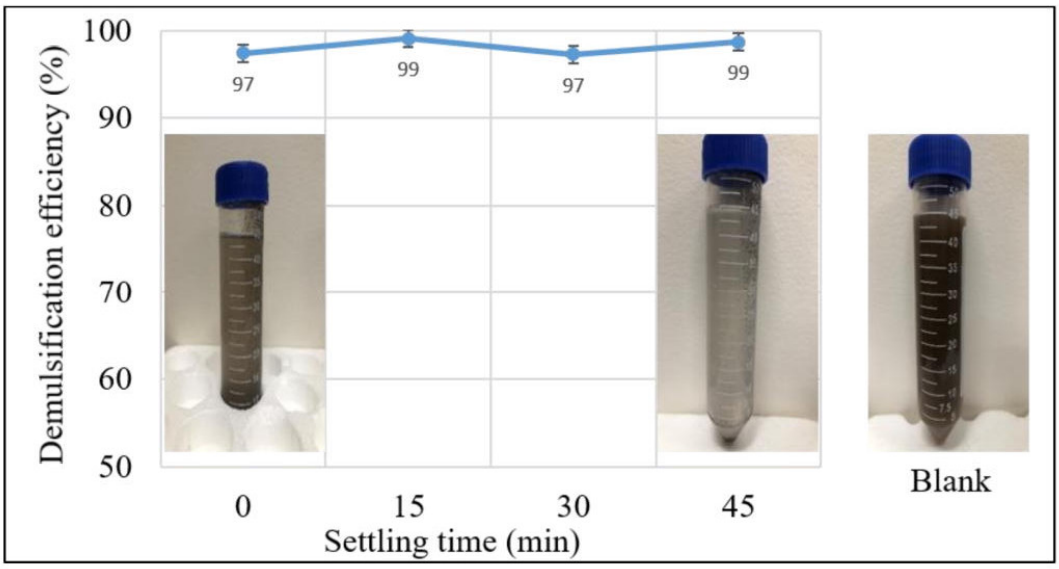

Figure 4.8. Effect of settling time on demulsification efficiency at a DSS concentration of 900 mg/L, an oil concentration of 1000 mg/L, a shaking time of 15 min, and a salinity of 36 g/L.

4.3.3. Demulsification mechanism by DSS

Figure 4.9 shows the schematic diagram of the demulsification process by DSS. After adding DSS to the emulsion and mixing, DSS molecules dissolved in the emulsion and reached

the oil−water interface quickly due to their low molecular weight. Then, DSS molecules saturated the oil−water interface. DSS is an anionic surfactant with a negative surface charge. Asphaltenes of crude oil that formed the rigid film at the oil−water interface also have a negative surface charge at pH > 4 (Ezzat et al., 2021). The presence of positive ions (e.g., Na^{+}, Mg^{2+}, and Ca^{2+}) in the emulsion contributed to DSS saturation of the oil−water interface by reducing the repulsive force among the negative surface charge molecules. This was confirmed by the high demulsification efficiency when the water phase had high salinity. DSS possesses high surface activity and adsorption capacity due to its double-chain structure, which displaced natural emulsifying agents of crude oil like asphaltenes and resins and ruptured the rigid film at the oil−water interface. Hence, the unstable emulsion flocculated and coalesced, as shown in Figure 4.10, leading to oil and water separation. The transmittance of the emulsion at different shaking times was measured (Figure 4.11). The transmittance of the emulsion increased within short shaking times (<15 min), which also proved the quick aggregation and coalescence of emulsified oil in water. At 15 min, coalesced oil droplets were still suspended in the separated water phase, resulting in 60% transmittance in the separated water. The low TEPH concentration in separated water (7.8 mg/L) without gravity separation (0 min settling time) indicated that although turbidity reached 60%, the efficiency of the demulsification process reached 97%. After 45 min of gravity separation, the suspended oil droplets settled, and the TEPH was reduced to 3.9 mg/L (demulsification efficiency reached 99%).

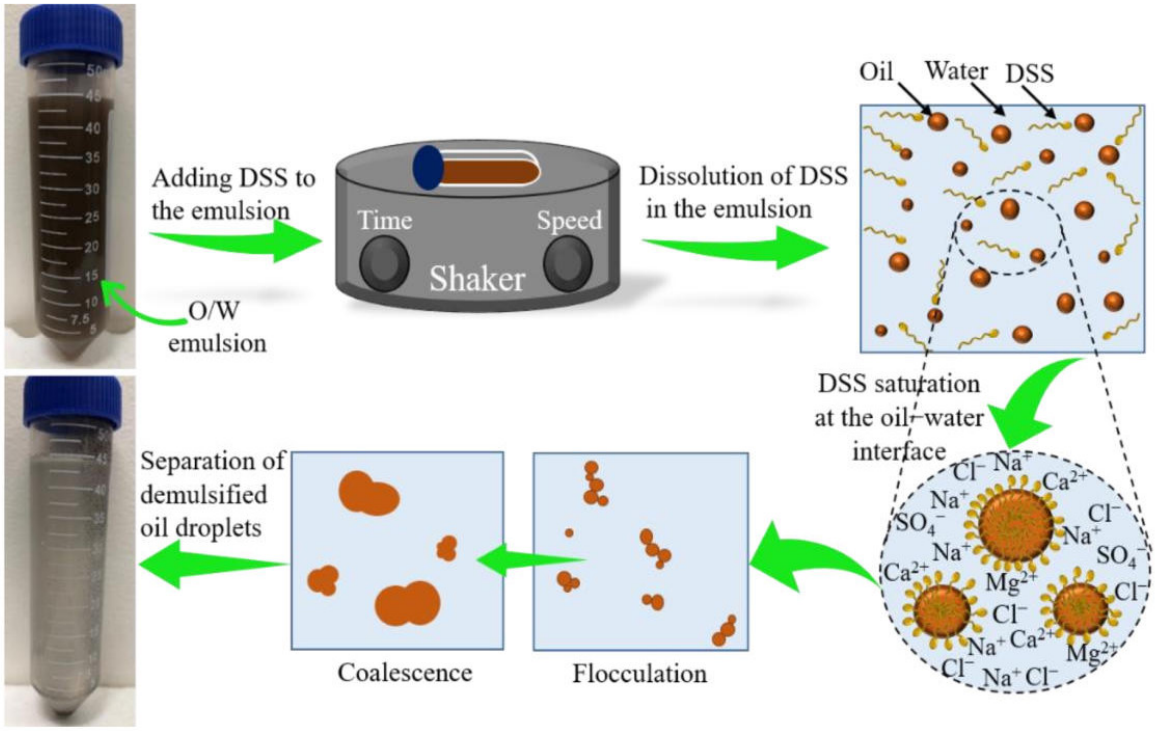

Figure 4.9. Schematic diagram of the demulsification process by DSS.

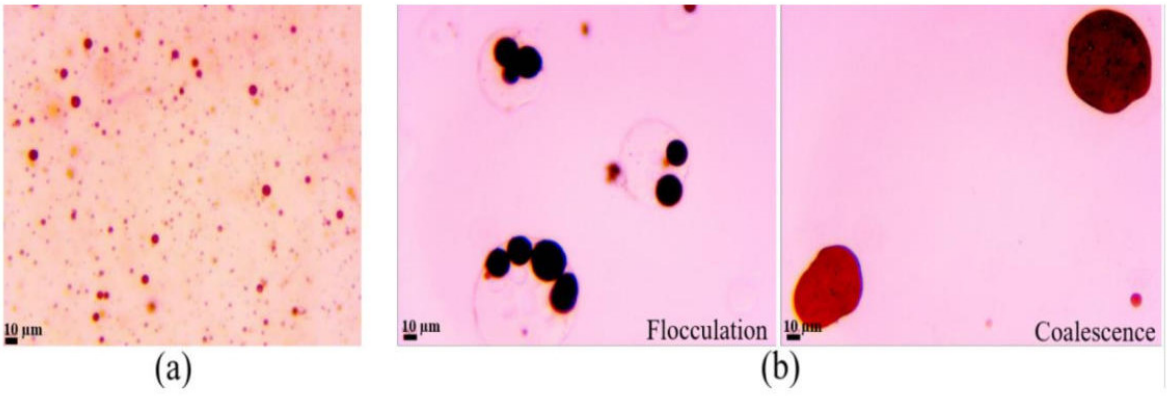

Figure 4.10. Microscopic images of a) emulsified O/W (1000 mg/L), b) demulsified O/W (1000 mg/L) by DSS (flocculation and coalescence of oil droplets) under optimum conditions of the demulsification process by DSS.

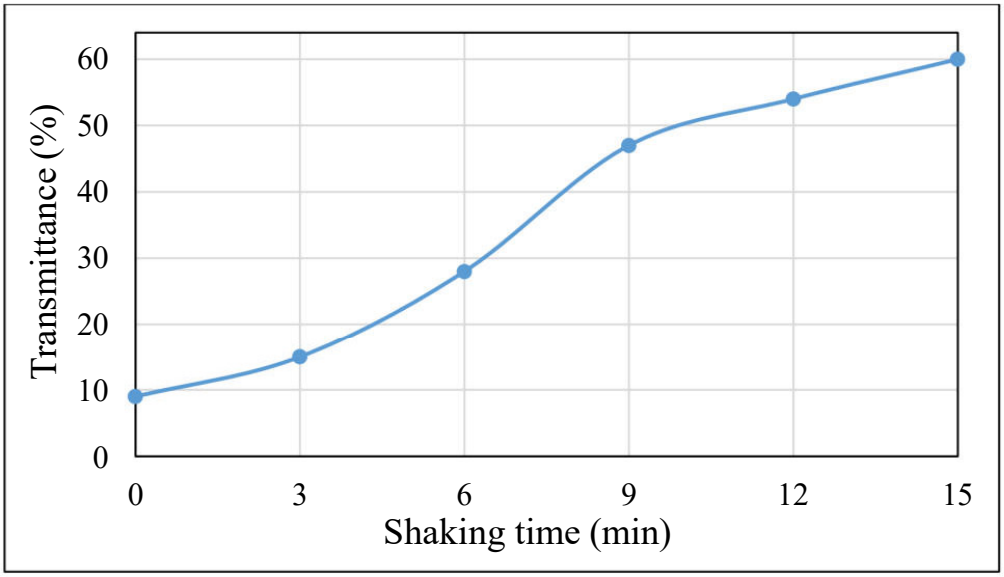

Figure 4.11. The transmittance of the O/W emulsion against shaking time under optimum conditions of the demulsification process by DSS.

4.4. Summary

The performance of DSS as a new anionic surfactant in the demulsification of crude O/W emulsions was investigated. Effects of the DSS concentration, crude oil concentration, and shaking time were investigated, and the optimum conditions were obtained. DSS is a low molecular weight demulsifier that diffuses in the emulsion quickly and demulsifies the emulsion within a short time. The optimum conditions of DSS concentration and shaking time were 900 mg/L and 15 min, respectively, when the oil concentration was 1000 mg/L. Under these optimum conditions, the effect of salinity, crude oil conditions (fresh and weathered oil with different R/A ratios), and settling time of gravity separation were investigated. Since DSS is an anionic surfactant, it was more efficient at demulsifying O/W emulsions when salt ions (e.g., Na^{+}, Mg^{2+}, Ca^{2+}) were in the emulsion (98% demulsification efficiency) compared to

when there was no salt (63% demulsification efficiency). Demulsification efficiency was not affected by the crude oil conditions and different R/A ratios of crude oils (i.e., emulsion stability). DSS demulsified the emulsion effectively even when the R/A ratio was low (demulsification efficiency > 98%, TEPH = 3.1 mg/L), which proved that the surface activity of DSS was higher than asphaltenes and resins (natural emulsifying agents). DSS demulsification significantly reduced the settling time of gravity separation. The demulsification mechanism by DSS was the displacement of natural emulsifying agents and weakening of the rigid film at the oil−water interface. This led to aggregation, flocculation, and then coalescence of oil droplets which were shown by capturing microscopic images and measuring the transmittance of emulsion. This research investigated the application of DSS in the demulsification process as a reliable demulsifier for different industrial applications.

Chapter 5

NEW AMMONIUM-BASED IONIC LIQUID WITH HYDROXYL FUNCTIONAL GROUPS IN THE SIDE CHAINS IN DEMULSIFYING OIL IN WATER EMULSION

Abstract

In this research, the performance of tris(2-hydroxyethyl) methylammonium methylsulfate (MTEOA $MeOSO_3$) ionic liquid with hydroxyl functional groups (OH^-) in the side chains was evaluated for the first time to demulsify heavy crude oil-in-water emulsion. Effects of MTEOA $MeOSO_3$ concentration, demulsification temperature, gravity separation settling time, and emulsifier type on the demulsification efficiency were investigated. The results showed that MTEOA $MeOSO_3$ demulsified emulsion at concentrations of ≤ 100 mg/L. A concentration higher than that brought about an abundance of OH^- in the emulsion, resulting in a repulsive force among negative surface charge molecules (OH^- and oil droplets) rather than adsorption of MTEOA $MeOSO_3$ molecules at the oil-water interface. Higher demulsification temperature (50 °C) increased the oil droplets' collision and accelerated the flocculation and coalescence process resulting in higher demulsification efficiency. Optical microscopic images showed that flocculation and coalescence of oil droplets occurred within the first 15 min of gravity settling, and the demulsification process reached equilibrium at 90 min settling. It was also found that the emulsifier type significantly affected the MTEOA $MeOSO_3$ performance in the demulsifying emulsion, and the spectrophotometry analysis supported it. MTEOA $MeOSO_3$ demulsified emulsion stabilized by natural emulsifiers effectively (demulsification efficiency: 92%) at a low MTEOA $MeOSO_3$ concentration (25 mg/L), while its efficiency was reduced (demulsification efficiency: 36%) notably in demulsifying emulsion stabilized by Tween 20+natural emulsifiers. The demulsification mechanism was concluded to be hydrogen bond

reconstruction due to hydroxyl groups in the ionic liquid structure. This study showed that a biodegradable ionic liquid with hydroxyl functional groups rather than alkyl chains could be an effective demulsifier in the demulsifying emulsion.

5.1. Introduction

Crude oil in water (O/W) and water in oil (W/O) emulsions generate widely in oil and gas industries during crude oil production processes and in oceans due to oil spills. In the former one, O/W emulsion generates when ocean water surrounding oil wells mixes with crude oil during extraction from resources and forms emulsion due to the action of shear and pressure drop at the wellhead, chokes, and valves (Al-Ghouti et al., 2019; Liu et al., 2021b; Raya et al., 2020). Also, it generates, to a great extent, during enhanced oil recovery processes due to flooding crude oil resources with ocean water and surfactants (Austad et al., 2011; Zahid et al., 2011). Marine oil spills also happen frequently due to ship accidents and natural seepage, leading to a large volume of O/W emulsion. Previous research noted that almost 9,000,000 tons of oil had been spilled since 1965 (Motta et al., 2018). Emulsion stabilizes by natural emulsifiers in crude oils (e.g., asphaltenes) and surfactants if used in oil and gas industries (Sousa et al., 2021). Emulsifiers create complex inter-and intra-molecular interactions (e.g., π–π stacking, hydrogen bond), forming a rigid film around emulsified droplets in the continuous phase and preventing their coalescence and separation (Chen et al., 2018; Farooq et al., 2021; Ma et al., 2021). Toxicity associated with crude oil compounds (e.g., polycyclic aromatic hydrocarbon) is a significant environmental concern that limits discharging of oil and grease to the environment to the maximum of 42 mg/L/day based on the United States Environmental Protection Agency regulation (Ruberg et al., 2021; Shokri and Fard, 2022). Therefore, treating O/W emulsion gets much attention to meet environmental regulations and develop recycling and reuse in oil and gas industries (Franco et al., 2014).

Several technologies have been used to demulsify O/W emulsion, including gravity settling (Mohayeji et al., 2016), biological treatment (Lusinier et al., 2019), flotation (Piccioli et al.,

2020), centrifugation (Kumar et al., 2021), electrical treatment (Ren and Kang, 2018), membrane separation (Zhao et al., 2021) and chemical demulsification using chemical demulsifiers (Wang et al., 2021). Of these methods, the latter has the advantages of simplicity, effectiveness, and rapid and cheap process (Yang et al., 2021; Yonguep and Chowdhury, 2021). Demulsifiers are surface-active agents that demulsify emulsion by diffusion in emulsion and reach the oil-water interface, replacing a rigid film around emulsified droplets to form a soft film facilitating their coalescence and separation of them by gravity (Abdullah and Al-Lohedan, 2019). Although different demulsifiers (e.g., polymers, ionic liquids, nanoparticles) have been used in the demulsification process, it is reported that no demulsifier can be applied for all kinds of crude oil emulsion due to the complicated components of crude oils and commercial limitations (Kang et al., 2018; Wang et al., 2021; Yuan et al., 2022,). Environmental regulations make it essential to investigate new demulsifiers to effectively demulsify emulsions with less potential environmental risk (Atta et al., 2016a).

Among various demulsifiers, ionic liquids get much attention because of their unique characteristics, including non-flammability, thermal stability, and low vapor pressure (Hassanshahi et al., 2020). These features make ionic liquids desirable substitutions for commercial demulsifiers and organic solvents in industrial applications (Bera et al., 2020; Singh and Savoy, 2020). Ionic liquids are liquid salts with a melting point below 100 °C which, if it is below room temperature, are called room-temperature ionic liquids (Javed et al., 2018). Ionic liquids are produced by the combination of different organic cations (e.g., imidazolium, pyridinium, and ammonium) and organic or inorganic anions (e.g., alkyl-sulfonate, tosylate) (Nasirpour et al., 2020). Ionic liquids characteristics (e.g., surface activity) are tunable by applying different cation and anion types and the cation's alkyl chain length. The surface

activity of ionic liquids increases by increasing their cation's alkyl chain length, making them effective in demulsifying emulsion (Hassanshahi et al., 2020).

Different ionic liquids (e.g., imidazolium- and ammonium-based) were used to demulsify the emulsion. The results showed that ionic liquid type and concentration, emulsifier type, temperature, and settling time were the most influential parameters in the demulsification process (Abdullah and Al-Lohedan, 2019; Atta et al., 2016a; Husain et al., 2021; Khan et al., 2021; Li et al., 2016,). Imidazolium-based ionic liquids were used successfully to demulsify emulsion (Ezzat et al., 2018; Hazrati et al., 2016; Santos et al., 2019; Silva et al., 2013). However, their high cost and toxicity are their main drawbacks which limit their applications in industries (Ezzat et al., 2022; Romero et al., 2008). Ammonium-based ionic liquids are considered environmentally friendly because they are readily biodegradable and less toxic if they have short alkyl chains (Deng et al., 2015; Sun et al., 2020). Three ammonium-based ionic liquids with different anions and structures (trioctylmethyl ammonium chloride, trioctylmethyl ammonium bromide, 1-hexadecyltrimethyl ammonium bromide) were investigated to demulsify W/O emulsion (Biniaz et al., 2016). Their results showed that the highest demulsification efficiency (100%) was achieved by the most hydrophobic ionic liquid (trioctylmethylammonium chloride). The optimum demulsification conditions for this ionic liquid were at a concentration of 1039.22 mg/L and a temperature of 78.49 °C (Biniaz et al., 2016). Another research investigated the effect of different ammonium-based ionic liquids (trihexylmethylamminium methylsulfate, trioctylmethylammonium chloride, trioctylmethylammonium ethylsulfate, and trioctylmethylammonium methylsulfate) on demulsification of W/O emulsion for different crude oil types. Based on their results, the efficiency of ionic liquids in the demulsification process depended on the crude oil types (i.e.,

different amounts of natural emulsifiers) (Oropeza et al., 2016). Ammonium-based ionic liquids used in previous research still have high toxicity due to the long cation's alkyl chains in their structure, limiting their industrial applications (Deng et al., 2015). The ionic liquid structure should be manipulated to reduce its toxicity and be environmentally friendly. In previous research, ionic liquid toxicity and biodegradability analysis showed that substituting hydroxyl functional groups for cation's alkyl chains is one solution to reduce ionic liquid toxicity significantly and increase the ionic liquid biodegradability (Deng et al., 2015; Gathergood and Scammells, 2002). However, there is no research to study whether substituting hydroxyl groups with the alkyl chains affects the ionic liquid performance in the crude oil demulsification process. This research investigates the performance of a new ammonium-based ionic liquid containing hydroxyl groups to demulsify crude oil emulsion. This worthwhile investigation shows the role of hydroxyl groups on the ionic liquid performance in the demulsification process and develops the application of an environmentally friendly ionic liquid in industries.

This research evaluates the efficiency of tris(2-hydroxyethyl) methylammonium methylsulfate (MTEOA $MeOSO_3$), which has three hydroxyl groups in the side chains, in demulsifying crude O/W emulsion. The effects of crucial demulsification parameters, including MTEOA $MeOSO_3$ concentration, demulsification temperature, gravity separation settling time, and emulsifier type, were investigated in the demulsification process. Spectrophotometric analysis of the emulsion was measured before and after the demulsification process to investigate this ionic liquid's potency in the demulsifying emulsion. Microscopic images of the emulsion were also taken before and after the demulsification process to monitor the changes in emulsified oil droplets' size in the aqueous phase.

5.2. Materials and methods

5.2.1. Materials

Cold Lake Blend (CLB) heavy crude oil used in this study was obtained by Multi-Partner Research Initiative (MPRI) in Canada. The physicochemical properties of CLB crude oil is listed in Table 3.1 (Chapter 3). MTEOA $MeOSO_3$ ionic liquid (≥95%) and Tween 20 (≥40%) were purchased from Sigma-Aldrich Company, Canada. Required salts to make synthetic ocean water were magnesium chloride hexahydrate ($MgCl_2.6H_2O$, 99.4%), calcium chloride anhydrous ($CaCl_2$, ≥96.0%), sodium bicarbonate ($NaHCO_3$, 100.1%), sodium sulfate anhydrous (Na_2SO_4, 99.5%), sodium hydroxide (NaOH, ≥97.0%) which were purchased from Fisher Scientific Company, Canada as well as strontium chloride hexahydrate ($SrCl_2.6H_2O$, 99.0%), potassium chloride (KCl, 99.0–100.5%), potassium bromide (KBr, ≥99.0%), boric acid (H_3BO_3, ≥99.5%), sodium fluoride (NaF, ≥99.0%), sodium chloride (NaCl, ≥99.0%), which were purchased from Sigma-Aldrich Company, Canada. All the chemical materials were at American Chemical Society reagent grade and used without further purification. Anhydrous silica gel (75-150 μm, 30 Å pore size, Davisil Grade 923) and sodium sulfate (granular anhydrous) were purchased from Sigma-Aldrich Company, Canada. They were dried at 200 – 250 °C for 24 hours. Hexane and dichloromethane were at high-performance liquid chromatography (HPLC) grade and were purchased from Sigma-Aldrich Company, Canada. A water purification system produced the ultrapure water used in this research (Milli-Q Advantage A10).

5.2.2. Methods

5.2.2.1. Synthesis of ocean water

The ocean water was synthesized based on the ASTMD1141 method (ASTM, 2013). The synthetic ocean water's chemical concentrations are listed in Table 4.2 (Chapter 4). A few mL of sodium hydroxide solution (0.1N) were used to adjust the pH of synthetic ocean water to 8.2 by a Mettler Toledo FG2 portable pH meter before starting each experiment.

5.2.2.2. Ionic liquid characterization

The water solubility of MTEOA $MeOSO_3$ ionic liquid was determined following the previous research method (Yuan et al., 2022). To this aim, 1 g of MTEOA $MeOSO_3$ was dissolved in 99 g of water, and the water solubility was evaluated. The thermal stability of MTEOA $MeOSO_3$ was investigated by thermogravimetric analysis (TGA) (TA instruments Discovery TGA). TGA analysis was conducted under a nitrogen atmosphere from 30 °C to 300 °C at a heating rate of 10 °C/min. Other characteristics of MTEOA $MeOSO_3$ ionic liquid reported by the Sigma-Aldrich Company are listed in Table 5.1. The schematic structure of MTEOA $MeOSO_3$ ionic liquid is shown in Figure 5.1.

Table 5.1. Properties of MTEOA $MeOSO_3$ ionic liquid (data is based on the safety data sheet from Sigma-Aldrich company).

Parameter	Result
Formula	$C_8H_{21}NO_7S$
Molecular weight	275.32 g/mol
Relative density	1.320 g/cm^3 at 20 °C
pH	7.0-8.0 at 20 g/L at 20 °C
Initial boiling point	> 180 °C
Biodegradability	Readily biodegradable
Toxicity to fish (LC50)	Danio rerio (zebrafish) - > 5,000 mg/L - 96 h

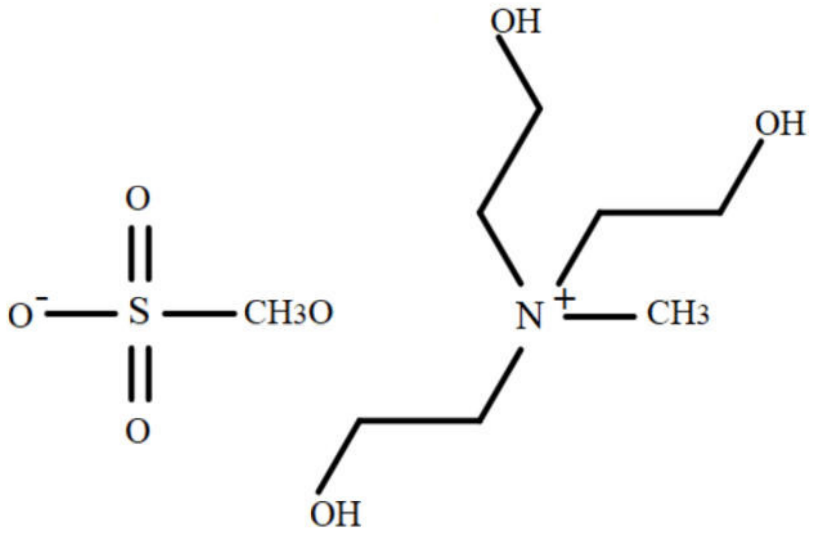

Figure 5.1. Schematic structure of MTEOA $MeOSO_3$ ionic liquid.

5.2.2.3. O/W emulsion preparation

Two types of O/W emulsion (I) and (II) were prepared to simulate generated emulsion in oil and gas industries and oceans with different emulsifiers, respectively. O/W emulsion (I) was prepared by dissolving 0.2 g Tween 20 in 100 mL of synthetic ocean water (salinity: ~36 g/L, pH: 8.2) and mixed by hand a few times. Tween 20 was selected because it is a common surfactant used in the petroleum industry (Chew et al., 2017). Then 0.3 g of CLB crude oil was poured into the 100 mL of synthetic ocean water and sonicated using a Q700 Sonicator (Qsonica, 20 kHz, solid titanium probe diameter = 12.7 mm, USA) to make emulsion at 3000 mg/L. Sonicator conditions were at the amplitude of 100%, sonication time of 10 min at a pulse condition of 20:20 seconds (On/ Off). O/W emulsion (II) was prepared without adding Tween 20. CLB crude oil (1.5 g) was poured into 100 mL of synthetic ocean water (salinity: ~36 g/L, pH: 8.2) and heated at 50 °C on a heater (Thermo Scientific) for 5 min to reduce the oil viscosity. Then their mixture was sonicated continuously for 15 min, starting at the amplitude

of 50% and then increasing to 80% and 100% and sonicating the solution at each amplitude for 5 min. Figures 5.2a and 5.2b show the oil droplets' size distribution in emulsion (I) and emulsion (II), respectively. There was no significant sign of emulsion breaking during the experimental time. The effect of emulsifier type (natural emulsifiers (e.g., asphaltenes) and Tween 20+natural emulsifiers) on the ionic liquid performance in crude oil demulsification was investigated by comparing the demulsification efficiency of emulsion (I) and emulsion (II).

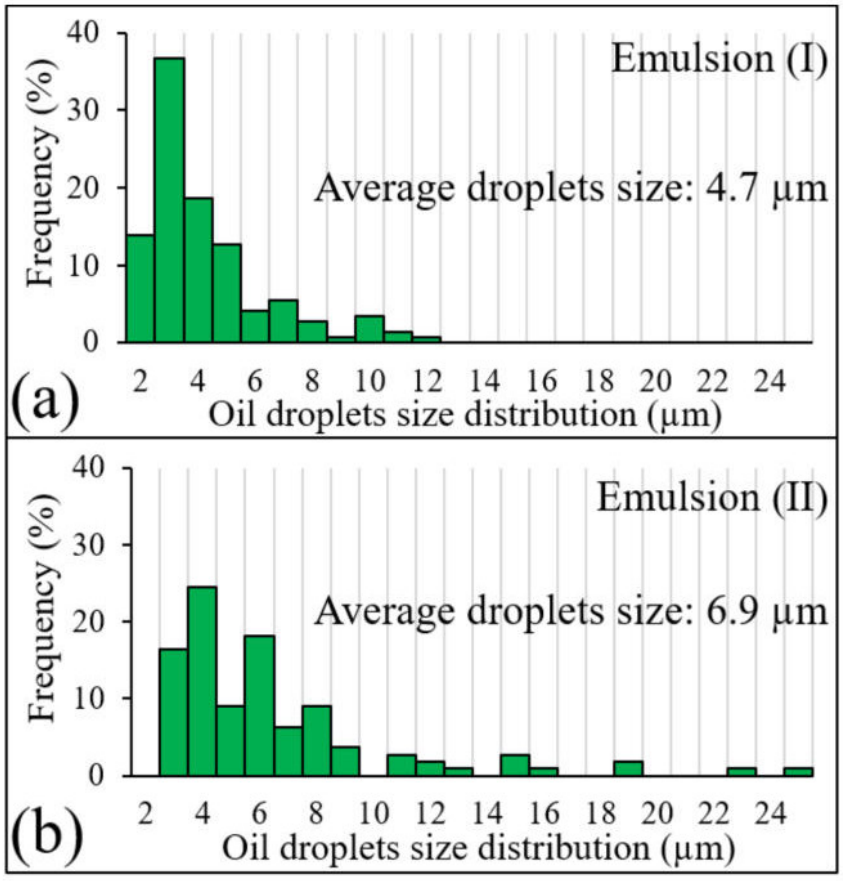

Figure 5.2. Oil droplets size distribution in the emulsion a) emulsion (I), b) emulsion (II).

5.2.2.4. Demulsification process

The demulsification process was conducted in a batch system. Specific amounts of MTEOA $MeOSO_3$ (25−1000 mg/L) were added to 100 mL of prepared emulsion (I) and were shaken at 250 rpm by a Talboy 3500 Orbital Shaker for 10 min. Then the mixture was settled in a water bath at different temperatures (25,40,50 ± 2°C) and settling times (30−120 min). Experiments considering the effect of settling times were repeated three times to ensure the reproducibility of the results, and the average was reported. A similar process was conducted on emulsion (II) by adding different MTEOA $MeOSO_3$ concentrations (25,50,100 mg/L) at room temperature (~ 25 °C) to investigate the effect of emulsifier type (natural emulsifiers and Tween 20+natural emulsifiers) on the demulsification efficiency. A portion of the separated water was collected for liquid-liquid extraction to analyze the total extractable petroleum hydrocarbons (TEPH) in the separated water based on the method explained in the following section. Demulsification efficiency was calculated following equation (5.1) (Hassanshahi et al., 2022). A gravity separation experiment was also performed without adding ionic liquid (control experiment).

$$Demulsification\ efficiency = \frac{C_i - C_f}{C_i} \times 100 \quad (5.1)$$

Where, C_i and C_f are the initial and final concentrations of TEPH in the emulsion and the separated water, respectively.

5.2.2.5. Analysis of TEPH in separated water and emulsion

TEPH in separated water was extracted following the liquid-liquid extraction method in the British Columbia laboratory manual (British Columbia laboratory manual, 2017). A water

sample (40 mL) was taken from the separated water (bottom layer) and mixed with 2 mL of solvent (hexane/ dichloromethane (1:1 vol.)). The volume ratio of solvent to sample was 1 to 20. The mixture of solvent and sample was shaken vigorously for 30 min. After that, the solvent and water were allowed to separate in a separatory funnel. The solvent was then collected in a 20 mL glass vial ($vial_1$). The extraction process was repeated with another fresh 2 mL of solvent, and then the solvent was collected in $vial_1$. After that, the separatory funnel was rinsed with 2 mL of solvent and collected in $vial_1$. Anhydrous sodium sulfate (0.3 g) was added to the $vial_1$ and mixed to remove the moisture. Then the extraction solvent was poured into another 20 mL glass vial ($vial_2$) containing 3 g of silica gel and mixed to remove polar organic compounds. Then the extraction was poured into another 20 mL glass vial ($vial_3$). $Vial_1$ and $vial_2$ were washed with 2 mL of solvent sequentially, and then the solvent was collected in $vial_3$. This process was repeated with 3 mL of solvent twice to ensure the TEPH was collected. A portion of extraction in $vial_3$ was taken to analyze TEPH using an Agilent 6890 gas chromatograph with a flame ionization detector (GC-FID). The hydrocarbons mixtures were grouped in (nC_{10}–nC_{19}), (nC_{19}–nC_{32}) and (nC_{32}–nC_{50}). Decane (nC_{10}), nonadecane (nC_{19}), eicosane (nC_{20}), dotriacontane (nC_{32}), tetriacontane (nC_{34}) and pentacontane (nC_{50}) were used as the external standards. A ZB-1HT INFERNO capillary column (Phenomenex) with a length of 30 m, an inner diameter of 0.32 mm, and a film thickness of 0.25 µm was used. The carrier gas was helium at a rate of 1.6 mL/min. TEPH extract (1 µL) was injected into the system, and a split ratio of 10:1 was performed for each run. During analysis, the injector and detector temperatures were kept at 290 °C and 320 °C, respectively. The initial temperature of the oven was at 130 °C, then increased to 310 °C and 340 °C at 20 °C/min and 5 °C/min, respectively,

and held at 340 °C for 8 min. A similar procedure was conducted to determine the TEPH in the emulsion.

5.2.2.6. Optical microscopic analysis

A sample drop was poured onto a clear glass slide and placed under a compound microscope (Fisher Scientific, AX800) with a 200X objective magnification to analyze the oil droplets visually. The captured microscopic images of the emulsion were analyzed using SeBaView software (version 4.7). According to the images, the oil droplets' size distribution was determined before and after the demulsification process (Kuang et al., 2020b; Yuan et al., 2022).

5.2.2.7. Spectrophotometric analysis

The spectra of emulsion before and after the demulsification process was monitored at the wavelength ranges of 200−600 nm using UV-Vis Spectrophotometers 8100 (OrionTM AquaMate UV-Vis spectrophotometer, Perkin Elmer). The sample was taken at 3.5 mL of quartz Suprasil cell with 1.0 cm path length and polytetrafluoroethylene lid, and measurement was conducted at room temperature (25 °C).

5.3. Results and discussion

5.3.1. Ionic liquid characterization

Water solubility analysis showed that MTEOA $MeOSO_3$ dissolved in the water completely and is suitable for the demulsification process where water is the continuous phase. The ionic liquid's thermal stability is shown in Figure 5.3 based on TGA analysis. The results indicated that MTEOA $MeOSO_3$ ionic liquid remained stable at higher temperatures before reaching its

initial boiling point (> 180 °C). At a temperature higher than that, mass loss started. Based on the TGA graph, MTEOA $MeOSO_3$ was thermal stable within the experimental temperatures.

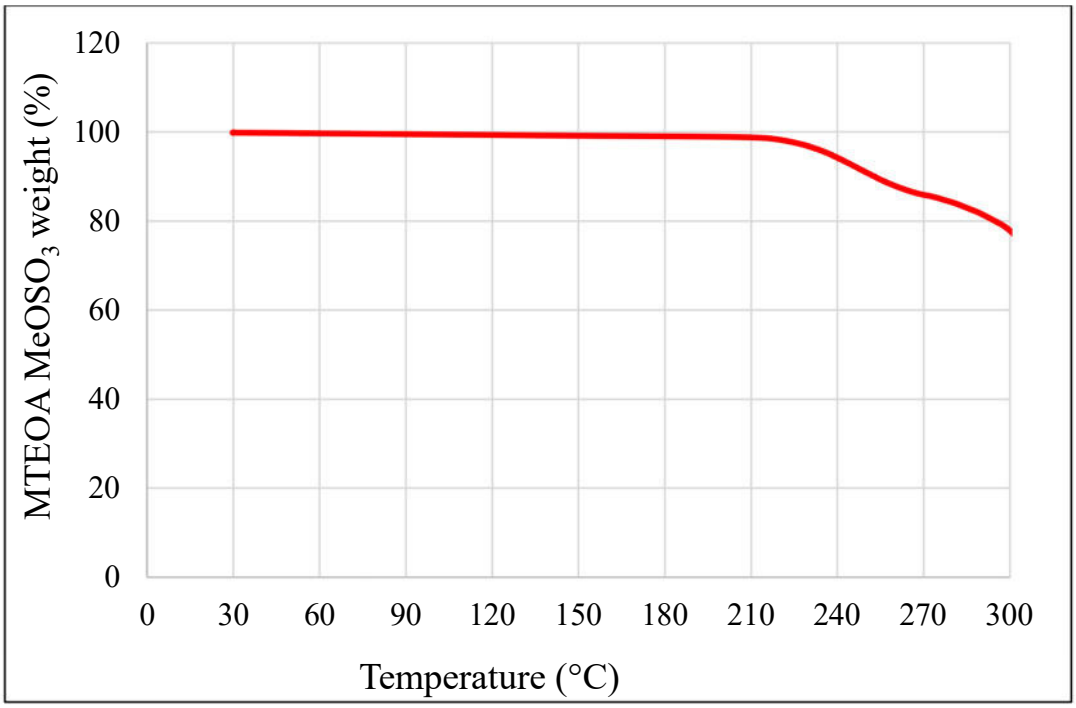

Figure 5.3. TGA analysis of MTEOA $MeOSO_3$ ionic liquid (heating rate: 10 °C/min, under a nitrogen atmosphere).

5.3.2. Parameters influencing the demulsification process

5.3.2.1. Ionic liquid concentration and demulsification temperature

The effect of MTEOA $MeOSO_3$ concentration (25−1000 mg/L) in demulsifying emulsion (I) at 25 °C (room temperature) after 90 min settling is shown in Figure 5.4a. By increasing MTEOA $MeOSO_3$ concentration from 25 mg/L to 100 mg/L, demulsification efficiency reached around 51%, and the TEPH was reduced to 428 mg/L (Table 5.2). Hydroxyl groups in the side chains of MTEOA $MeOSO_3$ weakened the rigid film around emulsified oil droplets by breaking the generated hydrogen bond between emulsifiers (Tween 20+natural emulsifiers)

and water and reconstructing it between MTEOA $MeOSO_3$ molecules and water. This helped with the coalescence of emulsified oil droplets and separation from the water phase (Ma et al., 2021; Ma et al., 2022). However, increasing ionic liquid concentration to 300 mg/L reduced demulsification efficiency significantly (demulsification efficiency: ~17%). Hydroxyl groups (OH^-) in the side chains have a negative charge on the ionic liquid surface (Jia et al., 2020). Asphaltenes of crude oil (i.e., natural emulsifier) that formed the rigid film at the oil-water interface also have a negative surface charge at pH > 4 (Ezzat et al., 2021). Increasing MTEOA $MeOSO_3$ concentration to 300 mg/L led to the abundance of hydroxyl groups in the emulsion, which brought about a repulsive force among MTEOA $MeOSO_3$ molecules and oil droplets. Hence, MTEOA $MeOSO_3$ molecules were distributed in the emulsion (I) rather than adsorbing at the oil-water interface. This was confirmed by decreasing the demulsification efficiency and increasing the TEPH in the separated water (Table 5.2). A further increase in MTEOA $MeOSO_3$ concentration to 700 mg/L increased demulsification efficiency slightly (reached ~28%), and then it decreased (to 24%) at a higher MTEOA $MeOSO_3$ concentration (1000 mg/L). This slight increase in demulsification efficiency might be due to many MTEOA $MeOSO_3$ molecules in the emulsion (I), which pushed them to reach the oil-water interface.

The effect of demulsification temperature on the demulsification efficiency of emulsion (I) was investigated by conducting a set of experiments at different MTEOA $MeOSO_3$ concentrations (25−500 mg/L) and demulsification temperatures (40, 50 °C ± 2°C) for 90 min settling (Figure 5.4b). The results indicated that temperature directly affected the demulsification efficiency for all the ionic liquid concentrations. Compared with room temperature (25 °C, Figure 5.4a), increasing the temperature to 50 °C improved the demulsification efficiency by increasing the oil droplets' movement and the chance of their

collision in the emulsion (I). This was proved by increasing the demulsification efficiency from 36% to 46% at 25 °C and 50 °C, respectively, when 25 mg/L of MTEOA $MeOSO_3$ was used. Higher temperatures (50 °C) accelerated the rise and separation of coalesced oil droplets. The best demulsification condition to demulsify emulsion (I) was at the MTEOA $MeOSO_3$ concentration of 50 mg/L and the temperature of 50 °C, which resulted in 61% demulsification efficiency.

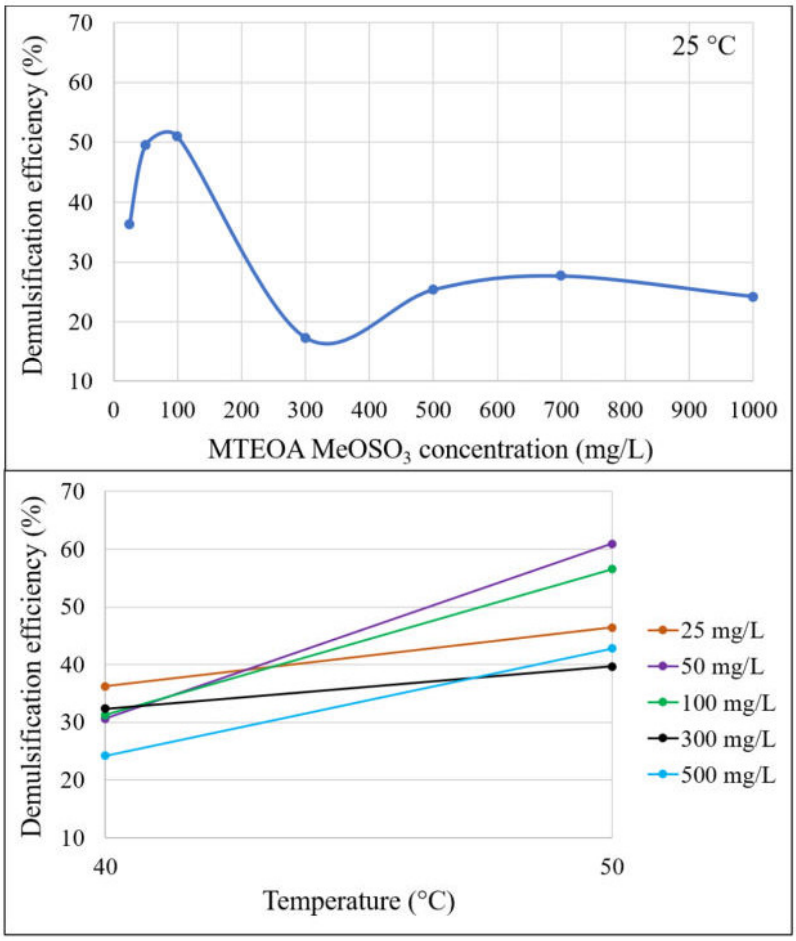

Figure 5.4. Effect of MTEOA $MeOSO_3$ concentrations and temperatures on demulsification efficiency of emulsion (I) after 90 min settling.

Table 5.2. TEPH concentration and EPH fractions in the separated water at different MTEOA $MeOSO_3$ concentrations and temperatures after 90 min of settling time.

Experimental parameters		EPH in separated water			
MTEOA $MeOSO_3$ concentration (mg/L)	Temperature (°C ± 2)	TEPH concentration (mg/L)	EPH (C_{10}–C_{19}) fraction (%)	EPH (C_{19}–C_{32}) fraction (%)	EPH (C_{32}–C_{50}) fraction (%)
25	25	556	39	55	6*
50		440	45	53	2*
100		428	49	50	1*
300		721	42	53	5*
500		651	41	54	5*
700		631	41	53	6*
1000		661	41	53	6*
25	40	556	38	54	8*
50		605	42	53	5*
100		599	42	54	4*
300		590	41	54	5*
500		661	38	54	8*
25	50	467	38	57	5*
50		341	39	55	6*
100		379	38	57	5*
300		526	37	54	9
500		499	36	55	9*

* Data was below the detection limit.

5.3.2.2. Settling time

As indicated earlier, the best demulsification efficiency of emulsion (I) was achieved at the MTEOA $MeOSO_3$ concentration of 50 mg/L and demulsification temperature of 50 °C. The effect of gravity settling time (30, 60, 90, 120 min) on the demulsification efficiency of emulsion (I) was investigated under this condition. As shown in Figure 5.5, settling time impacted demulsification efficiency significantly. By increasing the settling time from 30 min to 90 min, the demulsification efficiency increased from 37% to 61%, and the TEPH decreased from 547 mg/L to 341 mg/L (Table 5.3), respectively. At 120 min, the demulsification efficiency reached 69% (slightly changed compared to 90 min settling), indicating reaching the equilibrium state of the demulsification process at 90 min settling. Oil droplets' size distribution (Figure 5.6) also indicated that the demulsification efficiency started once the MTEOA $MeOSO_3$ was added to the emulsion (I). Oil droplets' size distribution in the blank (i.e., emulsion (I)) is shown in Figure 5.6a. Most oil droplets in the blank were lower than 5 μm in diameter, indicating high emulsion (I) stability. After mixing MTEOA $MeOSO_3$ in the emulsion (I), the oil droplet's size increased to 50 μm (10 folds) within 1 min of settling time (Figure 5.6b), indicating the rigid film ruptured at the oil-water interface, and the oil droplets flocculated and coalesced. The hydrophilicity of MTEOA $MeOSO_3$ (i.e., water solubility) and its low molecular weight (275.32 g/mol) brought about this quick diffusion of MTEOA $MeOSO_3$ molecules in the emulsion (I) and reaching the oil-water interface. Oil droplets in the emulsion (I) reached a wider range of sizes after 5 min of settling, Figure 5.6c. Flocculating and coalescing of the oil droplets in the emulsion (I) continued after 15 min of settling time (Figure 5.6d), and its rate gradually reduced, as shown by the reduction in oil droplets' size in the emulsion (I) in Figures 5.6e and 5.6f. Hence, additional settling time (≥ 30 min) provided

sufficient time for separating the coalesced oil droplets. After 90 min settling time (Figures 5.6g and 5.6h), coalesced oil droplets separated, and the persistent emulsified oil droplets remained in the separated water (bottom layer). The oil droplets in the separated water were as small as those in the blank (Figure 5.6a). No further flocculation and coalescence happened after 90 minutes of settling time, indicating that the demulsification process reached equilibrium.

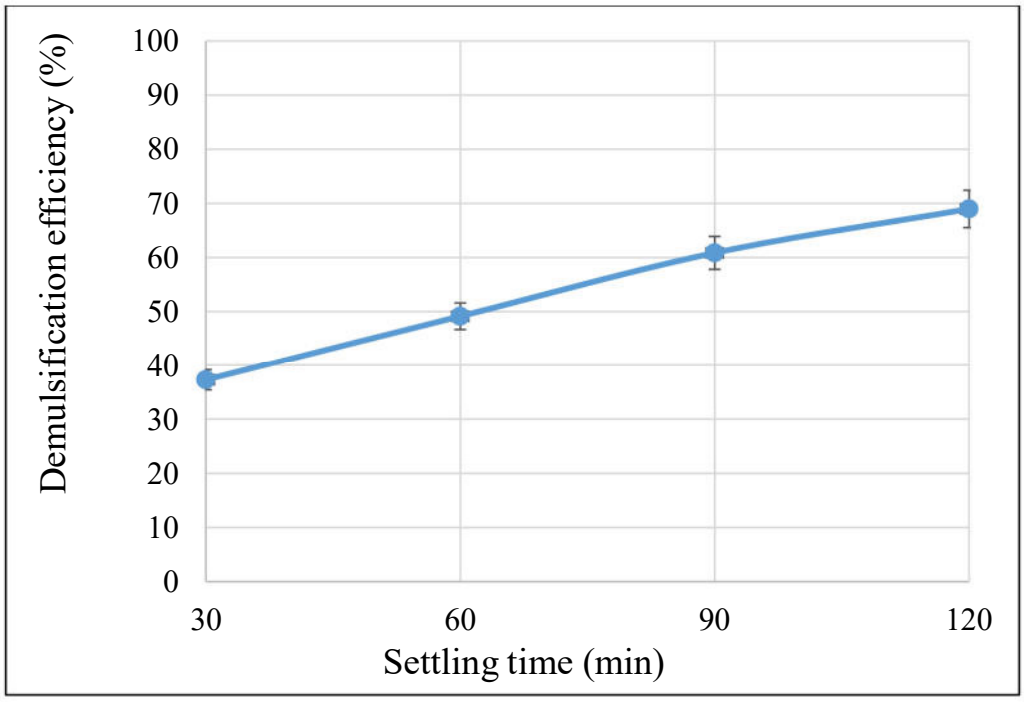

Figure 5.5. Effect of settling time on demulsification efficiency of emulsion (I) at the MTEOA $MeOSO_3$ concentration of 50 mg/L and demulsification temperature of 50 °C.

Table 5.3. TEPH concentration and EPH fraction in separated water at different settling times at MTEOA $MeOSO_3$ concentration of 50 mg/L and demulsification temperature of 50 °C.

Experimental parameter		EPH in separated water			
		TEPH concentration (mg/L)	EPH (C_{10}–C_{19}) fraction (%)	EPH (C_{20}–C_{32}) fraction (%)	EPH (C_{32}–C_{50}) fraction (%)
Settling time (min)	30	547	33	52	15
	60	443	33	50	17
	90	341	34	50	16
	120	270	37	50	13

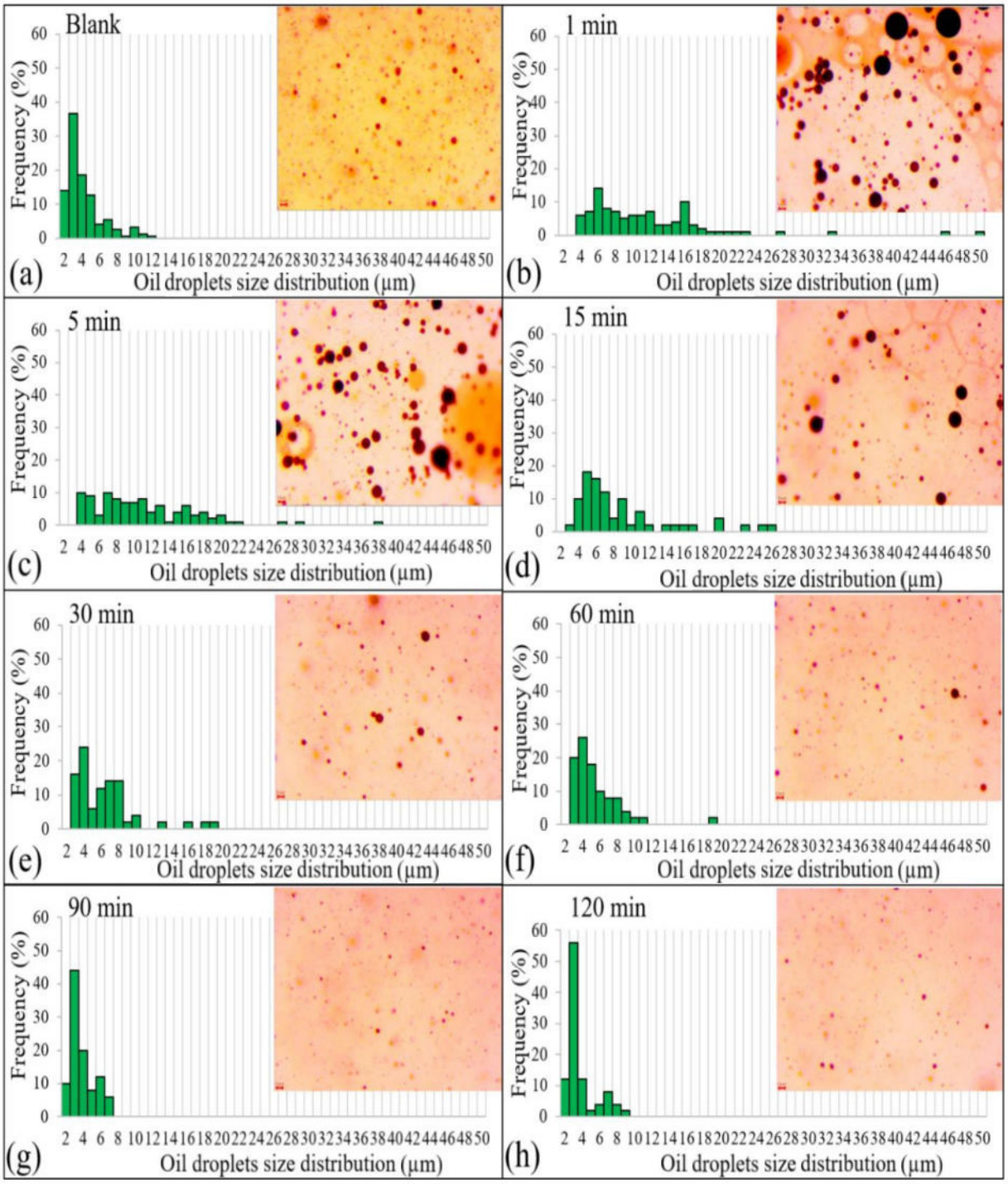

Figure 5.6. Oil droplets size distribution in the emulsion (I) a) blank: without MTEOA $MeOSO_3$, b-h) after adding 50 mg/L of MTEOA $MeOSO_3$ at the demulsification temperature of 50 °C at different settling times.

5.3.2.3. Emulsifier type

Emulsifiers form a rigid film at various thicknesses at the oil-water interface, which determines the emulsion stability. When a mixture of emulsifiers is in an emulsion, various molecular interactions occur at the oil-water interface (e.g., electrostatic, hydrogen bonding), which affects the interface thickness (McClements and Jafari, 2018). Emulsion with a thick film at the interface has high stability, which may affect the ionic liquid performance. As shown in Figure 5.2, the average oil droplets size in the emulsion (I) and (II) were 4.7 μm and 6.9 μm, respectively, indicating that a mixture of Tween 20+natural emulsifiers generated emulsion (I) with smaller oil droplets size distribution (i.e., higher stability). The effect of emulsifier type, including Tween 20+natural emulsifiers (emulsion (I)) and natural emulsifiers (emulsion (II)), on the performance of MTEOA $MeOSO_3$ in the demulsification process, was studied. Different MTEOA $MeOSO_3$ concentrations (25,50,100 mg/L) were added to emulsion (II) at room temperature (25 °C) and were shaken at 250 rpm for 10 min without considering a gravity settling. The results were shown in Figure 5.7 and compared with similar experimental conditions on emulsion (I) after 90 min gravity settling. It was found that emulsifier type significantly affects the MTEOA $MeOSO_3$ performance. The synergistic interaction of Tween 20 and natural emulsifiers (e.g., asphaltenes) in emulsion (I) led to a thick rigid film at the oil-water interface that MTEOA $MeOSO_3$ could not break it effectively. Hence, emulsified oil droplets remained in the separated water, resulting in low demulsification efficiency (≤51%). In contrast, MTEOA $MeOSO_3$ was most effective in breaking the rigid film at the oil-water interface created by natural emulsifiers (e.g., asphaltenes), resulting in outstanding demulsification efficiency (≥92%). At the MTEOA $MeOSO_3$ concentration of 25 mg/L, the TEPH in the separated water reduced to 33 mg/L, and

a further increase in the MTEOA $MeOSO_3$ concentration (100 mg/L) reduced the TEPH to 17 mg/L (demulsification efficiency: 96%). Hence, the optimum demulsification efficiency (92%) on Emulsion (II) occurred at MTEOA $MeOSO_3$ concentration of 25 mg/L at room temperature (25 °C) without settling.

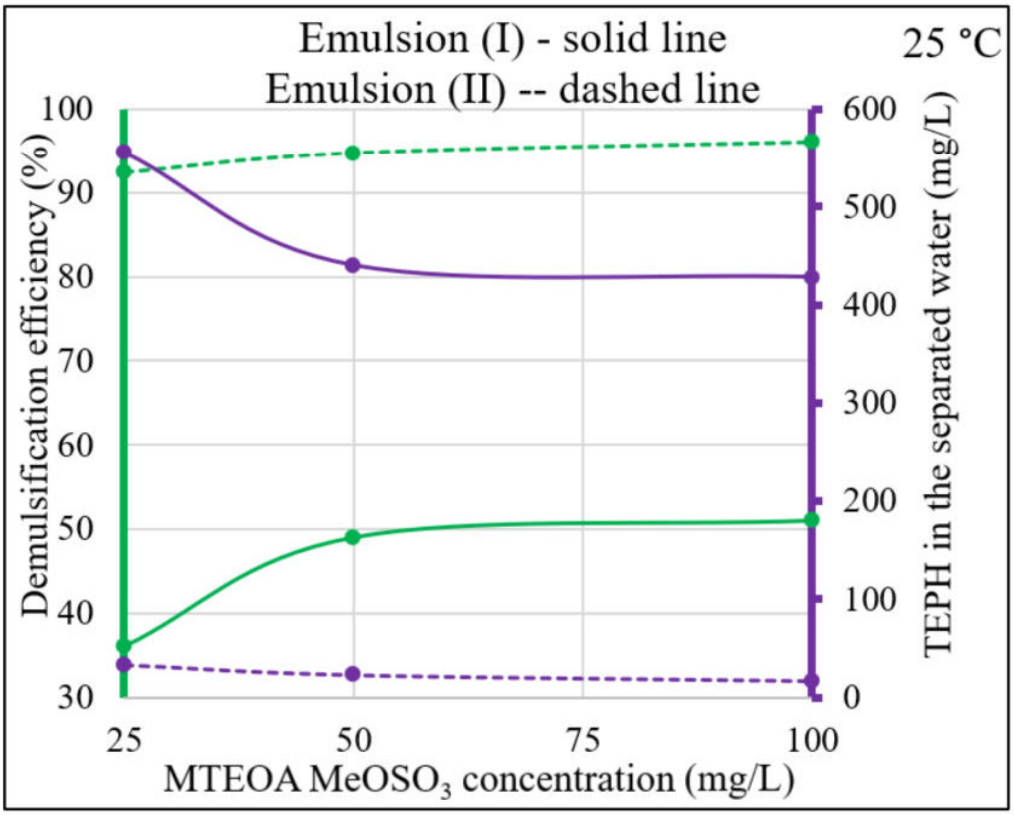

Figure 5.7. Effect of emulsifier type on demulsification efficiency by MTEOA $MeOSO_3$.

Spectrophotometric analysis and optical microscopic images of emulsions (I) and (II) and the separated waters at their best demulsification condition are shown in Figure 5.8 and Figure 5.9, respectively. Figure 5.8 shows two peaks in emulsions (I) and (II) at 235 nm and 260 nm, corresponding to benzenic and naphthenic compounds in crude oil, respectively. As shown in Figure 5.8a, the peaks dropped slightly after demulsifying emulsion (I), which shows that the

oil concentration in the separated water was still high. In contrast, Figure 5.8b shows that the peaks dropped significantly, indicating low oil concentration in the separated water after demulsifying emulsion (II). This result is consistent with the real and optical microscopic images of emulsions (I) and (II) and their separated waters (Figure 5.9). Figure 5.9a shows that the separated water was turbid and contained highly emulsified oil droplets, indicating that MTEOA $MeOSO_3$ could not demulsify all of the oil droplets, which Tween 20+natural emulsifiers stabilized. On the contrary, Figure 5.9b shows that the separated water was clear, and the number of emulsified oil droplets in the separated water was low. This observation proved that MTEOA $MeOSO_3$ ionic liquid could effectively demulsify emulsion (II) generated by natural emulsifiers.

Based on the above results, it was concluded that MTEOA $MeOSO_3$ with the hydroxyl groups in the side chains rather than alkyl chains effectively demulsified emulsion (II) stabilized by natural emulsifiers. However, its efficiency was reduced when Tween 20 (a commercial surfactant) and natural emulsifiers stabilized the emulsion (I). This indicated that the rigid film around emulsified oil droplets by Tween 20+natural emulsifiers was thicker than the one with only natural emulsifiers. Hence, MTEOA $MeOSO_3$ is effective at a low concentration in demulsifying emulsion generated due to marine oil spills, in which natural emulsifiers in crude oil stabilize oil droplets.

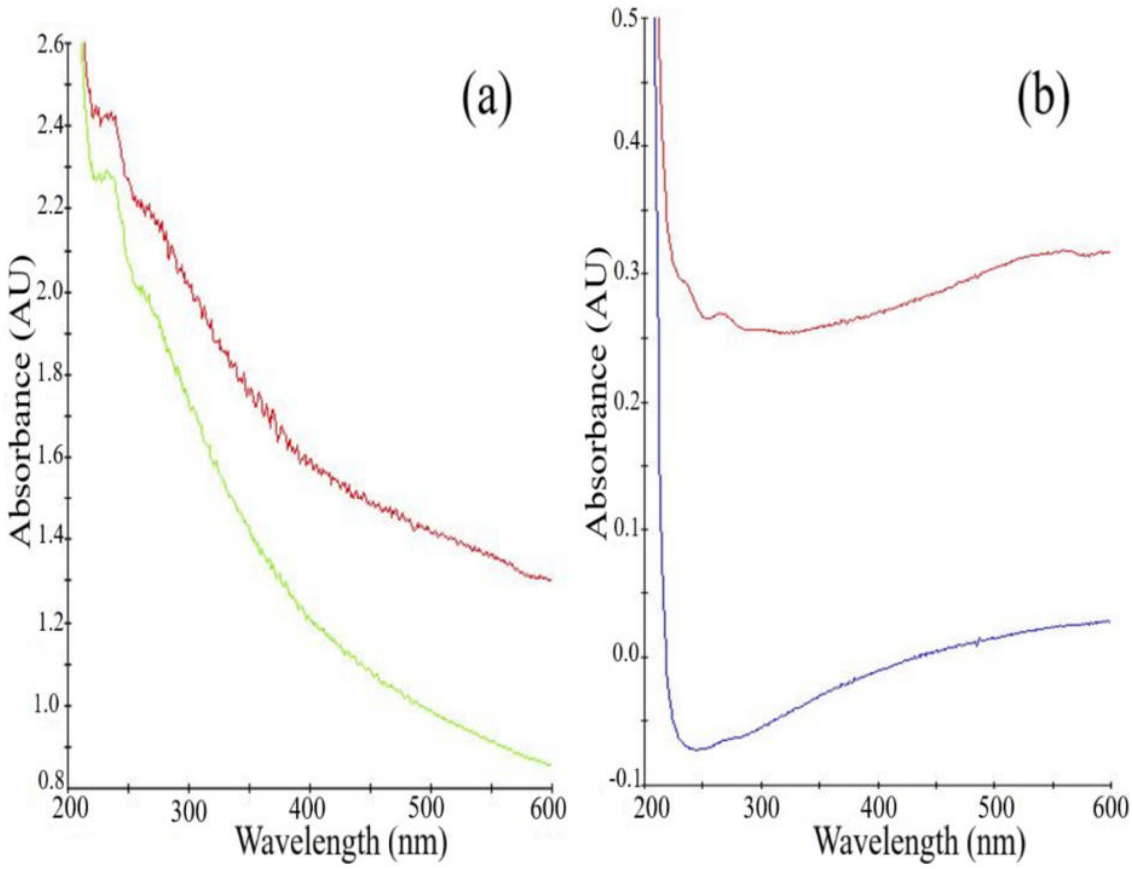

Figure 5.8. Spectrophotometric of emulsion (I) and (II) and the separated water

a) emulsion (I) (red line) and the separated water (green line) at the best demulsification condition (MTEOA $MeOSO_3$ concentration: 50 mg/L, temperature: 50 °C, settling time: 90 min)

b) emulsion (II) (red line) and the separated water (blue line) at the optimum demulsification condition (MTEOA $MeOSO_3$ concentration: 25 mg/L, temperature: 25 °C, without settling).

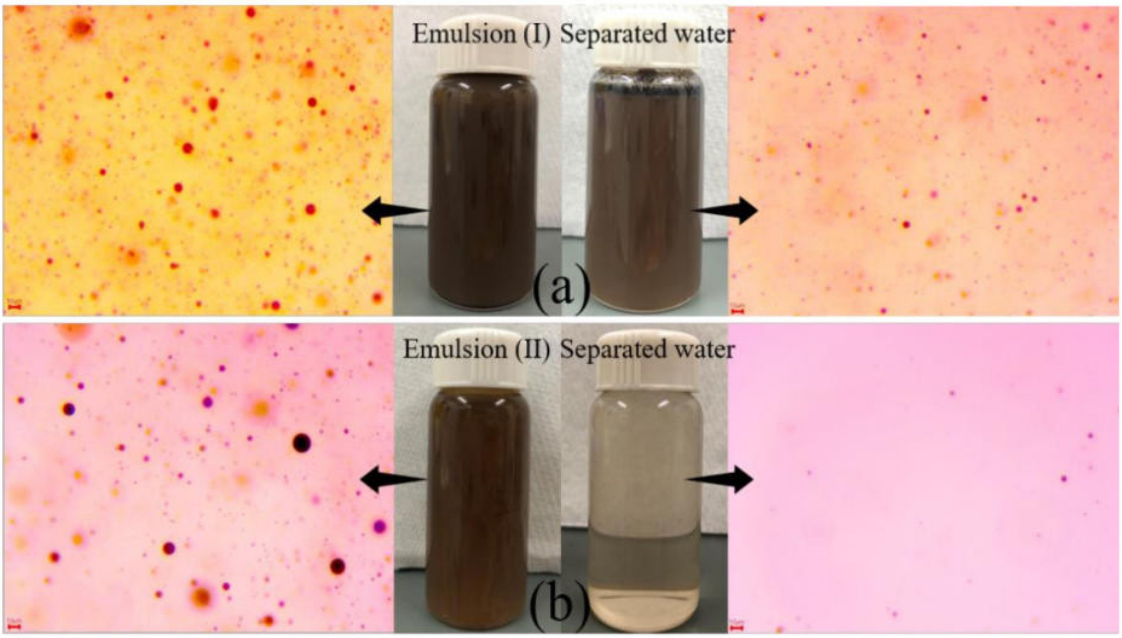

Figure 5.9. Real and optical microscopy images of emulsion (I) and (II) and the separated water at their best demulsification condition

a) MTEOA $MeOSO_3$ concentration: 50 mg/L, temperature: 50 °C, settling time: 90 min

b) MTEOA $MeOSO_3$ concentration: 25 mg/L, temperature: 25 °C, without settling.

5.3.3. Demulsification mechanism

The proposed demulsification mechanism by MTEOA $MeOSO_3$ is shown in Scheme 5.1. Emulsion (I) generated by Tween 20+natural emulsifiers formed a rigid film around oil droplets through hydrogen bonding among oxygen molecules of Tween 20 and asphaltenes (i.e., natural emulsifiers) and hydrogen molecules of water. Emulsion (II) generated by natural emulsifiers also formed a rigid film around oil droplets due to hydrogen bonding among oxygen molecules of asphaltenes and hydrogen molecules of water. The latter film might be thinner than the one in emulsion (I) in the absence of Tween 20. MTEOA $MeOSO_3$ is a low molecular weight (275.32 g/mol) ionic liquid that diffused quickly in the emulsion. At the oil-

water interface, the hydroxyl groups (OH^-) of MTEOA $MeOSO_3$ broke the hydrogen bond between water molecules and emulsifiers (Tween 20 and/or asphaltenes) and reconstructed it among oxygen molecules of MTEOA $MeOSO_3$ and hydrogen molecules of water. This helped with the flocculation and coalescence of emulsified oil droplets and separation from the water phase. The results showed that MTEOA $MeOSO_3$ molecules were more efficient in breaking the rigid film formed by the natural emulsifiers.

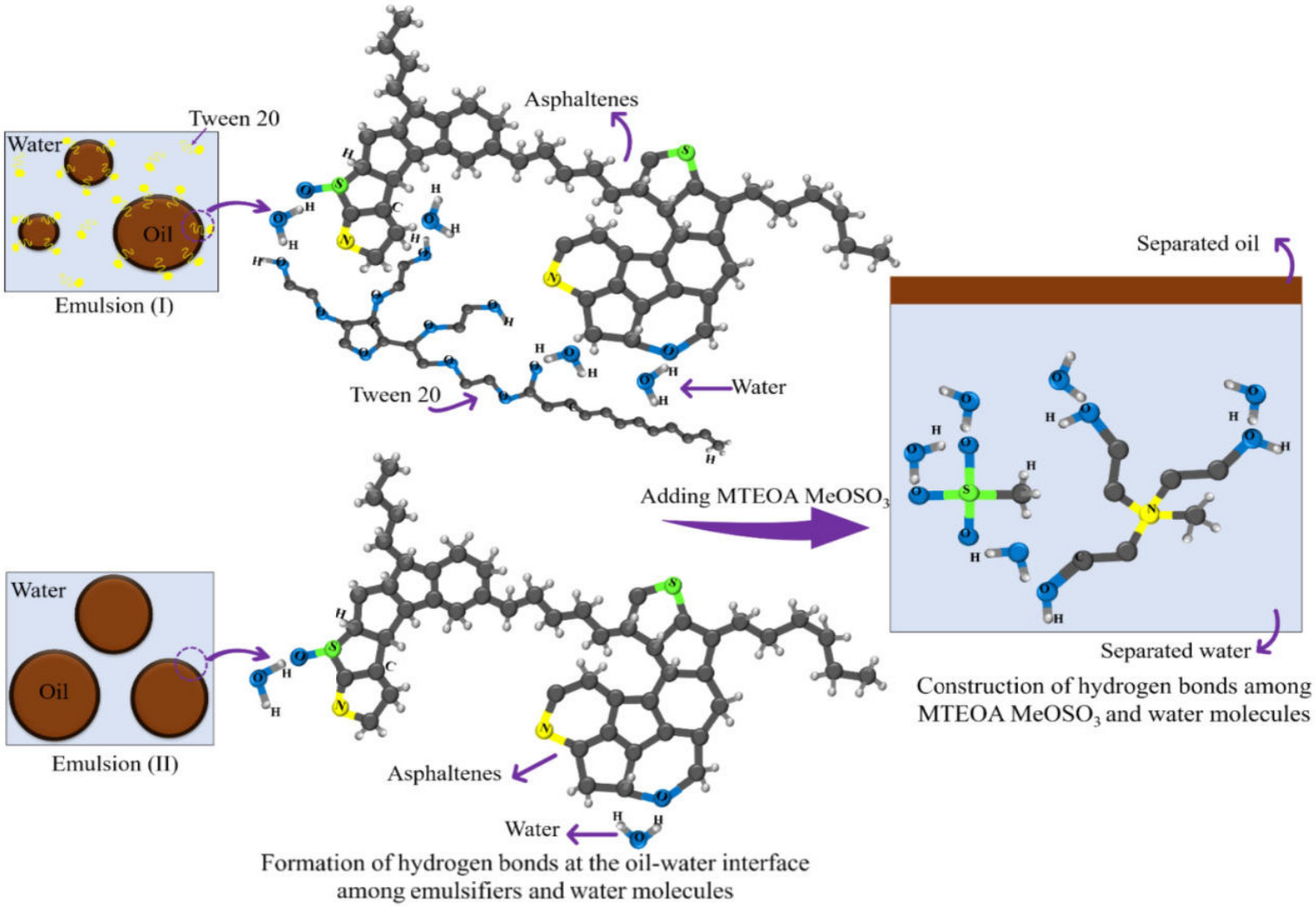

Scheme 5.1. Demulsification mechanism by MTEOA $MeOSO_3$.

5.4. Summary

This research evaluated the performance of MTEOA $MeOSO_3$ ionic liquid in demulsifying crude O/W emulsion. The effects of crucial experimental parameters on demulsification efficiency were investigated, including MTEOA $MeOSO_3$ concentration, demulsification temperature, gravity separation settling time, and emulsifier type. The results showed that MTEOA $MeOSO_3$ effectively demulsified emulsion at a low concentration (≤ 100 mg/L). Increasing MTEOA $MeOSO_3$ concentration more than that reduced the demulsification efficiency significantly due to the presence of many hydroxyl groups (OH^-) in the emulsion, which brought about a repulsive force among negative surface charge molecules (OH^- and oil droplets). Microscopic images showed that flocculation and coalescence of oil droplets occurred within 15 min of settling time. Further settling time provided sufficient time for the coalesced oil droplets to separate until the demulsification process reached equilibrium at 90 min. Increasing demulsification temperature (50 °C) increased the rate of oil droplets collision and hastened the separation process. The MTEOA $MeOSO_3$ performance was significantly affected by the emulsifier type (natural emulsifiers and Tween 20+natural emulsifiers). MTEOA $MeOSO_3$ was effective in demulsifying emulsion (II) stabilized by natural emulsifiers at a low MTEOA $MeOSO_3$ concentration (25 mg/L) without settling time at room temperature (demulsification efficiency: 92%, TEPH: 33 mg/L). However, its efficiency was reduced when it was used for emulsion (I) generated by Tween 20+natural emulsifiers at the same experimental condition after 90 min settling (demulsification efficiency: 36%, TEPH: 556 mg/L). Spectrophotometry analysis and optical microscopic images also supported the achieved results. The rigid film formed around emulsified oil droplets in emulsion (I) might be thicker than emulsion (II), affecting MTEOA $MeOSO_3$ efficiency. The demulsification

mechanism was proposed to break the hydrogen bond among oxygen molecules of emulsifiers and hydrogen of water and reconstruct it with oxygen molecules of MTEOA $MeOSO_3$ and hydrogen of water. This study showed that MTEOA $MeOSO_3$ ionic liquid with hydroxyl functional groups rather than alkyl chains is effective in demulsifying emulsion generated by natural emulsifiers in the marine environment and develops the application of a biodegradable, low-toxic ionic liquid in industries.

Chapter 6

STUDY ON AMMONIUM-BASED IONIC LIQUIDS WITH A DIFFERENT SIDE CHAIN IN DEMULSIFYING CRUDE OIL IN WATER EMULSION

Abstract

This research investigated the performance of three ionic liquids with a different side chain on crude oil-in-water demulsification. These include dodecyl trimethylammonium chloride (DTAC), [2-(Methacryloyloxy)ethyl] trimethylammonium chloride (METAC), and (3-Acrylamidopropyl) trimethylammonium chloride (APTAC). Response surface methodology was used to investigate the effects of ionic liquid concentration, gravity separation settling time, and ionic liquid types (i.e., different side chains) on demulsification efficiency. The results showed that the selected ionic liquids effectively demulsified the emulsion with an efficiency ≥85%, and the demulsification equilibrium was achieved after a short gravity settling time (20 min). Increasing ionic liquid concentration resulted in higher demulsification efficiency for METAC and APTAC, but had an insignificant effect on the demulsification efficiency of DTAC. APTAC with the amide group on the side chain resulted in the highest demulsification efficiency (96%) compared to METAC (ester group) and DTAC (alkyl group), indicating the superiority of the amide group in demulsifying the emulsion. The demulsification mechanism for DTAC was found to be electrostatic attraction, and for METAC and APTAC it was the combination of electrostatic attraction and hydrogen bond reconstruction. Spectrophotometry and optical microscopy analysis were conducted to validate the results. This research indicated that the alkyl group substitution with amide or ester groups improved the ionic liquid potency in demulsifying oil-in-water emulsion.

Keywords: Chemical demulsification, oil in water emulsion, ionic liquid, side chains, response surface methodology.

6.1. Introduction

Emulsification is inevitable when oil is spilled and contacts water, leading to the generation of water-in-oil (W/O) or oil-in-water (O/W) emulsion (Silva et al., 2022; Wang et al., 2021; Yonguep et al., 2022). Crude oils contain a mixture of toxic organic compounds (e.g., aliphatic hydrocarbons, naphthenic acids, and polycyclic aromatic hydrocarbons), and thus their spill to water would result in adverse impacts on humans and the environment if not properly treated (Ruberg et al., 2021). Natural emulsifiers in crude oils (e.g., asphaltenes) create a rigid film by different inter- and intra-molecular interactions (e.g., hydrogen bond) around emulsified droplets that prevent coalescence and separation (Sousa et al., 2021). It is thus of importance to find effective ways to break the emulsion for oil spill treatment (Shokri and Fard, 2022).

Various physical, biological and chemical methods have been used for oil/water demulsification (Abdulredha et al., 2020). Physical methods, such as gravity separation, centrifugal separation, and electrocoalescence, have the main drawbacks of large space requirements, high maintenance and energy cost, and poor efficiency (Abdulredha et al., 2020; Less and Vilagines, 2012; Tian et al., 2022). Biological method using biodemulsifiers has the advantage of being environmentally friendly (e.g., biodegradability), but it is susceptible to operational issues (Hadi and Ali, 2022a). Chemical method using chemical demulsifiers is effective to quickly break emulsion with easy operation (Raya et al., 2020). Demulsifiers are surface-active compounds that diffuse in the emulsion and reach the oil-water interface, and break the rigid film around emulsified droplets, thus leading to enhanced oil/water separation. Critical parameters affecting demulsification include demulsifier type, demulsifier concentration, and gravity separation settling time (Ma et al., 2022; Saad et al., 2019). Demulsifiers are classified based on their structures into polymeric surfactants, ionic liquids,

and nanoparticles (Hadi and Ali, 2022b; Ma et al., 2022). Ionic liquids are liquid salts with a melting point below 100 °C (Nasirpour et al., 2020). They have been used in demulsification because of their unique properties of high thermal stability, low vapor pressure, and non-flammability (Hassanshahi et al., 2020; Nasirpour et al., 2020). Ionic liquids are produced by combining different organic cations and organic or inorganic anions. Common cations include imidazolium, phosphonium, ammonium, and pyridinium, while the anions include chloride, dicyanamide, hexafluorophosphate, and tetrafluoroborate (Singh and Savoy, 2020). The properties of ionic liquids are tunable by altering the types of cation and anion as well as the alkyl chain length of cation. For example, surface activity and hydrophobicity of ionic liquid were found to increase by increasing the cation's alkyl chain length (Hassanshahi et al., 2020).

Various ionic liquids were studied to investigate their effects on demulsification. Masri et al. (2022) found that increasing ionic liquid concentration (1000 mg/L) and settling time (60 min) increased demulsification efficiency, while ionic liquid type was a crucial parameter affecting the demulsification process (Masri et al., 2022). Other studies investigated the effects of ionic liquid type (including cation and anion types and cation alkyl chain length) and found that the cation type (e.g., imidazolium and pyridinium) did not affect demulsification process, while anion type (e.g., halide and non-halide) affected the demulsification processing time (Elmobarak and Almomani, 2021; Guzman-Lucero et al., 2010; Hazrati et al., 2018; Li et al., 2016; Silva et al., 2013). Increasing cation alkyl chain length could increase ionic liquid's surface activity, resulting in higher demulsification efficiency (Guzman-Lucero et al., 2010; Hazrati et al., 2018; Silva et al., 2013). Zolfaghari et al. (2018) investigated the effect of dodecyltrimethylammonium chloride, which has a long-alkyl-chain (10 carbons) cation and a halide anion, on oil/water demulsification, and their results showed that at the ionic liquid

concentration of 1000 mg/L, the demulsification efficiency reached 89.4% after 3 hours settling (Zolfaghari et al., 2018).

By manipulating the structure, ionic liquids could be applied successfully as demulsifiers. However, their industrial application is limited due to their toxicity (Hadi and Ali, 2022a; Romero et al., 2008). The toxicity of ionic liquids mainly depends on their cation type and alkyl chain length. In contrast, anion type has insignificant effect on toxicity (Romeo et al., 2008). Previous research noted that ionic liquid's toxicity reduced significantly by using an environmentally benign cation (e.g., ammonium) and substituting the alkyl group on the side chain with functional groups (e.g., ester, amide) (Cho et al., 2021; Magina et al., 2021). Functional groups have a high surface activity, low toxicity, and high biodegradability (Gathergood et al., 2004; Gathergood et al., 2006; Wang et al., 2020). Thus, an ionic liquid with ammonium cation and functional groups on the side chain may be environmentally friendly. However, such ionic liquid needs to be investigated to find if its potency on oil/water demulsification changes. It also requires to examine which functional groups (e.g., amide and ester) would be more effective to substitute the alkyl group. Hence, this research is to investigate the effects of three ammonium-based ionic liquids with similar anions but different side chain (alkyl, ester, amide groups) on oil/water demulsification. They include dodecyl trimethylammonium chloride (DTAC), [2-(Methacryloyloxy)ethyl] trimethylammonium chloride (METAC), and (3-Acrylamidopropyl) trimethylammonium chloride (APTAC). Response surface methodology (RSM) was used to investigate the effects of ionic liquid concentration, gravity separation settling time, and ionic liquid type (i.e., different side chains) on demulsification efficiency and obtain the optimum demulsification condition.

6.2. Materials and methods

6.2.1. Materials

Heavy Cold Lake Blend (CLB) crude oil used in this study was obtained from Multi-Partner Research Initiative (MPRI) in Canada. The crude oil physicochemical properties are listed in Table 3.1 (Chapter 3). DTAC (≥99.0%), METAC (75% wt. in H_2O) and APTAC (75% wt. in H_2O) ionic liquids were purchased from Sigma-Aldrich Canada, and their structures and molecular weights are listed in Table 6.1. The salts to make synthetic ocean water include magnesium chloride hexahydrate ($MgCl_2.6H_2O$, 99.4%), calcium chloride anhydrous ($CaCl_2$, ≥96.0%), sodium bicarbonate ($NaHCO_3$, 100.1%), sodium sulfate anhydrous (Na_2SO_4, 99.5%), sodium hydroxide (NaOH, ≥97.0%) which were purchased from Fisher Scientific Canada as well as strontium chloride hexahydrate ($SrCl_2.6H_2O$, 99.0%), potassium chloride (KCl, 99.0–100.5%), potassium bromide (KBr, ≥99.0%), boric acid (H_3BO_3, ≥99.5%), sodium fluoride (NaF, ≥99.0%), sodium chloride (NaCl, ≥99.0%), which were purchased from Sigma-Aldrich Canada. All the chemical materials were at American Chemical Society reagent grade and used without further purification. Anhydrous silica gel (75-150 μm, 30 Å pore size, Davisil Grade 923) and sodium sulfate (granular anhydrous) were purchased from Sigma-Aldrich Canada. They were dried at 200 – 250 °C for 24 hours. Hexane and dichloromethane were at high-performance liquid chromatography (HPLC) grade and were purchased from Sigma-Aldrich Canada. A water purification system (Milli-Q Advantage A10) produced the ultrapure water used in this research.

Table 6.1. Summary of the studied ammonium-based ionic liquids.

Name	Chemical structure	Molecular weight (g/mole)	Abbreviation
Dodecyl trimethylammonium chloride	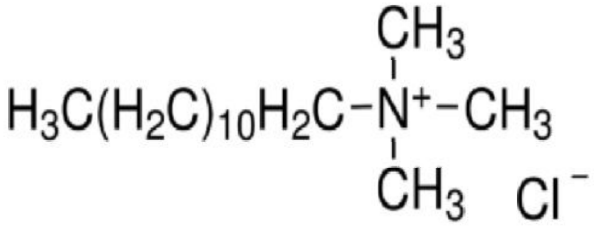	263.89	DTAC
[2-(Methacryloyloxy)ethyl] trimethylammonium chloride	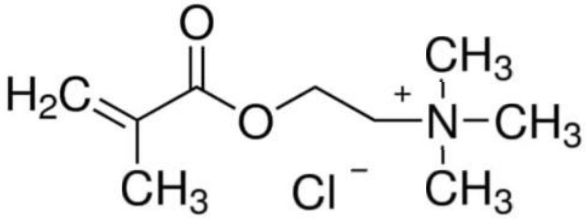	207.7	METAC
(3-Acrylamidopropyl) trimethylammonium chloride	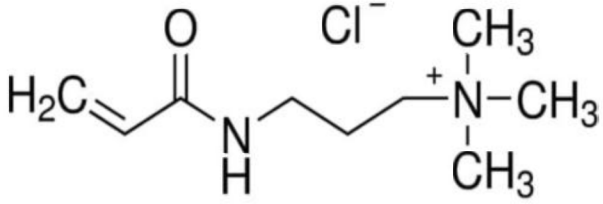	206.71	APTAC

6.2.2. Methods

6.2.2.1. Synthesis of ocean water

Ocean water was synthesized following the ASTM D1141 method (ASTM method, 2013), with chemical concentrations being listed in Table 4.2 (Chapter 4). Before each experiment, a few milliliters of sodium hydroxide solution (0.1 N) were used to adjust the pH to 8.2 (i.e. average ocean pH). Mettler Toledo FG2 portable pH meter was used to measure the pH.

6.2.2.2. Oil/water emulsion preparation

Oil/water emulsion was prepared by pouring 1.5 g of CLB on the surface of 100 mL of synthetic ocean water in a 200 mL beaker (salinity: ~36 g/L, pH: 8.2) and heating them at 50 °C for 5 min on a heater (Thermo Scientific) to reduce the oil viscosity. Then the solution was sonicated continuously for 15 min using a Q700 Sonicator (Qsonica, 20 kHz, solid titanium probe diameter = 12.7 mm) to produce stable emulsion (Hassanshahi et al., 2022). The sonicating process started at the amplitude of 50% and then increased to 80% and 100% and the solution was sonicated at each amplitude for 5 min. Figure 6.1 shows the oil droplets' size distribution in the obtained oil/water emulsion.

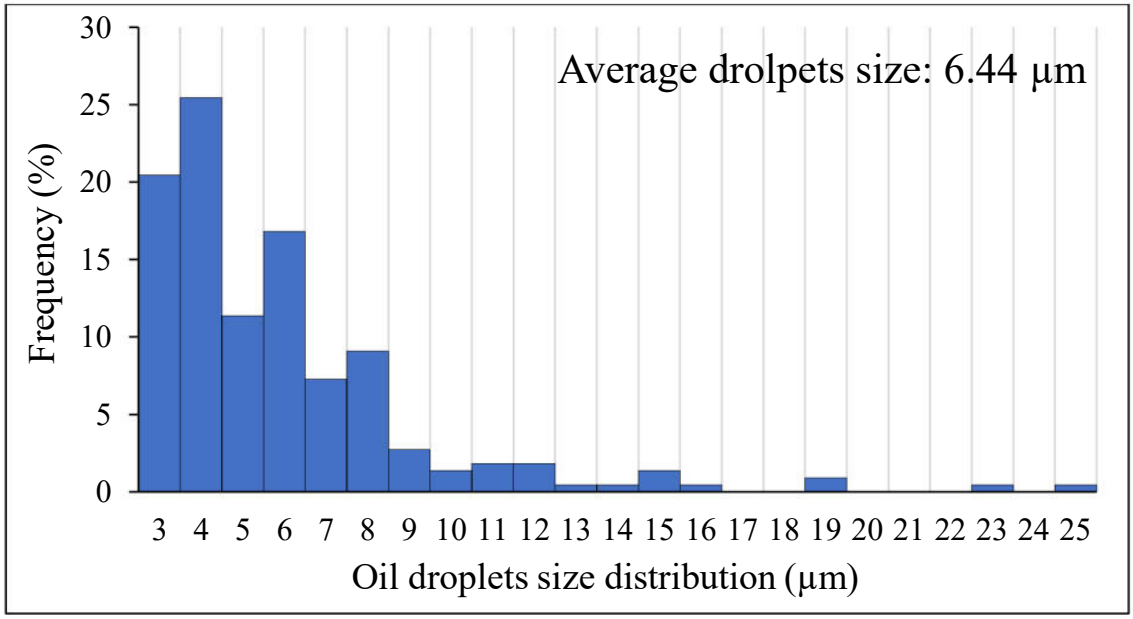

Figure 6.1. Oil droplet size distribution in the emulsion.

6.2.2.3. Experimental design

Critical parameters affecting the demulsification process, including ionic liquid concentration, gravity separation settling time, and ionic liquid type (i.e., different side chains), were considered based on previous studies (Ma et al., 2022; Masri et al., 2022; Saad et al., 2019). Design expert software (version 12.0.11.0, Stat-Ease, Inc.) was used to design the experiments. Central composite design (CCD) was used as a response surface method (RSM) to investigate the effect of each parameter on the demulsification efficiency. For each parameter with numeric values (i.e. concentration and settling time), five levels (coded with $\pm\alpha$, ±1, 0) were considered, and for the categoric parameter (i.e. ionic liquid type), three levels were considered in CCD (Table 6.2). Experimental data from CCD were fitted using equation (6.1) (Hassanshahi et al., 2022).

$$Y = \beta_0 + \sum_{i=1}^{k} \beta_i X_i + \sum_{i=1}^{k} \beta_{ii} X_i^2 + \sum_{i<j} \sum_j \beta_{ij} X_i X_j \quad (6.1)$$

where Y is the predicted response, β_0 is a constant coefficient, β_i is the linear effect of X_i variable, β_{ii} is the second-order effect of variable X_i, and β_{ij} is the effect of the linear interaction between parameters X_i and X_j. The statistical significance of each parameter was determined by analysis of variance (ANOVA).

Table 6.2. Independent experimental parameters and levels in RSM.

Numeric parameters	Range and level					
	Unit	−α	−1	0	+1	+α
Ionic liquid concentration	mg/L	5	10	25	40	45
Settling time	min	0	5	15	25	30
Categoric parameter		Level				
		1		2		3
Ionic liquid type (side chain)	-	DTAC (Alkyl group)		METAC (Ester group)		APTAC (Amide group)

6.2.2.4. Demulsification experiment

Demulsification experiment was conducted in a batch system using the bottle test method (Li et al., 2016). Ionic liquid (DTAC, METAC, APTAC) at different concentrations (5−45 mg/L) was added to 100 mL of the prepared emulsion (1.5 g_{CLB}/100 $mL_{ocean\ water}$) in a 250 mL glass bottle and were mixed on a Talboy 3500 Orbital Shaker at 250 rpm for 10 min at room temperature (~25 °C). Then the solution was allowed to settle at different settling times (0−30 min) for oil-water gravity separation. After that, samples were taken from the separated water (bottom layer) for the liquid-liquid extraction process to measure the total extractable petroleum hydrocarbons (TEPH). Demulsification efficiency was calculated using equation

(6.2). A gravity separation experiment without adding ionic liquid was conducted as a control experiment.

$$DE = \frac{C_i - C_f}{C_i} \times 100 \quad (6.2)$$

Where DE, C_i and C_f are demulsification efficiency (%), initial and final TEPH concentrations (mg/L) in the emulsion and in the separated water, respectively.

6.2.2.5. Analysis of TEPH in emulsion and separated water

TEPH in emulsion and separated water were extracted following the liquid-liquid extraction method (British Columbia laboratory manual, 2017). A 20 mL sample was taken from the emulsion or the separated water (bottom layer) and mixed with 1 mL of solvent (hexane: dichloromethane at 1:1 vol.). The volume ratio of solvent to sample was 1 to 20. The mixture of solvent and sample was shaken vigorously by a Thermo Scientific Digital Vortex Mixer (MODEL NO: 88882009) at 3000 rpm for 15 min. After that, solvent and water were allowed to separate in a separatory funnel. The solvent was then collected in a 20 mL glass vial ($vial_1$). The extraction process was repeated with another fresh 1 mL of solvent, and then the solvent was collected in $vial_1$. Anhydrous sodium sulfate (0.5 g) was added to the $vial_1$ and mixed to remove the moisture. Then the extraction solvent in $vial_1$ was poured into another 20 mL glass vial ($vial_2$) containing 0.3 g of silica gel to remove polar organic compounds. Then the extraction in $vial_2$ was poured into another 20 mL glass vial ($vial_3$). After that, the separatory funnel was rinsed with 1 mL of solvent that was then collected in $vial_1$ to rinse the sodium sulfate. The solvent was poured to $vial_2$ to rinse the silica gel and was then collected in $vial_3$. $Vial_1$ and $vial_2$ were washed with another 1 mL of solvent to ensure all the TEPH was extracted, and then the extraction was collected in $vial_3$. A portion of extraction in $vial_3$ was taken to

analyze TEPH using an Agilent 6890 gas chromatograph with a flame ionization detector (GC-FID). The petroleum hydrocarbons mixtures were grouped in (nC_{10}–nC_{18}), (nC_{18}–nC_{32}) and (nC_{32}–nC_{50}). Decane (nC_{10}), nonadecane (nC_{19}), eicosane (nC_{20}), dotriacontane (nC_{32}), tetriacontane (nC_{34}) and pentacontane (nC_{50}) were used as the external standards. The ZB-1HT INFERNO capillary column (Phenomenex) with a length of 30 m, an inner diameter of 0.32 mm, and a film thickness of 0.25 μm was used. The carrier gas was helium at a rate of 1.6 mL/min. TEPH extract (1 μL) was injected into the system, and a split ratio of 10:1 was performed for each run. During analysis, the injector and detector temperatures were kept at 290 °C and 320 °C, respectively. The initial temperature of the oven was at 130 °C, then increased to 310 °C and 340 °C at 20 °C/min and 5 °C/min, respectively, and held at 340 °C for 8 min.

6.2.2.6. Optical microscopic analysis

Oil droplets in the emulsion was monitored visually before and after demulsification under a compound microscope (Fisher Scientific, AX800) with a 200X objective magnification. A sample drop was poured onto a clear glass slide that was placed under the microscope to capture images. The images were analyzed by SeBaView software (version 4.7), and the oil droplets' size distribution was determined (Kuang et al., 2020b; Yuan et al., 2022; Zolfaghari et al., 2018).

6.2.2.7. Spectrophotometric analysis

Spectrophotometric analysis was conducted to measure the absorbance signal of emulsion in the wavelength ranges of 200 to 600 nm before and after the demulsification process (Cruz et al., 2018). The sample was put in the 3.5 mL quartz Suprasil cell with 1.0 cm path length and polytetrafluoroethylene lid, and measurement was conducted at room temperature (25 °C) using UV-Vis Spectrophotometers 8100 (Orion^{TM} AquaMate, Perkin Elmer).

6.3. Results and discussion

6.3.1. Demulsification results

A total of 33 experiments were designed by CCD, as shown in Table 6.3.

Table 6.3. CCD matrix for different types of ionic liquids (DTAC, METAC, APTAC) and the demuslification results.

Run	Numeric parameters		EPH in separated water			
	Ionic liquid concentration (mg/L)	Settling time (min)	TEPH concentration (mg/L)	EPH (C_{10}–C_{18}) fraction (%)	EPH (C_{18}–C_{32}) fraction (%)	EPH (C_{32}–C_{50}) fraction (%)
DTAC (alkyl group)						
1	5	15	41	33	49	18
2	10	5	39	35	50	15
3	10	25	31	43	48	9
4	25	0	63	36	49	15
5	25	15	45	48	41	11
6	25	30	38	41	48	11
7	25	15	38	44	46	10

Table 6.3. (continued)

Numeric parameters			EPH in separated water			
Run	Ionic liquid concentration (mg/L)	Settling time (min)	TEPH concentration (mg/L)	EPH (C_{10}–C_{18}) fraction (%)	EPH (C_{18}–C_{32}) fraction (%)	EPH (C_{32}–C_{50}) fraction (%)
8	25	15	31	38	51	11
9	40	5	47	39	52	9
10	40	25	34	42	45	13
11	45	15	26	41	49	10
METAC (ester group)						
12	5	15	37	32	49	19
13	10	5	56	39	48	13
14	10	25	43	41	46	13
15	25	0	51	32	53	15
16	25	15	39	35	55	10
17	25	30	25	34	53	13
18	25	15	27	37	52	11
19	25	15	26	32	51	17
20	40	5	40	33	52	15
21	40	25	32	40	48	12
22	45	15	25	35	53	12
APTAC (amide group)						
23	5	15	43	37	51	12
24	10	5	44	36	54	10
25	10	25	41	38	54	8
26	25	0	81	34	54	12
27	25	15	36	36	49	15
28	25	15	37	38	50	12

Table 6.3. (continued)

Run	Numeric parameters		EPH in separated water			
	Ionic liquid concentration (mg/L)	Settling time (min)	TEPH concentration (mg/L)	EPH (C_{10}–C_{18}) fraction (%)	EPH (C_{18}–C_{32}) fraction (%)	EPH (C_{32}–C_{50}) fraction (%)
29	25	15	42	35	52	13
30	25	30	22	35	52	13
31	40	5	45	39	50	11
32	40	25	20	39	50	11
33	45	15	27	35	52	13

Quadratic models were developed for demulsification by DTAC, METAC, and APTAC, as shown in equations (6.3), (6.4), and (6.5), respectively.

$$DE_D = +83.124 - 0.083X_1 + 0.624X_2 + 0.003X_1X_2 + 0.001X_1^2 - 0.017X_2^2 \quad (6.3)$$

$$DE_M = +82.587 - 0.007X_1 + 0.647X_2 + 0.003X_1X_2 + 0.001X_1^2 - 0.017X_2^2 \quad (6.4)$$

$$DE_A = +87.565 - 0.036X_1 + 0.583X_2 + 0.003X_1X_2 + 0.001X_1^2 - 0.017X_2^2 \quad (6.5)$$

Where DE_D, DE_M, and DE_A represents the demulsification efficiency (%) of DTAC, METAC, and APTAC, respectively; X_1 represents the ionic liquid concentration (mg/L); X_2 represents the settling time (min). Ionic liquid concentration and settling time are in the range of (5−45 mg/L) and (0−30 min), respectively.

Based on the ANOVA results (Table C1), the adequacy of the models and the significance of the effect of each independent parameter were determined. The models were significant (F-value: 8.03, P-value: <0.0001) in determining demulsification efficiency. The significant

parameters (P-values < 0.05) in the models were X_1, X_2, X_3, and X_2^2. Model summary statistics for the generated quadratic models by RSM are listed in C2.

6.3.1.1. Ionic liquid concentration effect

The effect of ionic liquid concentration on demulsification was investigated. ANOVA showed significant effect of this parameter (F-value: 5.41, P-value: 0.030). Figure 6.2 shows the effect of ionic liquid concentration (10−40 mg/L) on the demulsification efficiency for all three types of ionic liquids after 15 min of gravity settling. It was found that adding ionic liquids to the oil/water emulsion favored demulsification with a demulsification efficiency ≥88%. Among the three ionic liquids, APTAC was most effective at all addition concentrations. Increasing ionic liquid concentration from 10 mg/L to 40 mg/L increased the demulsification efficiency of METAC and APTAC, but it had an insignificant effect on the performance of DTAC. As shown in Table 6.3, the TEPH in the separated water was reduced from 43 mg/L to 32 mg/L and from 41 mg/L to 20 mg/L for METAC and APTAC, respectively, when the ionic liquid concentration increased from 10 mg/L to 40 mg/L after 25 min gravity settling. However, for demulsification by DTAC, the increase in ionic liquid concentration slightly increased TEPH in the separated water (from 31 mg/L to 34 mg/L). This indicated that ionic liquids with different side chains and hydrophilicity greatly influenced their performance in the demulsification, in which increasing the ionic liquid concentration may not improve the demulsification efficiency. All three ionic liquids have a quaternary ammonium head with a positive charge which could reach the oil-water interface and neutralize the negative charge of oil droplets, resulting in oil droplets' flocculation, coalescence, and separation (Wang et al., 2018). METAC and APTAC with ester and amide groups on the side chain, respectively, could break the rigid film through hydrogen bond reconstruction, resulting in oil droplets'

flocculation and coalescence (Ma et al., 2021). Hence, METAC and APTAC brought about higher demulsification efficiency than DTAC. Based on the results, the three ionic liquids had promising demulsification efficiency (≥88%) at a low concentration (≤40 mg/L), and APTAC had the best performance.

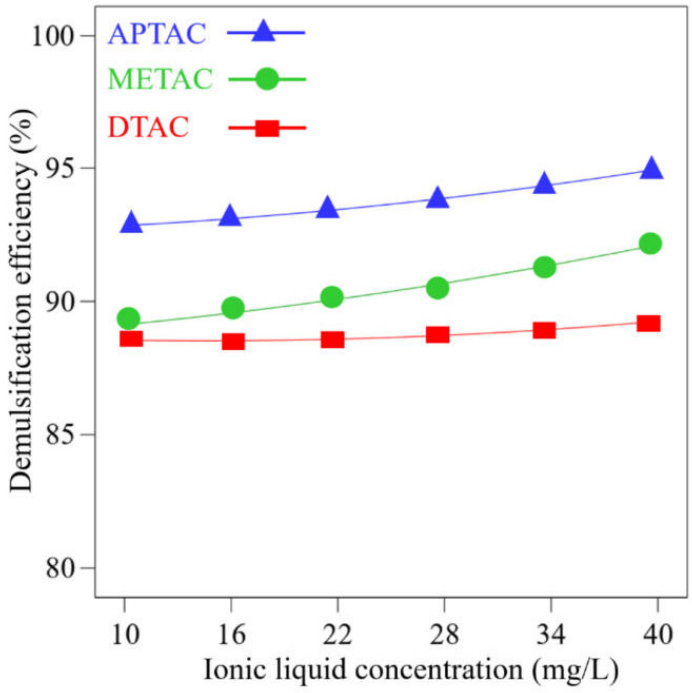

Figure 6.2. Effect of ionic liquid concentration on demulsification efficiency for DTAC, METAC, and APTAC at 15 min settling.

6.3.1.2. Effect of ionic liquid type (side chain)

The effect of ionic liquid type on the demulsification process was investigated. Based on the ANOVA analysis, the ionic liquid type was a significant parameter influencing the demulsification process (F-value: 17.98, P-value: <0.0001). Figure 6.3 shows the effect of ionic liquid type on the demulsification efficiency at ionic liquid concentration of 25 mg/L and

15 min gravity settling. APTAC with the amide group had the highest demulsification efficiency (94%), followed by METAC (ester group) (91%) and DTAC (alkyl group) (88%). The long alkyl group on the DTAC side chain increases its hydrophobicity, while the ester and amide groups on the METAC and APTAC side chains increase their hydrophilicity (Hassanshahi et al., 2020; Magina et al., 2021). Hydrophobic DTAC molecules encounter a barrier in distributing in the oil/water emulsion and reaching the oil-water interface where the continuous phase is water (Kang et al., 2018). This led to the lower efficiency of DTAC compared to METAC and APTAC in breaking the oil/water emulsion. The higher demulsification efficiency of APTAC compared to METAC indicated that the amide group was more effective than the ester group in breaking the rigid film at the oil-water interface. As shown in Table 6.3, under the same experimental conditions (ionic liquid concentration: 25 mg/L, settling time 30 min), the TEPH in the separated water were 38 mg/L, 25 mg/L, and 22 mg/L for DTAC, METAC, and APTAC, respectively. This also proved the superiority of amide group over the ester and alkyl groups in demulsification. Figure 6.4 shows the spectrophotometric analysis of emulsion (before demulsification) and the separated water after demulsification by DTAC, METAC, and APTAC. The emulsion had high absorbance due to many emulsified oil droplets. Its absorbance was notably reduced after the demulsification process, indicating a significant reduction in the amount of oil droplets in the emulsion. The lowest absorbance was for APTAC, consistent with its highest demulsification efficiency. The peaks at the wavelength range of 240−300 nm are relevant characteristics of aromatic compounds in crude oil (Mehraban et al., 2021). Although demulsification efficiency by METAC was higher than DTAC, the spectrophotometric analysis indicated that DTAC was

more efficient than METAC in removing the aromatic compounds, one of the main toxic compounds in crude oils.

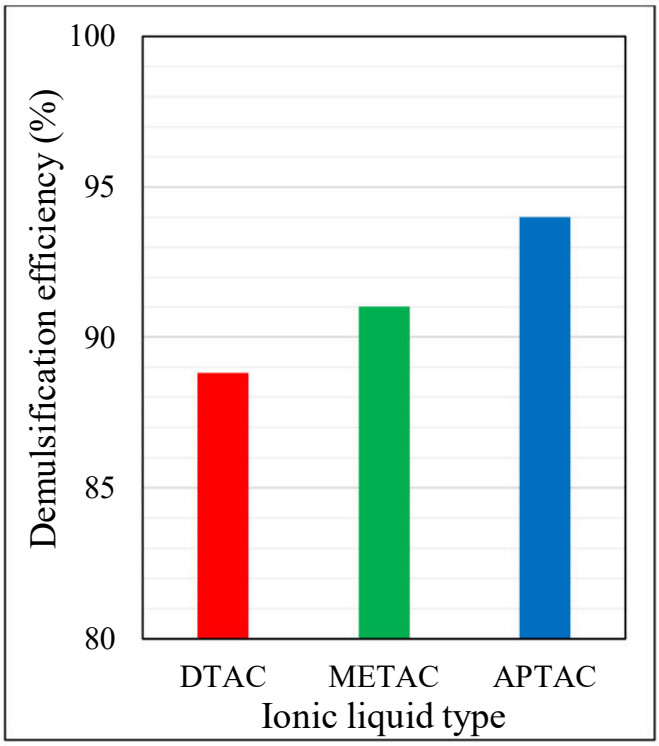

Figure 6.3. Effect of ionic liquid type (side chain) on the demulsification efficiency (ionic liquid concentration: 25 mg/L, settling time: 15 min).

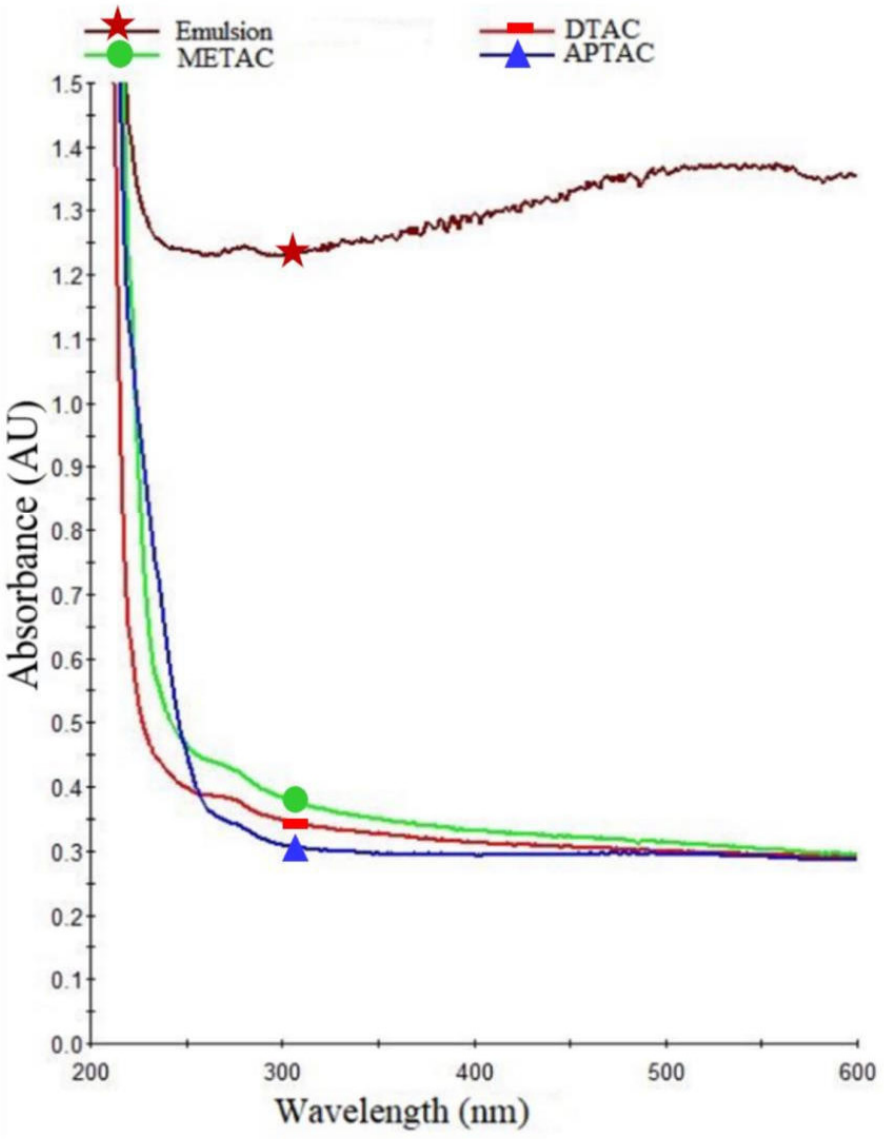

Figure 6.4. Spectrophotometric of emulsion and the separated water after demulsification by DTAC, METAC and APTAC (ionic liquid concentration: 25 mg/L, settling time: 15 min).

6.3.1.3. Effect of settling time

Settling time was another significant parameter affecting the demulsification process (F-value: 27.40, P-value: <0.0001). Figure 6.5 indicates the effect of settling time (5−25 min) on the demulsification efficiency of DTAC, METAC, and APTAC (ionic liquid concentration: 25 mg/L). Increasing settling time from 5 min to 20 min allowed the oil droplets to coalesce and separate from the water phase, resulting in higher demulsification efficiency. Beyond 20 min settling, the separation rate was insignificant, indicating that the demulsification reached the equilibrium. As noted in previous research, the equilibrium state of the demulsification process usually occurs after 90 min settling (Zhang et al., 2018b). This study showed that DTAC, METAC, and APTAC effectively broke emulsion at a short settling time (20 min) and achieved a high demulsification efficiency (≥85%). This might be due to the low molecular weight of the ionic liquids (< 3000 g/mole). Ionic liquids with a low molecular weight distribute and diffuse quickly in the emulsion and reach the oil-water interface as compared to high-molecular-weight ionic liquids (> 10,000 g/mole), which require a long time to function (Hassanshahi et al., 2020). Figure 6.6 shows the visual observation and optical microscopic images of separated water without gravity settling and with 30 min of gravity settling after the demulsification process by DTAC, METAC, and APTAC. Without gravity separation (settling time: 0 min), all the separated waters were visually clear after demulsification. However, as shown in the microscopic images, tiny oil droplets were still contained in the separated waters, which resulted in high TEPH (Table 6.3). After 30 min of gravity settling, the coalesced oil droplets were separated from the water phase, and the amount of oil droplets in the water reduced as shown in the microscopic images; hence, the TEPH decreased significantly

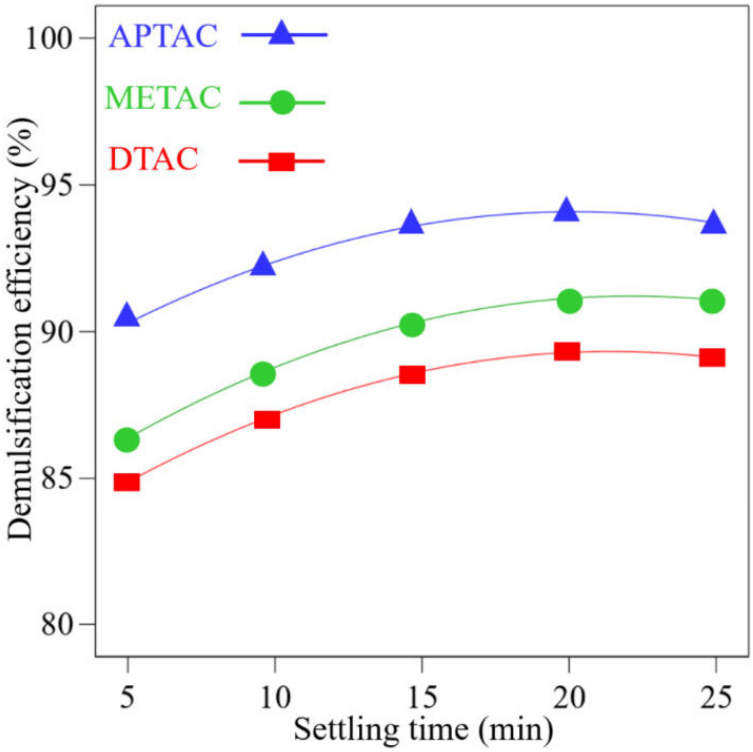

Figure 6.5. Effect of settling time on demulsification efficiency for DTAC, METAC and APTAC at the concentration of 25 mg/L.

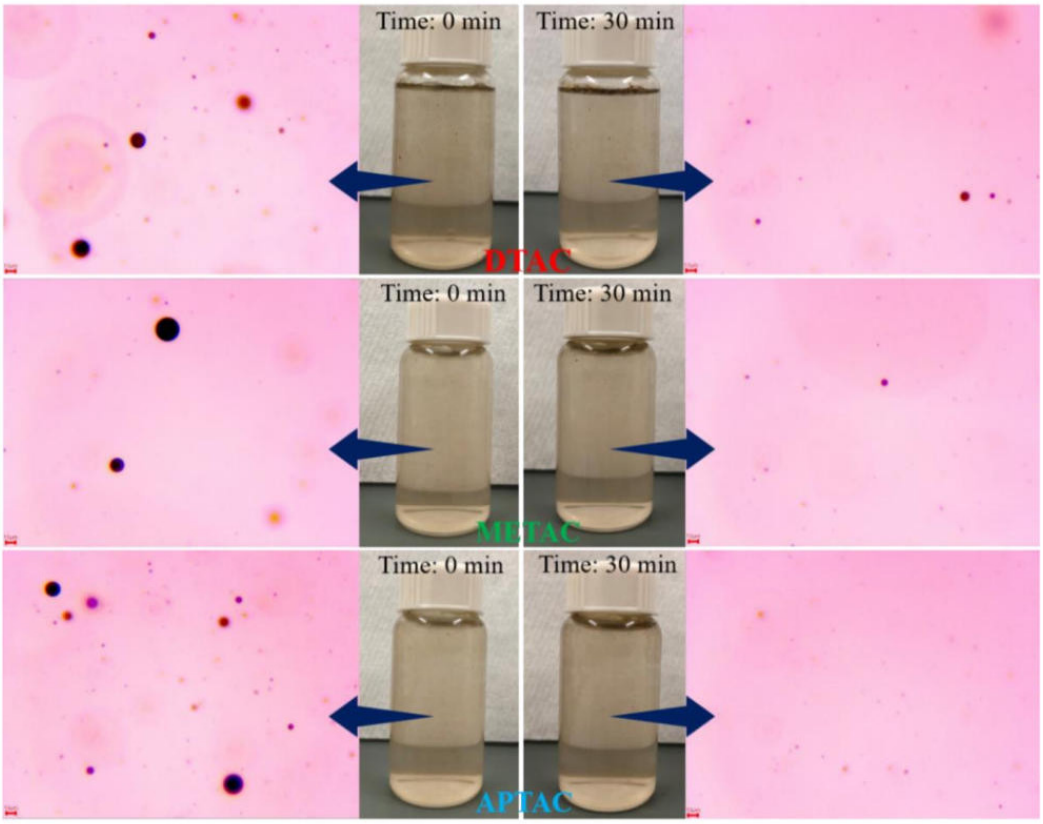

Figure 6.6. Visual observation and optical microscopy images of separated water at settling times of 0 and 30 min after the demulsification process by DTAC, METAC, and APTAC at the concentration of 25 mg/L.

6.3.1.4. Interaction of parameters and their optimum condition

The effect of the interaction between ionic liquid concentration and settling time for each ionic liquid type is shown in Figure 6.7. The interaction of parameters in the demulsification process resulted in a higher demulsification efficiency at a lower ionic liquid concentration. As shown in Figure 6.7a, increasing the DTAC concentration had a negligible effect on the demulsification efficiency (~85%) at 5 min gravity settling; however, higher demulsification efficiency (90%) was achieved at a longer settling time (20 min). Figure 6.7b shows similar

demulsification efficiency (88%) at METAC concentration and settling time of 40 mg/L and 6 min as that at 10 mg/L and 12 min, indicating the interaction effect of parameters in the demulsification process. Similar observation was obtained for the demulsification by APTAC, as shown in Figure 6.7c. Hence, the interaction effect of parameters indicates that lower ionic liquid concentration but longer gravity settling time could still bring satisfactory demulsification performance.

Table 6.4 lists the optimum condition of demulsification as suggested by RSM. As indicated earlier, the amide group was more effective than the ester group in the demulsification process. Hence, a lower optimum APTAC concentration (16 mg/L) than METAC concentration (19 mg/L) is suggested by RSM, which leads to a higher demulsification efficiency (91%). The suggested optimum DTAC concentration is 25 mg/L, higher than METAC and APTAC. DTAC has a long alkyl chain in the structure which increases the hydrophobicity of the ionic liquid. Hydrophobic ionic liquids encounter a barrier in the diffusion in the emulsion where the continuous phase is water. Hence higher DTAC concentration (25 mg/L) is required for distribution in the oil/water emulsion and reaching the oil-water interface. Moreover, hydrophobic DTAC requires a longer settling time (21 min) to function and achieve high demulsification efficiency compared to hydrophilic METAC and APTAC (12 min and 10 min, respectively).

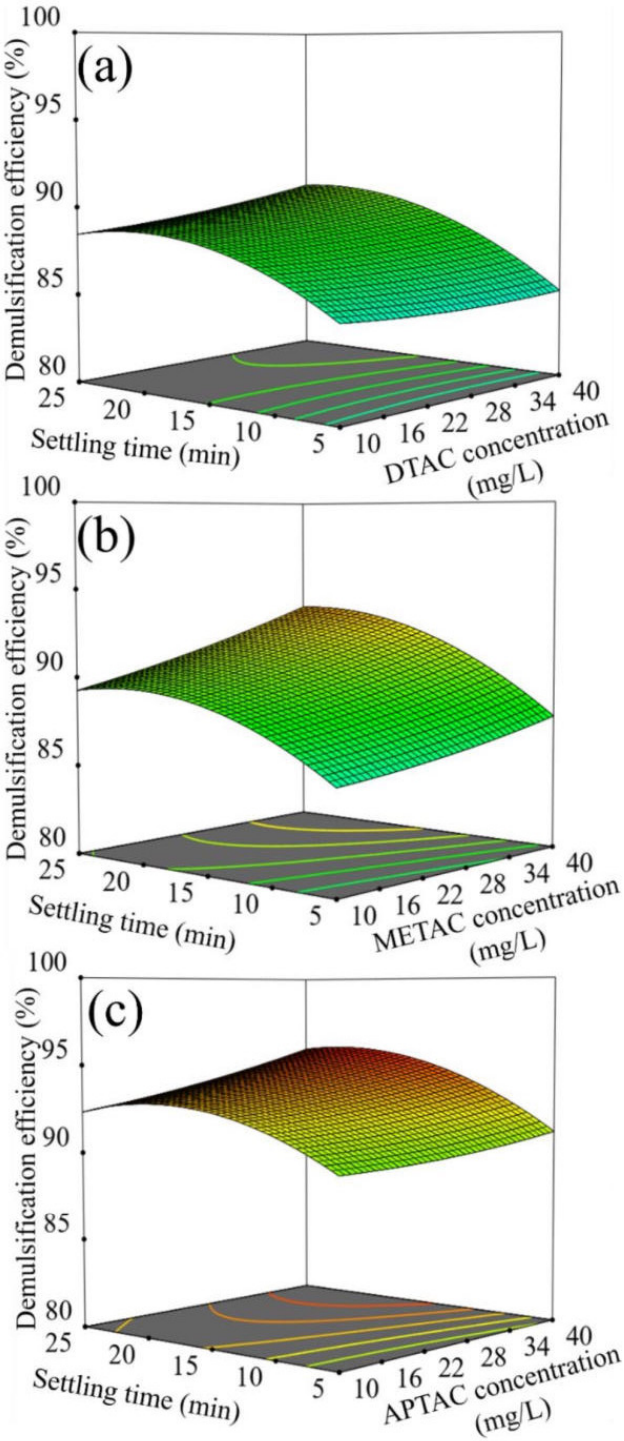

Figure 6.7. Effect of interaction of different parameters on demulsification efficiency a) DTAC concentration and settling time, b) METAC concentration and settling time, c) APTAC concentration and settling time.

Table 6.4. Optimum condition of demulsification process by ionic liquids.

Number	Ionic liquid concentration (mg/L)	Settling time (min)	Ionic liquid type (side chain)	Demulsification efficiency (%)
1	25	21	DTAC (alkyl group)	89
2	19	12	METAC (ester group)	89
3	16	10	APTAC (amide group)	91

6.3.2. Demulsification mechanism

Scheme 6.1 shows the demulsification mechanism by DTAC, METAC, and APTAC. Oil/water emulsion is generated due to the formation of different complex inter- and intra-molecular interactions (e.g., hydrogen bond) among the natural emulsifiers in crude oil (e.g., asphaltenes) and water molecules (Sousa et al., 2021). Emulsified oil droplets have a negative surface charge at the solutions with pH >4, which deter their coalescence (Ezzat et al., 2021). After adding ionic liquids to the emulsion and mixing them, ionic liquids molecules distribute in the emulsion and reach the oil-water interface. DTAC, METAC, and APTAC are ionic liquids with quaternary ammonium groups and possess a positive charge (Wang et al., 2018). Hence, ionic liquid molecules neutralized the repulsive force among emulsified oil droplets molecules, resulting in their flocculation, coalescence, and separation. Besides that, METAC and APTAC have ester and amide groups on the side chain, respectively, that broke the generated hydrogen bond among the oxygen molecules of asphaltenes and hydrogen of water molecules and reconstructed it among ionic liquid and water molecules (Ma et al., 2021; Wang et al., 2020). This also brought about the flocculation and coalescence of oil droplets. Hence, METAC and APTAC resulted in higher demulsification efficiency than DTAC. Substituting

the alkyl group with the ester and amide groups resulted in demulsification through the combination of electrostatic attraction and hydrogen bond reconstruction, which improved demulsification efficiency.

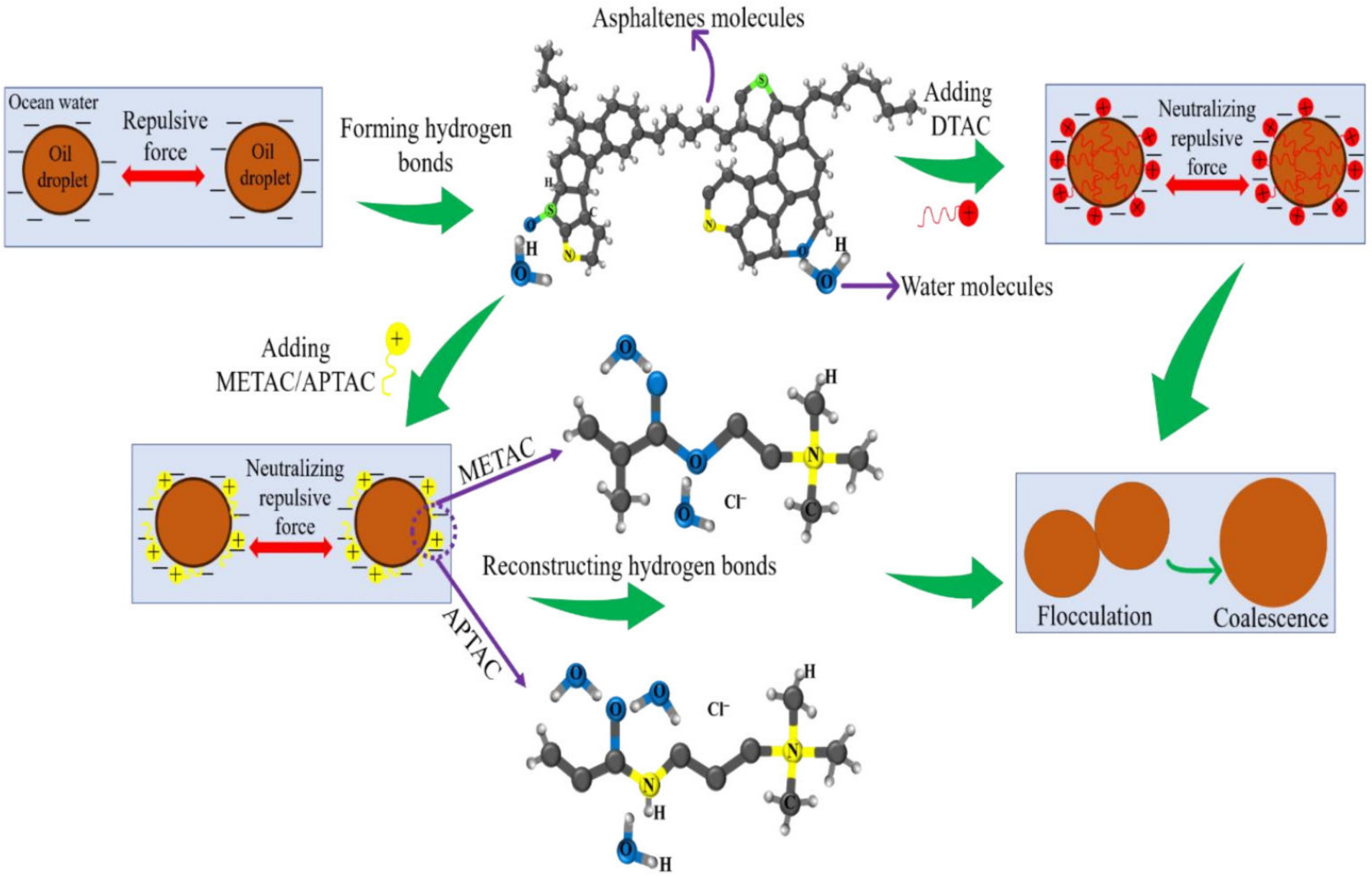

Scheme 6.1. Demulsification mechanism of O/W emulsion by DTAC, METAC, and APTAC.

6.4. Summary

This research studied the performance of three ionic liquids (DTAC, METAC, APTAC) with different side chains (alkyl, ester, amide groups) in demulsifying crude oil/water emulsion. Effects of ionic liquid concentration, gravity separation settling time, and ionic liquid type on the demulsification efficiency were investigated. The optimum demulsification condition for each ionic liquid was obtained. The results indicated the effectiveness of the three ionic liquids. Increasing ionic liquid concentration improved the demulsification by METAC and APTAC, but had no notable effect on the demulsification by DTAC. The demulsification equilibrium state occurred at a short settling (20 min). The results indicated that substituting the alkyl group on the side chain with the ester and amide groups improved the performance of ionic liquid in demulsification. APTAC with the amide group on the side chain achieved the highest demulsification efficiency, indicating the amide group's superiority over the ester and alkyl groups. The demulsification mechanism for DTAC was suggested to be the electrostatic attraction, while for METAC and APTAC, it was the combination of electrostatic attraction and hydrogen bond reconstruction.

Chapter 7

CONCLUSION AND RECOMMENDATION

7.1. Synthesis and conclusion

A primary environmental concern is generating a large volume of oily wastewater in oil and gas industries and the marine environment due to oil production processes and natural seepage or ship accidents, respectively (Abdulredha et al., 2020; Motta et al., 2018). Crude oil contains complex hydrocarbon compounds which aliphatic and polycyclic aromatic hydrocarbons are the most toxic compounds in crude oils. These toxic compounds severely risk human health and the marine environment, which require removal from the water by an effective and environmentally friendly process (Ruberg et al., 2021). Different systems were applied to treat oily wastewater, including physical, biological, and chemical (Abdulredha et al., 2020). Physical and biological systems had some limitations in demulsifying emulsion effectively due to the complexity of crude oils and commercial limitations. Their main drawbacks are large space requirements, long-time processing, susceptibility to operational issues, and poor efficiency (Abdulredha et al., 2020; Hadi and Ali, 2022a; Less and Vilagines, 2012; Tian et al., 2022). The chemical treatment system is effective, cheap, and easy to operate (Yang et al., 2021; Yonguep and Chowdhury, 2021). However, the previous research noted that demulsifiers' toxicity and high synthesizing costs had limited their industrial applications (Hadi and Ali, 2022a; Romero et al., 2008). Also, no demulsifier can be used for all types of crude oils, and their efficiency is affected by various parameters, including crude oil type, concentration, and water salinity. A practical and environmentally friendly demulsifier must be investigated to demulsify emulsion effectively. This study proposed applying different

demulsifiers (anionic surfactant and ionic liquids) to demulsify stable oil in water (O/W) emulsions.

Chapter 3 proposed the generation of stable O/W emulsion using ultrasonic homogenization. This research applied the experimental design (response surface methodology (RSM)) of ultrasonic processing parameters (power and sonication time) and emulsion characteristics (water salinity and pH) to investigate their significance and interactions on emulsion stability. Statistical analysis of these parameters was conducted, which is required for future research projects to account for scientific results (Sousa et al., 2021). Empirical correlations of parameters on emulsion stability are required to determine the energy needed for emulsion generation. The results showed that the optimum conditions were at a power level of 76–80 W, sonication time of 16 mins, water salinity of 15 g/L NaCl, and pH of 8.3. Based on the interaction of parameters, the required energy to generate a stable emulsion was within 60−70 kJ. The effect of CLB crude oil condition (fresh and weathered) was evaluated at the optimum conditions of parameters on crude O/W emulsion stability. Based on the results, fresh CLB crude O/W emulsion was more stable than the weathered one. This technique was used to generate a stable emulsion for the chemical demulsification process.

Chapter 4 investigated an anionic surfactant (dioctyl sodium sulfosuccinate (DSS)) with a double-chain structure in demulsifying crude O/W emulsions. The DSS is expected to overcome the drawbacks of single-chain anionic surfactants reported in previous research and the drawbacks of previously reported demulsifier-impeding interfacial adsorption. Such a surfactant would effectively demulsify highly saline stable emulsions without requiring a long settling time, as previously reported demulsifiers (e.g., dendrimers, nonionic, and cationic) showed poor efficiency (Kuang et al., 2020a; Yonguep and Chowdhury, 2021; Zhang et al.,

2016). The effects of DSS concentration, oil concentration, and shaking time were investigated using RSM, and their optimum conditions were determined. Further single-factor experiments were conducted to investigate the effect of salinity, crude oil condition, and gravity separation settling time. The results indicated that DSS effectively demulsified emulsions at 15 min shaking time without settling. DSS performance did not affect by the crude oil concentration (500−3000 mg/L) and crude oil type (fresh and weathered with different resins/asphaltenes). These are the advantages of DSS over other used demulsifiers, which require a long settling time and show poor efficiency at a low oil concentration (e.g., 3000 mg/L). Increasing DSS concentration from 300 mg/L to 900 mg/L (critical micelle concentration) increased the demulsification efficiency to 99% and reduced the total extractable petroleum hydrocarbons (TEPH) to lower than 10 mg/L. DSS is an anionic surfactant with a negative surface charge, showing a promising result at higher salinity (36 g/L) than no salt. The optimum conditions of the demulsification process by DSS were at a DSS concentration of 900 mg/L and a shaking time of 15 min when the oil concentration was 1000 mg/L. This study showed that DSS is a reliable demulsifier for different industrial applications.

Ionic liquids are liquid salts with the unique features of non-flammability, thermal stability, and low vapor pressure. These features are essential for industrial applications; however, their toxicity has limited their applications. By manipulating the ionic liquid structure and substituting the alkyl chain group with functional groups, (e.g., hydroxyl, ester, and amide), ionic liquid toxicity reduces significantly. In chapter 5, an ionic liquid (tris(2-hydroxyethyl) methylammonium methylsulfate (MTEOA $MeOSO_3$)) with three hydroxyl groups on the side chains was selected to investigate if it affects ionic liquid performance in demulsifying O/W emulsion. The effects of MTEOA $MeOSO_3$ concentration, demulsification temperature,

gravity separation settling time, and emulsifier type were studied. It was found that the emulsifier type significantly affected the ionic liquid performance. For emulsion (I) generated by natural emulsifiers+Tween 20, the optimum demulsification conditions were at the MTEOA $MeOSO_3$ concentration of 50 mg/L, the demulsification temperature of 50 °C, and the gravity separation settling time of 90 min. The TEPH was reduced to 341 mg/L at this demulsification condition. However, for emulsion (II) generated by natural emulsifiers, the optimum demulsification conditions were at the MTEOA $MeOSO_3$ concentration of 25 mg/L, room temperature (~ 25 °C), and without settling time, where the TEPH was reduced to 33 mg/L. The rigid film formed around emulsified oil droplets in emulsion (I) might be thicker than emulsion (II), affecting MTEOA $MeOSO_3$ efficiency. The demulsification mechanism was concluded to be hydrogen bond reconstruction due to hydroxyl groups in the ionic liquid structure. This study showed that MTEOA $MeOSO_3$ ionic liquid with hydroxyl functional groups rather than alkyl chains is effective in demulsifying emulsion generated by natural emulsifiers in the marine environment and develops the application of a biodegradable, low-toxic ionic liquid in industries.

In chapter 6, three ionic liquids, namely dodecyl trimethylammonium chloride (DTAC), [2-(Methacryloyloxy)ethyl] trimethylammonium chloride (METAC), and (3-Acrylamidopropyl) trimethylammonium chloride (APTAC) were selected to investigate if the potency of the ionic liquid changes by substituting the alkyl group with the ester and amide functional groups and which of them would be more effective to be substituted. The effects of ionic liquids concentration, settling time, and ionic liquid type (i.e., side chain) were studied using RSM, and their optimum conditions were determined. The results indicated that substituting the alkyl group on the side chain with the ester and amide groups improved the potency of ionic liquid

in the demulsifying O/W emulsion. APTAC with the amide group on the side chain achieved the highest demulsification efficiency and the lowest TEPH in the separated water, proving the amide group's superiority over the ester and alkyl groups. Increasing ionic liquid concentration increased the demulsification efficiency for METAC and APTAC, while it had an insignificant effect on the performance of DTAC. This emphasizes the importance of ionic liquids' hydrophilicity in demulsifying emulsions where the continuous phase is water. The hydrophobicity of DTAC is high due to the long alkyl chain on the side chain, in which increasing the ionic liquid concentration did not improve the demulsification efficiency. The low molecular weight of ionic liquids brought about reaching the demulsification equilibrium state at a short settling (20 min). The demulsification mechanism for DTAC was concluded to be an electrostatic attraction, and METAC and APTAC were the combinations of electrostatic attraction and hydrogen bond reconstruction.

In summary, all the applied demulsifiers (anionic surfactant and ionic liquids) demulsified stable O/W emulsions effectively. Chapter 3 revealed the generation of stable O/W emulsion using an ultrasonic homogenizer. A promising application of an anionic surfactant in the demulsifying O/W emulsion was indicated in chapter 4. Chapter 5 showed that the presence of hydroxyl groups on the ionic liquid side chain rather than the long alkyl chain did not affect the ionic liquid efficiency in the demulsifying emulsion. Chapter 6 showed that substituting the alkyl group with the ester and amide group improved the potency of ionic liquids in the demulsifying emulsion, and the amide group showed the best performance.

7.2. Limitations and future research

This dissertation investigated the effect of ultrasonic homogenization on the generation of stable crude O/W emulsion. The ultrasonic homogenizer could successfully generate a stable O/W emulsion on the lab scale, and the required energy was determined. It is recommended to do further research on applying ultrasonic homogenizer to generate O/W emulsion on a large scale. It is applicable for emulsion washing to remedy oil-contaminated soil and for the field-scale experimental demulsification process.

The chemical demulsification process using different demulsifiers (anionic surfactant and ionic liquids) on a lab scale was investigated in this study. The results indicated an effective demulsifying process and a significant reduction in the total extractable petroleum hydrocarbons in separated water. Further mesoscale studies must be conducted before applying the laboratory test results in large-scale applications.

All the applied demulsifiers were water soluble and ended in the separated water phase after the demulsification process. Hence, it is recommended to do further research on the recovery of the demulsifiers. Although these demulsifiers were commercially available and cheaper than those synthesized, their recovery may reduce the process cost if the recovery process cost is low.

This research aimed to investigate effective environmentally friendly demulsifiers in demulsifying crude O/W emulsion. Ionic liquids with a novel structure were selected to reduce their toxicity. Although the studied demulsifiers were much more environmentally benign than previously used ones, conducting a toxicity and biodegradability analysis at different temperatures is still highly recommended.

It was found that the presence of a commercial emulsifier (Tween 20) in oily wastewaters significantly affects the performance of ionic liquid (tris(2-hydroxyethyl) methylammonium methylsulfate) in the demulsifying O/W emulsion. Increasing the demulsification temperature accelerated the demulsification process and resulted in higher efficiency. However, the remaining TEPH in separated water was still high (beyond the standard limitations). Thus, finding a strategy to overcome this drawback of ionic liquid is recommended.

References

Abbas, S., Bashari, M., Akhtar, W., Li, W. W., Zhang, X. (2014). Process optimization of ultrasound-assisted curcumin nanoemulsions stabilized by OSA-modified starch. *Ultrasonics Sonochemistry*, *21*(4), 1265-1274.

Abdullah, M. M., Al-Lohedan, H. A. (2019). Demulsification of Arabian heavy crude oil emulsions using novel amphiphilic ionic liquids based on glycidyl 4-nonylphenyl ether. *Energy & Fuels*, *33*(12), 12916-12923.

Abdullah, M. M., AlQuraishi, A. A., Allohedan, H. A., AlMansour, A. O., Atta, A. M. (2017). Synthesis of novel water soluble poly (ionic liquids) based on quaternary ammonium acrylamidomethyl propane sulfonate for enhanced oil recovery. *Journal of Molecular Liquids*, *233*, 508-516.

Abdulredha, M. M., Aslina, H. S., Luqman, C. A. (2020). Overview on petroleum emulsions, formation, influence and demulsification treatment techniques. *Arabian Journal of Chemistry*, *13*(1), 3403-3428.

Abranches, D. O., Silva, L. P., Martins, M. A., Pinho, S. P., Coutinho, J. A. (2020). Understanding the formation of deep eutectic solvents: betaine as a universal hydrogen bond acceptor. *ChemSusChem*, *13*(18), 4916-4921.

Abu-Eishah, S. I. (2011). Ionic liquids recycling for reuse. *Ionic Liquids-Classes and Properties*, 239-272.

Abullah, M. M., Al-Lohedan, H. A., Attah, A. M. (2016). Synthesis and application of amphiphilic ionic liquid based on acrylate copolymers as demulsifier and oil spill dispersant. *Journal of Molecular Liquids*, *219*, 54-62.

Adetunji, A. I., Olaniran, A. O. (2021). Treatment of industrial oily wastewater by advanced technologies: a review. *Applied Water Science*, *11*(6), 1-19.

Adewunmi, A. A., Kamal, M. S. (2019). Demulsification of water-in-oil emulsions using ionic liquids: Effects of counterion and water type. *Journal of Molecular Liquids*, *279*, 411-419.

Adilbekova, A. O., Omarova, K. I., Karakulova, A., Musabekov, K. B. (2015). Nonionic surfactants based on polyoxyalkylated copolymers used as demulsifying agents. *Colloids and Surfaces A: Physicochemical and Engineering Aspects*, *480*, 433-438.

Adzigbli, L., Yuewen, D. (2018). Assessing the impact of oil spills on marine organisms. *Journal of Oceanography and Marine Research*, *6*(179), 472-479.

Al-Ghouti, M. A., Al-Kaabi, M. A., Ashfaq, M. Y., Da'na, D. A. (2019). Produced water characteristics, treatment and reuse: A review. *Journal of Water Process Engineering*, *28*, 222-239.

Alves, D., Lourenço, E., Franceschi, E., Santos, A. F., Santana, C. C., Borges, G., Dariva, C. (2017). Influence of ionic liquids on the viscoelastic properties of crude oil emulsions. *Energy & Fuels*, *31*(9), 9132-9139.

Ardakani, E. K., Kowsari, E., Ehsani, A. (2020). Imidazolium-derived polymeric ionic liquid as a green inhibitor for corrosion inhibition of mild steel in 1.0 M HCl: Experimental and computational study. *Colloids and Surfaces A: Physicochemical and Engineering Aspects*, *586*, 124195.

Ashokkumar, M. (2011). The characterization of acoustic cavitation bubbles–an overview. *Ultrasonics Sonochemistry*, *18*(4), 864-872.

Aslan, D., Dogan, M. (2018). The influence of ultrasound on the stability of dairy-based, emulsifier-free emulsions: rheological and morphological aspect. *European Food Research and Technology*, *244*(3), 409-421.

ASTM D1141-98. (2013). Standard Practice for the Preparation of Substitute Ocean Water. West Conshohocken, PA.

Atta, A. M., Al-Lohedan, H. A., Abdullah, M. M. (2016a). Dipoles poly (ionic liquids) based on 2-acrylamido-2-methylpropane sulfonic acid-co-hydroxyethyl methacrylate for demulsification of crude oil water emulsions. *Journal of Molecular Liquids*, *222*, 680-690.

Atta, A. M., Al-Lohedan, H. A., Abdullah, M. M., ElSaeed, S. M. (2016b). Application of new amphiphilic ionic liquid based on ethoxylated octadecylammonium tosylate as demulsifier and petroleum crude oil spill dispersant. *Journal of Industrial and Engineering Chemistry*, *33*, 122-130.

Atta, A. M., Ezzat, A. O., Hashem, A. I. (2017). Synthesis and application of monodisperse hydrophobic magnetite nanoparticles as an oil spill collector using an ionic liquid. *RSC Advances*, *7*(27), 16524-16530.

Austad, T., Shariatpanahi, S. F., Strand, S., Black, C. J. J., Webb, K. J. (2012). Conditions for a low-salinity enhanced oil recovery (EOR) effect in carbonate oil reservoirs. *Energy & Fuels*, *26*(1), 569-575.

Azadi, F., Karimi-Jashni, A., Zerafat, M. M. (2021). Desalination of brackish water by gelatin-coated magnetite nanoparticles as a novel draw solute in forward osmosis process. *Environmental Technology*, *42*(18), 2885-2895.

Balsamo, M., Erto, A., Lancia, A. (2017). Chemical demulsification of model water-in-oil emulsions with low water content by means of ionic liquids. *Brazilian Journal of Chemical Engineering*, *34*, 273-282.

Bancroft, W. D. (2002). The theory of emulsification, V. *The Journal of Physical Chemistry*, *17*(6), 501-519.

Becherini, S., Mezzetta, A., Chiappe, C., Guazzelli, L. (2019). Levulinate amidinium protic ionic liquids (PILs) as suitable media for the dissolution and levulination of cellulose. *New Journal of Chemistry*, *43*(11), 4554-4561.

Beland, L. P., Oloomi, S. (2019). Environmental disaster, pollution and infant health: Evidence from the Deepwater Horizon oil spill. *Journal of Environmental Economics and Management*, *98*, 102265.

Bera, A., Agarwal, J., Shah, M., Shah, S., Vij, R. K. (2020). Recent advances in ionic liquids as alternative to surfactants/chemicals for application in upstream oil industry. *Journal of Industrial and Engineering Chemistry*, *82*, 17-30.

Berthod, A., Ruiz-Angel, M. J., Carda-Broch, S. (2008). Ionic liquids in separation techniques. *Journal of Chromatography A*, *1184*(1-2), 6-18.

Berton, P., Manouchehr, S., Wong, K., Ahmadi, Z., Abdelfatah, E., Rogers, R. D., Bryant, S. L. (2019). Ionic liquids-based bitumen extraction: enabling recovery with environmental footprint comparable to conventional oil. *ACS Sustainable Chemistry & Engineering*, *8*(1), 632-641.

Bi, Y., Tan, Z., Wang, L., Li, W., Liu, C., Wang, Z., Liu, X., Jia, X. (2020). The demulsification properties of cationic hyperbranched polyamidoamines for polymer flooding emulsions and microemulsions. *Processes*, *8*(2), 176.

Bin-Dahbag, M. S., Al Quraishi, A. A., Benzagouta, M. S., Kinawy, M. M., Al Nashef, I. M., Al Mushaegeh, E. (2014). Experimental study of use of ionic liquids in enhanced oil recovery. *Journal of Petroleum & Environmental Biotechnology*, *4*(165), 1-7.

Bin Dahbag, M. S., Hossain, M. E., AlQuraishi, A. A. (2016). Efficiency of ionic liquids as an enhanced oil recovery chemical: simulation approach. *Energy & Fuels*, *30*(11), *9260*-9265.

Biniaz, P., Farsi, M., Rahimpour, M. R. (2016). Demulsification of water in oil emulsion using ionic liquids: Statistical modeling and optimization. *Fuel*, *184*, 325-333.

Borges, B., Rondón, M., Sereno, O., Asuaje, J. (2009). Breaking of water-in-crude-oil emulsions. 3. Influence of salinity and water− oil ratio on demulsifier action. *Energy & Fuels*, *23*(3), 1568-1574.

British Columbia environmental laboratory manual of extractable petroleum hydrocarbons (EPH) in water by GC/FID. (2017).

Cabrera-Trujillo, M. A., Sotelo-Díaz, L. I., Quintanilla-Carvajal, M. X. (2016). Effect of amplitude and pulse in low frequency ultrasound on oil/water emulsions. *Dyna*, *83*(199), 63-68.

Canevari, G. P. (1982). The formulation of an effective demulsifier for oil spill emulsions. *Marine Pollution Bulletin*, *13*(2), 49-54.

Cao, Y., Mu, T. (2014). Comprehensive investigation on the thermal stability of 66 ionic liquids by thermogravimetric analysis. *Industrial & Engineering Chemistry Research*, *53*(20), 8651-8664.

Capek, I. (2004). Preparation of metal nanoparticles in water-in-oil (w/o) microemulsions. *Advances in Colloid and Interface Science*, *110*(1-2), 49-74.

Capello, C., Fischer, U., Hungerbühler, K. (2007). What is a green solvent? A *comprehensive* framework for the environmental assessment of solvents. *Green Chemistry*, *9*(9), 927-934.

Chantereau, G., Sharma, M., Abednejad, A., Vilela, C., Costa, E. M., Veiga, M., Antunes, F., Pintado, M. M., Sebe, G., Coma, V., Freire, M. G., Freire, C. S. R., Silvestre, A. J. D. (2020). Bacterial nanocellulose membranes loaded with vitamin B-based ionic *liquids* for dermal care applications. *Journal of Molecular Liquids*, *302*, 112547.

Chen, D., Li, F., Gao, Y., Yang, M. (2018). Pilot performance of chemical demulsifier on the demulsification of produced water from polymer/surfactant flooding in the Xinjiang oilfield. *Water*, *10*(12), 1874.

Chen, D. X., OuYang, X. K., Wang, Y. G., Yang, L. Y., He, C. H. (2013). Liquid–liquid extraction of caprolactam from water using room temperature ionic liquids. *Separation and Purification Technology*, *104*, 263-267.

Chew, N. G. P., Zhao, S., Loh, C. H., Permogorov, N., Wang, R. (2017). Surfactant effects on water recovery from produced water via direct-contact membrane distillation. *Journal of Membrane Science*, *528*, 126-134.

Cho, C. W., Pham, T. P. T., Zhao, Y., Stolte, S., Yun, Y. S. (2021). Review of the toxic effects of ionic liquids. *Science of The Total Environment*, *786*, 147309.

Chong, J. Y., Machado, M. B., Arora, N., Bhattacharya, S., Ng, S., Kresta, S. M. (2016). Demulsifier performance in diluted bitumen dewatering: effects of mixing and demulsifier dosage. *Energy & Fuels*, *30*(11), 9962-9974.

Chowdhury, M. R., Moshikur, R. M., Wakabayashi, R., Tahara, Y., Kamiya, N., Moniruzzaman, M., Goto, M. (2019). Development of a novel ionic liquid–curcumin complex to enhance its solubility, stability, and activity. *Chemical Communications*, *55*(54), 7737-7740.

Clarke, C. J., Bui-Le, L., Hallett, J. P., Licence, P. (2020). Thermally stable imidazolium dicationic ionic liquids with pyridine functional groups. *ACS Sustainable Chemistry & Engineering, 8,* 8762-8772.

Consoli, L., de Figueiredo Furtado, G., da Cunha, R. L., Hubinger, M. D. (2017). High solids emulsions produced by ultrasound as a function of energy density. *Ultrasonics Sonochemistry*, *38*, 772-782.

Costa, A. L. R., Gomes, A., Cunha, R. L. (2018). One-step ultrasound producing O/W emulsions stabilized by chitosan particles. *Food Research Iinternational*, *107*, 717-725.

Cruz, E. E. B., Rivas, N. V. G., García, U. P., Martinez, A. M. M., Banda, J. A. M. (2018). Characterization of crude oils and the precipitated asphaltenes fraction using UV spectroscopy, dynamic light scattering and microscopy. *Recent Insights in Petroleum Science and Engineering*, 117.

Daaou, M., Bendedouch, D. (2012). Water pH and surfactant addition effects on the stability of an Algerian crude oil emulsion. *Journal of Saudi Chemical Society*, *16*(3), 333-337.

Deng, Y., Beadham, I., Ghavre, M., Costa Gomes, M. F., Gathergood, N., Husson, P., Legeret, B., Quilty, B., Sancelme, M., Besse-Hoggan, P. (2015). When can ionic liquids be considered readily biodegradable? Biodegradation pathways of pyridinium, pyrrolidinium and ammonium-based ionic liquids. *Green Chemistry*, *17*(3), 1479-1491.

Dharaskar Swapnil, A. (2012). Ionic liquids (a review): the green solvents for petroleum and hydrocarbon industries. Research *Journal of Chemical Sciences ISSN*, *2231*, 606X.

Dickhout, J. M., Moreno, J., Biesheuvel, P. M., Boels, L., Lammertink, R. G. H., De Vos, W. M. (2017). Produced water treatment by membranes: A review from a colloidal perspective. *Journal of Colloid and Interface Science*, *487*, 523-534.

Dimitrijević, A., Tavares, A. P. M., Almeida, M. R., Vraneš, M., Sousa, A. C. A., Cristóvão, A. C., Trtic-Petrovic, T., Gadzuric, S., Freire, M. G. (2020). Valorization of expired energy drinks by designed and integrated ionic liquid-based aqueous biphasic systems. *ACS Sustainable Chemistry & Engineering*, *8*(14), 5683-5692.

Doshi, B., Sillanpää, M., Kalliola, S. (2018). A review of bio-based materials for oil spill treatment. *Water Research*, *135*, 262-277.

Duan, M., He, J., Li, D., Wang, X., Jing, B., Xiong, Y., Fang, S. (2019). Synthesis of a novel copolymer of block polyether macromonomer and diallyldimethylammonium chloride and its reverse demulsification performance. *Journal of Petroleum Science and Engineering*, *175*, 317-323.

Duan, S., Jiang, Y., Geng, T., Ju, H., Wang, Y. (2020). Wetting, foaming, and emulsification properties of novel methyltriphenylphosphonium carboxylate ionic liquid surfactants. *Journal of Dispersion Science and Technology*, *41*(1), 47-53.

Dudek, M., Chicault, J., Øye, G. (2019). Microfluidic investigation of crude oil droplet coalescence: effect of oil/water composition and droplet aging. *Energy & Fuels*, *34*(5), 5110-5120.

Elmobarak, W. F., Almomani, F. (2021). Evaluation of the efficiency of ionic liquids in the demulsification of oil-in-water emulsions. *Environmental Technology & Innovation*, *24*, 102003.

Ezzat, A. O., Atta, A. M., Al-Lohedan, H. A. (2021). Demulsification of stable seawater/Arabian heavy crude oil emulsions using star-like tricationic pyridinium ionic liquids. *Fuel*, *304*, 121436.

Ezzat, A. O., Atta, A. M., Al-Lohedan, H. A., Hashem, A. I. (2018). Synthesis and application of new surface active poly (ionic liquids) based on 1, 3-dialkylimidazolium as demulsifiers for heavy petroleum crude oil emulsions. *Journal of Molecular Liquids*, *251*, 201-211.

Ezzat, A. O., Tawfeek, A. M., Al-Lohedan, H. A. (2022). Synthesis and application of novel gemini pyridinium ionic liquids as demulsifiers for arabian heavy crude oil emulsions. *Colloids and Surfaces A: Physicochemical and Engineering Aspects*, *634*, 127961.

Fard, A. K., Rhadfi, T., Mckay, G., Al-marri, M., Abdala, A., Hilal, N., Hussien, M. A. (2016). Enhancing oil removal from water using ferric oxide nanoparticles doped carbon nanotubes adsorbents. *Chemical Engineering Journal*, *293*, 90-101.

Farooq, U., Patil, A., Panjwani, B., Simonsen, G. (2021). Review on application of nanotechnology for asphaltene adsorption, crude oil demulsification, and produced water treatment. *Energy & Fuels*, *35*(23), 19191-19210.

Feng, X., Wang, S., Hou, J., Wang, L., Cepuch, C., Masliyah, J., Xu, Z. (2011). Effect of hydroxyl content and molecular weight of biodegradable ethylcellulose on demulsification of water-in-diluted bitumen emulsions. *Industrial & Engineering Chemistry Research*, *50*(10), 6347-6354.

Fernandez-Avila, C., Trujillo, A. J. (2016). Ultra-high pressure homogenization improves oxidative stability and interfacial properties of soy protein isolate-stabilized emulsions. *Food Chemistry*, *209*, 104-113.

Fingas, M., Fieldhouse, B. (2004). Formation of water-in-oil emulsions and application to oil spill modelling. *Journal of Hazardous Materials*, *107*(1-2), 37-50.

Fingas, M., Fieldhouse, B., Mullin, J. (1994). Studies of water-in-oil emulsions and techniques to measure emulsion treating agents. In *Artic and Marine Oil Spill Program Technical Seminar* (pp. 213-213). Ministry of supply and services, Canada.

Flores, C. A., Flores, E. A., Hernández, E., Castro, L. V., García, A., Alvarez, F., Vázquez, F. S. (2014). Anion and cation effects of ionic liquids and ammonium salts evaluated as dehydrating agents for super-heavy crude oil: Experimental and theoretical points of view. *Journal of Molecular Liquids*, *196*, 249-257.

Florindo, C., Branco, L. C., Marrucho, I. M. (2019). Quest for green-solvent design: from hydrophilic to hydrophobic (Deep) eutectic solvents. *ChemSusChem*, *12*(8), 1549-1559.

Florindo, C., Monteiro, N. V., Ribeiro, B. D., Branco, L. C., Marrucho, I. M. (2020). Hydrophobic deep eutectic solvents for purification of water contaminated with Bisphenol-A. *Journal of Molecular Liquids*, *297*, 111841.

Forsyth, S. A., Pringle, J. M., MacFarlane, D. R. (2004). Ionic liquids—an overview. Australian *Journal of Chemistry*, *57*(2), 113-119.

Fortuny, M., Oliveira, C. B., Melo, R. L., Nele, M., Coutinho, R. C., Santos, A. F. (2007). Effect of salinity, temperature, water content, and pH on the microwave demulsification of crude oil emulsions. *Energy & Fuels*, *21*(3), 1358-1364.

Franco, C. A., Nassar, N. N., Cortés, F. B. (2014). Removal of oil from oil-in-saltwater emulsions by adsorption onto nano-alumina functionalized with petroleum vacuum residue. *Journal of Colloid and Interface Science*, *433*, 58-67.

Gathergood, N., Garcia, M. T., Scammells, P. J. (2004). Biodegradable ionic liquids: Part I. Concept, preliminary targets and evaluation. *Green Chemistry*, *6*(3), 166-175.

Gathergood, N., Scammells, P. J. (2002). Design and preparation of room-temperature ionic liquids containing biodegradable side chains. *Australian Journal of Chemistry*, *55*(9), 557-560.

Gathergood, N., Scammells, P. J., Garcia, M. T. (2006). Biodegradable ionic liquids Part III. The first readily biodegradable ionic liquids. *Green Chemistry*, *8*(2), 156-160.

Ghandi, K. (2014). A review of ionic liquids, their limits and applications. *Green and Sustainable Chemistry*, *2014, 4,* 44-53.

Gitipour, S., Hedayati, M., Madadian, E. (2015). Soil washing for reduction of aromatic and aliphatic contaminants in soil. *CLEAN–Soil, Air, Water*, *43*(10), 1419-1425.

Gondal, H. Y., Mumtaz, S., Abbaskhan, A., Mumtaz, N., Cano, I. (2020). New alkoxymethyl-functionalized pyridinium-based chiral ionic liquids: synthesis, characterization and properties. *Chemical Papers*, *74*, 2951-2963.

Goodarzi, F., Zendehboudi, S. (2019). A comprehensive review on emulsions and emulsion stability in chemical and energy industries. *The Canadian Journal of Chemical* Engineering, *97*(1), 281-309.

Grenoble, Z., Trabelsi, S. (2018). Mechanisms, performance optimization and new developments in demulsification processes for oil and gas applications. *Advances in Colloid and Interface Science*, *260*, 32-45.

Griffin, W. C. (1949). Classification of surface-active agents by" HLB". *Journal of the Society of Cosmetic Chemists.*, *1*, 311-326.

Gu, Y., Chen, S., Li, J., Liu, Y., Wang, L. (2020). Remediation of diesel oil contaminated sand by micro-emulsion. *Chinese Journal of Chemical Engineering*, *28*(2), 526-531.

Guglielmero, L., Mezzetta, A., Pomelli, C. S., Chiappe, C., Guazzelli, L. (2019). Evaluation of the effect of the dicationic ionic liquid structure on the cycloaddition of CO_2 to epoxides. *Journal of CO_2 Utilization*, *34*, 437-445.

Gundolf, T., Weyhing-Zerrer, N., Sommer, J., Kalb, R., Schoder, D., Rossmanith, P., Mester, P. (2019). Biological impact of ionic liquids based on sustainable fatty acid anions examined with a tripartite test system. *ACS Sustainable Chemistry & Engineering*, *7*(19), 15865-15873.

Guzman-Lucero, D., Flores, P., Rojo, T., Martínez-Palou, R. (2010). Ionic liquids as demulsifiers of water-in-crude oil emulsions: study of the microwave effect. *Energy & Fuels*, *24*(6), 3610-3615.

Hadi, A. A., Ali, A. A. (2022a). A review of petroleum emulsification types, formation factors, and demulsification methods. *Materials Today: Proceedings*.

Hadi, A. A., Ali, A. A. (2022b). Chemical demulsification techniques in oil refineries: A review. *Materials Today: Proceedings*.

Han, D., Row, K. H. (2010). Recent applications of ionic liquids in separation technology. *Molecules*, *15*(4), 2405-2426.

Han, M., Zhang, J., Chu, W., Chen, J., Zhou, G. (2019). Research progress and prospects of marine oily wastewater treatment: a review. *Water*, *11*(12), 2517.

Hanamertani, A. S., Pilus, R. M., Irawan, S. (2017). A review on the application of ionic liquids for enhanced oil recovery. *ICIPEG 2016*. 133-147.

Hao, L., Jiang, B., Zhang, L., Yang, H., Sun, Y., Wang, B., Yang, N. (2016). Efficient demulsification of diesel-in-water emulsions by different structural dendrimer-based demulsifiers. *Industrial & Engineering Chemistry Research*, *55*(6), 1748-1759.

Hashtjin, A. M., Abbasi, S. (2015). Optimization of ultrasonic emulsification conditions for the production of orange peel essential oil nanoemulsions. *Journal of Food Science and Technology*, *52*(5), 2679-2689.

Hassan, S. A., Abdalla, B. K., Mustafa, M. A. (2019). Addition of silica nano-particles for the enhancement of crude oil demulsification process. *Petroleum Science and Technology*, *37*(13), 1603-1611.

Hassanshahi, N., Hu, G., Lee, K., Li, J. (2022) Effect of ultrasonic homogenization on crude oil-water emulsion stability. *Journal of Environmental Science and Health, Part A*.

Hassanshahi, N., Hu, G., Li, J. (2020). Application of ionic liquids for chemical demulsification: A review. *Molecules*, *25*(21), 4915.

Hassanshahi, N., Hu, G., Li, J. (2022). Investigation of dioctyl sodium sulfosuccinate in demulsifying crude oil in water emulsion. *ACS Omega.*

Hassanshahi, N., Karimi-Jashni, A. (2018). Comparison of photo-Fenton, O_3/H_2O_2/UV and photocatalytic processes for the treatment of gray water. *Ecotoxicology and Environmental Safety*, *161*, 683-690.

Hassanshahian, M., Emtiazi, G., Caruso, G., Cappello, S. (2014). Bioremediation (bioaugmentation/biostimulation) trials of oil polluted seawater: a mesocosm simulation study. *Marine Environmental Research*, *95*, 28-38.

Hazrati, N., Beigi, A. A. M., Abdouss, M. (2018). Demulsification of water in crude oil emulsion using long chain imidazolium ionic liquids and optimization of parameters. *Fuel*, *229*, 126-134.

Hezave, A. Z., Dorostkar, S., Ayatollahi, S., Nabipour, M., Hemmateenejad, B. (2013a). Dynamic interfacial tension behavior between heavy crude oil and ionic liquid solution (1-dodecyl-3-methylimidazolium chloride ($[C_{12}mim][Cl]^+$ distilled or saline water/heavy crude oil)) as a new surfactant. *Journal of Molecular Liquids*, *187*, 83-89.

Hezave, A. Z., Dorostkar, S., Ayatollahi, S., Nabipour, M., Hemmateenejad, B. (2013b). Effect of different families (imidazolium and pyridinium) of ionic liquids-based surfactants on interfacial tension of water/crude oil system. *Fluid Phase Equilibria*, *360*, 139-145.

Hezave, A. Z., Dorostkar, S., Ayatollahi, S., Nabipour, M., Hemmateenejad, B. (2013c). Investigating the effect of ionic liquid (1-dodecyl-3-methylimidazolium chloride ($[C_{12}mim][Cl]$)) on the water/oil interfacial tension as a novel surfactant. *Colloids and Surfaces A: Physicochemical and Engineering Aspects*, *421*, 63-71.

Hijo, A. A. C. T., Barros, H. D. F. Q., Maximo, G. J., Cazarin, C. B. B., da Costa, L. B. E., Pereira, J. F. B., Junior, M. R. M., Meirelles, A. J. A. (2020). Subacute toxicity assessment of biobased ionic liquids in rats. *Food Research International*, *134*, 109125.

Hu, G., Li, J., Huang, S., Li, Y. (2016). Oil recovery from petroleum sludge through ultrasonic assisted solvent extraction. *Journal of Environmental Science and Health, Part A*, *51*(11), 921-929.

Hu, G., Li, J., Thring, R. W., Arocena, J. (2014). Ultrasonic oil recovery and salt removal from refinery tank bottom sludge. *Journal of Environmental Science and Health, Part A*, *49*(12), 1425-1435.

Huang, W., Wu, X., Qi, J., Zhu, Q., Wu, W., Lu, Y., Chen, Z. (2019). Ionic liquids: Green and tailor-made solvents in drug delivery. *Drug Discovery Today, 25*, 901-908.

Husain, A., Adewunmi, A. A., Kamal, M. S., Mahmoud, M., Al-Harthi, M. A. (2021). Demulsification of heavy petroleum emulsion using pyridinium ionic liquids with distinct anion branching. *Energy & Fuels*, *35*(20), 16527-16533.

Huet, G., Araya-Farias, M., Alayoubi, R., Laclef, S., Bouvier, B., Gosselin, I., Cezard, C.,Roulard, R., Courty, M., Hadad, C., Husson, E., Sarazin, C., Nguyen Van Nhien, A. (2020). New biobased-zwitterionic ionic liquids: efficiency and biocompatibility for the development of sustainable biorefinery processes. *Green Chemistry*, *22*(9), 2935-2946.

Hulsbosch, J., De Vos, D. E., Binnemans, K., Ameloot, R. (2016). Biobased ionic liquids: solvents for a green processing industry?. *ACS Sustainable Chemistry & Engineering*, *4*(6), 2917-2931.

Hutin, A., Argillier, J. F., Langevin, D. (2016). Influence of pH on oil-water interfacial tension and mass transfer for asphaltenes model oils. Comparison with crude oil behavior. *Oil & Gas Science and Technology–Revue d'IFP Energies nouvelles*, *71*(4), 58.

Iqbal, M., Zafar, N., Fessi, H., Elaissari, A. (2015). Double emulsion solvent evaporation techniques used for drug encapsulation. *International Journal of Pharmaceutics*, *496*(2), 173-190.

Irge, D. D. (2016). Ionic liquids: a review on greener chemistry applications, quality ionic liquid synthesis and economical viability in a chemical processes. *American Journal of Physical Chemistry, 5*, 74-79.

Ismail, N. H., Salleh, W. N. W., Ismail, A. F., Hasbullah, H., Yusof, N., Aziz, F., Jaafar, J. (2020). Hydrophilic polymer-based membrane for oily wastewater treatment: A review. *Separation and Purification Technology*, *233*, 116007.

Javed, F., Ullah, F., Zakaria, M. R., Akil, H. M. (2018). An approach to classification and hi-tech applications of room-temperature ionic liquids (RTILs): A review. *Journal of Molecular Liquids*, *271*, 403-420.

Jia, H., Dai, J., Huang, P., Han, Y., Wang, Q., He, J., Song, J., Wei, X., Yan, H., Liu, D. (2020). Application of novel amphiphilic Janus-SiO_2 nanoparticles for an efficient demulsification of crude oil/water emulsions. *Energy & Fuels*, *34*(11), 13977-13984

Kammakakam, I., Bara, J. E., Jackson, E. M., Lertxundi, J., Mecerreyes, D., Tomé, L. C. (2020). Tailored CO_2-philic anionic poly (ionic liquid) composite membranes: synthesis, characterization, and gas transport properties. *ACS Sustainable Chemistry & Engineering*, *8*(15), 5954-5965.

Kang, W., Yin, X., Yang, H., Zhao, Y., Huang, Z., Hou, X., Sarsenbekuly, B., Zhu, Z., Wang, P., Zhang, X., Geng, J., Aidarova, S. (2018). Demulsification performance, behavior and mechanism of different demulsifiers on the light crude oil emulsions. *Colloids and Surfaces A: Physicochemical and Engineering Aspects*, *545*, 197-204.

Khan, A., Gusain, R., Sahai, M., Khatri, O. P. (2019). Fatty acids-derived protic ionic liquids as lubricant additive to synthetic lube base oil for enhancement of tribological properties. *Journal of Molecular Liquids*, *293*, 111444.

Khan, H. W., Reddy, A. V. B., Bustam, M. A., Goto, M., Moniruzzaman, M. (2021). Development and optimization of ionic liquid-based emulsion liquid membrane process for efficient recovery of lactic acid from aqueous streams. *Biochemical Engineering Journal*, *176*, 108216

Khandoozi, S., Sharifi, A., Riazi, M. (2022). Enhanced oil recovery using surfactants. *Chemical Methods*, 95-139.

Khezeli, T., Ghaedi, M., Bahrani, S., Daneshfar, A., Soylak, M. (2020). Deep eutectic solvent in separation and preconcentration of organic and inorganic species. In *New Generation Green Solvents for Separation and Preconcentration of Organic and Inorganic Species,* 381-423, Elsevier.

Khorshid, Z. B., Doroodmand, M. M., Abdollahi, S. (2021). UV–Vis. spectrophotometric method for oil and grease determination in water, soil and different mediates based on emulsion. *Microchemical Journal*, *160*, 105620.

Kirchhecker, S., Esposito, D. (2016). Amino acid based ionic liquids: a green and sustainable perspective. *Current Opinion in Green and Sustainable Chemistry*, *2*, 28-33.

Koh, L. L. A., Chandrapala, J., Zisu, B., Martin, G. J., Kentish, S. E., Ashokkumar, M. (2014). A comparison of the effectiveness of sonication, high shear mixing and homogenisation on improving the heat stability of whey protein solutions. *Food and Bioprocess Technology*, *7*(2), 556-566.

Kokal, S. L. (2005). Crude oil emulsions: A state-of-the-art review. *SPE Production & Facilities*, *20*(01), 5-13.

Kore, R., Uppara, P. V., Rogers, R. D. (2020). Replacing HF or $AlCl_3$ in the acylation of isobutylbenzene with chloroaluminate ionic liquids. *ACS Sustainable Chemistry & Engineering*, *8*(28), 10330-10334.

Kovács, A., Erős, I., Csóka, I. (2016). Optimization and development of stable w/o/w cosmetic multiple emulsions by means of the Quality by Design approach. *International Journal of Cosmetic Science*, *38*(2), 128-138.

Kuang, J., Jiang, X., Mi, Y., Ye, F., Zhang, Z., Huang, Z., Yuan, H., Luo, Y., Xie, F. (2020a). Demulsification of oil-in-water emulsions using hyperbranched poly (amido amine) demulsifiers with 4, 4-diaminodiphenyl methane as initial cores. *Journal of Applied Polymer Science*, *137*(26), 48846.

Kuang, J., Mi, Y., Zhang, Z., Ye, F., Yuan, H., Liu, W., Jiang, X., Luo, Y. (2020b). A hyperbranched Poly (amido amine) demulsifier with trimethyl citrate as initial cores and its demulsification performance at ambient temperature. *Journal of Water Process Engineering*, *38*, 101542.

Kuhn, B. L., Osmari, B. F., Heinen, T. M., Bonacorso, H. G., Zanatta, N., Nielsen, S. O., Ranathunga, D. T. S., Villetti, M. A., Frizzo, C. P. (2020). Dicationic imidazolium-based dicarboxylate ionic liquids: Thermophysical properties and solubility. *Journal of Molecular Liquids*, *308*, 112983.

Kumar, N., Mandal, A. (2018). Surfactant stabilized oil-in-water nanoemulsion: stability, interfacial tension, and rheology study for enhanced oil recovery application. *Energy & Fuels*, *32*(6), 6452-6466.

Kumar, S., Mahto, V. (2017). Use of a novel surfactant to prepare oil-in-water emulsion of an Indian heavy crude oil for pipeline transportation. *Energy & Fuels*, *31*(11), 12010-12020.

Kumar, S., Rajput, V. S., Mahto, V. (2021). Experimental studies on demulsification of heavy crude oil-in-water emulsions by chemicals, heating, and centrifuging. *SPE Production & Operations*, *36*(02), 375-386.

Kunz, W., Häckl, K. (2016). The hype with ionic liquids as solvents. *Chemical Physics* Letters, *661*, 6-12.

Kuppusamy, S., Maddela, N. R., Megharaj, M., Venkateswarlu, K. (2020). Impact of total petroleum hydrocarbons on human health. In *Total Petroleum Hydrocarbons.* 139-165, Speringer.

Langevin, D., Poteau, S., Hénaut, I., Argillier, J. F. (2004). Crude oil emulsion properties and their application to heavy oil transportation. *Oil & Gas Science and Technology*, *59*(5), 511–521.

Lee, R. F. (1999). Agents which promote and stabilize water-in-oil emulsions. *Spill Science & Technology Bulletin*, *5*(2), 117-126.

Lemus, J., Palomar, J., Heras, F., Gilarranz, M. A., Rodriguez, J. J. (2012). Developing criteria for the recovery of ionic liquids from aqueous phase by adsorption with activated carbon. *Separation and Purification Technology*, *97*, 11-19.

Lemos, R. C. B., da Silva, E. B., dos Santos, A., Guimaraes, R. C. L., Ferreira, B. M. S., Guarnieri, R. A., Dariva, C., Franceschi, E., Santos, A. F., Fortuny, M. (2010). Demulsification of water-in-crude oil emulsions using ionic liquids and microwave irradiation. *Energy & Fuels*, *24*(8), 4439-4444.

Less, S., Vilagines, R. (2012). The electrocoalescers' technology: Advances, strengths and limitations for crude oil separation. *Journal of Petroleum Science and Engineering*, *81*, 57-63.

Li, J., Song, X., Hu, G., Thring, R. W. (2013). Ultrasonic desorption of petroleum hydrocarbons from crude oil contaminated soils. *Journal of Environmental Science and Health, Part A*, *48*(11), 1378-1389.

Li, X., Kersten, S. R., Schuur, B. (2016). Efficiency and mechanism of demulsification of oil-in-water emulsions using ionic liquids. *Energy & Fuels*, *30*(9), 7622-7628.

Li, W., Zhang, Z., Han, B., Hu, S., Xie, Y., Yang, G. (2007). Effect of water and organic solvents on the ionic dissociation of ionic liquids. *The Journal of Physical Chemistry B*, *111*(23), 6452-6456.

Liang, X., Wu, J., Yang, X., Tu, Z., Wang, Y. (2018). Investigation of oil-in-water emulsion stability with relevant interfacial characteristics simulated by dissipative particle dynamics. *Colloids and Surfaces A: Physicochemical and Engineering Aspects*, *546*, 107-114.

Linke, C., Drusch, S. (2016). Turbidity in oil-in-water-emulsions—Key factors and visual perception. *Food Research International*, *89*, 202-210.

Liu, J. W.; Wei, K. H.; Xu, S. W.; Cui, J.; Ma, J.; Xiao, X. L.; Xi, B. D.; He, X. S. (2021a). Surfactant-enhanced remediation of oil-contaminated soil and groundwater: A review. *Science of the Total Environment*, *756*, 144142.

Liu, Y., Lu, H., Li, Y., Xu, H., Pan, Z., Dai, P., Wang, H., Yang, Q. (2021b). A review of treatment technologies for produced water in offshore oil and gas fields. *Science of The Total Environment*, *775*, 145485.

Liu, Z., Li, Y., Luan, H., Gao, W., Guo, Y., Chen, Y. (2019). Pore scale and macroscopic visual displacement of oil-in-water emulsions for enhanced oil recovery. *Chemical Engineering Science*, *197*, 404-414.

Logeshwaran, P., Megharaj, M., Chadalavada, S., Bowman, M., Naidu, R. (2018). Petroleum hydrocarbons (PH) in groundwater aquifers: An overview of environmental fate, toxicity, microbial degradation and risk-based remediation approaches. *Environmental Technology & Innovation*, *10*, 175-193.

Lu, H., Pan, Z., Miao, Z., Xu, X., Wu, S., Liu, Y., Wang, H., Yang, Q. (2021). Combination of electric field and medium coalescence for enhanced demulsification of oil-in-water emulsion. *Chemical Engineering Journal Advances*, *6*, 100103.

Luo, X., Gong, H., Cao, J., Yin, H., Yan, Y., He, L. (2019). Enhanced separation of water-in-oil emulsions using ultrasonic standing waves. *Chemical Engineering Science*, *203*, 285-292.

Lusinier, N., Seyssiecq, I., Sambusiti, C., Jacob, M., Lesage, N., Roche, N. (2019). Biological treatments of oilfield produced water: A comprehensive review. *SPE Journal*, *24*(05), 2135-2147.

Lyu, R., Xia, T., Liang, C., Zhang, C., Li, Z., Wang, L., Wang, Y., Wu, M., Luo, X., Ma, J., Wang, C., Xu, C. (2020). MPEG grafted alkylated carboxymethyl chitosan as a high-efficiency demulsifier for O/W crude oil emulsions. *Carbohydrate Polymers*, *241*, 116309.

Ma, J., Yang, Y., Li, X., Sui, H., He, L. (2021). Mechanisms on the stability and instability of water-in-oil emulsion stabilized by interfacially active asphaltenes: Role of hydrogen bonding reconstructing. *Fuel*, *297*, 120763.

Ma, J., Yao, M., Yang, Y., Zhang, X. (2022). Comprehensive review on stability and demulsification of unconventional heavy oil-water emulsions. *Journal of Molecular Liquids*, 118510.

Magina, S., Barros-Timmons, A., Ventura, S. P., Evtuguin, D. V. (2021). Evaluating the hazardous impact of ionic liquids–challenges and opportunities. *Journal of Hazardous Materials*, *412*, 125215.

Mandai, T., Yoshida, K., Ueno, K., Dokko, K., Watanabe, M. (2014). Criteria for solvate ionic liquids. *Physical Chemistry Chemical Physics*, *16*(19), 8761-8772.

Martínez-Palou, R., Aburto, J. (2015). Ionic liquids as surfactants–applications as demulsifiers of petroleum emulsions. *Ionic Liquids Current State of the Art*, 305-326.

Masri, A. N., Sulaimon, A. A., Zakaria, M. Z., Abidemi, A. S. (2022). Imidazolium-based ionic liquids as demulsifier for water-crude oil emulsion. *Materials Today: Proceedings*.

Maton, C., De Vos, N., Stevens, C. V. (2013). Ionic liquid thermal stabilities: decomposition mechanisms and analysis tools. *Chemical Society Reviews*, *42*(13), 5963-5977.

McClements, D. J., Jafari, S. M. (2018). Improving emulsion formation, stability and performance using mixed emulsifiers: A review. *Advances in Colloid and Interface Science*, *251*, 55-79.

Mehraban, M. F., Farzaneh, S. A., Sohrabi, M. (2021). Debunking the impact of salinity on crude oil/water interfacial tension. *Energy & Fuels*, *35*(5), 3766-3779.

Mezzetta, A., Łuczak, J., Woch, J., Chiappe, C., Nowicki, J., Guazzelli, L. (2019). Surface active fatty acid ILs: Influence of the hydrophobic tail and/or the imidazolium hydroxyl functionalization on aggregates formation. *Journal of Molecular Liquids*, *289*, 111155.

Mi, T., Cai, Y., Wang, Q., Habibul, N., Ma, X., Su, Z., Wu, W. (2020). Synthesis of Fe_3O_4 nanocomposites for efficient separation of ultra-small oil droplets from hexadecane–water emulsions. *RSC Advances*, *10*(17), 10309-10314.

Modarres-Gheisari, S. M. M., Gavagsaz-Ghoachani, R., Malaki, M., Safarpour, P., Zandi, M. (2019). Ultrasonic nano-emulsification–A review. *Ultrasonics Sonochemistry*, *52*, 88-105.

Mohayeji, M., Farsi, M., Rahimpour, M. R., Shariati, A. (2016). Modeling and operability analysis of water separation from crude oil in an industrial gravitational coalescer. *Journal of the Taiwan Institute of Chemical Engineers*, *60*, 76-82.

Mondal, D., Sharma, M., Quental, M. V., Tavares, A. P., Prasad, K., Freire, M. G. (2016). Suitability of bio-based ionic liquids for the extraction and purification of IgG antibodies. *Green Chemistry*, *18*(22), 6071-6081.

Moradi, M., Alvarado, V., Huzurbazar, S. (2011). Effect of salinity on water-in-crude oil emulsion: evaluation through drop-size distribution proxy. *Energy & Fuels*, *25*(1), 260-268.

Moshikur, R. M., Chowdhury, M. R., Wakabayashi, R., Tahara, Y., Kamiya, N., Moniruzzaman, M., Goto, M. (2020). Ionic liquids with N-methyl-2-pyrrolidonium cation as an enhancer for topical drug delivery: Synthesis, characterization, and skin-penetration evaluation. *Journal of Molecular Liquids*, *299*, 112166.

Motta, F. L., Stoyanov, S. R., Soares, J. B. (2018). Application of solidifiers for oil spill containment: A review. *Chemosphere*, *194*, 837-846.

Muschiolik, G., Dickinson, E. (2017). Double emulsions relevant to food systems: preparation, stability, and applications. *Comprehensive Reviews in Food Science and Food Safety*, 16(3), 532-555.

Nasirpour, N., Mohammadpourfard, M., Heris, S. Z. (2020). Ionic liquids: Promising compounds for sustainable chemical processes and applications. *Chemical Engineering Research and Design*, *160*, 264-300.

Olajire, A. A. (2014). Review of ASP EOR (alkaline surfactant polymer enhanced oil recovery) technology in the petroleum industry: Prospects and challenges. *Energy*, *77*, 963-982.

Oropeza, E. A. F., Sotelo, L. V. C., Ortega, A. L., Cortez, J. G. H., Ramírez, F. A., Moreno, F. S. V., Martinez, A. E., Cassou, M. L. Y. (2016). U.S. Patent No. 9,404,052. Washington, DC: U.S. Patent and Trademark Office.

Oulego, P., Faes, J., González, R., Viesca, J. L., Blanco, D., Battez, A. H. (2019). Relationships between the physical properties and biodegradability and bacteria toxicity of fatty acid-based ionic liquids. *Journal of Molecular Liquids*, *292*, 111451.

Pan, Z., Qu, W., Ma, H., Atungulu, G. G., McHugh, T. H. (2012). Continuous and pulsed ultrasound-assisted extractions of antioxidants from pomegranate peel. *Ultrasonics Sonochemistry*, *19*(2), 365-372.

Patel, D. D., Lee, J. M. (2012). Applications of ionic liquids. *The Chemical Record*, *12*(3), 329-355.

Patinha, D. J., Wang, H., Yuan, J., Rocha, S. M., Silvestre, A. J., Marrucho, I. M. (2020). Thin porous poly (ionic liquid) coatings for enhanced headspace solid phase microextraction. *Polymers*, *12*(9), 1909.

Patsos, N., Lewis, K., Picchioni, F., Kobrak, M. N. (2019). Extraction of acids and bases from aqueous phase to a pseudoprotic ionic liquid. *Molecules*, *24*(5), 894.

Pekdemir, T., Copur, M., Urum, K. (2005). Emulsification of crude oil–water systems using biosurfactants. *Process Safety and Environmental Protection*, *83*(1), 38-46.

Peña, A. A., Hirasaki, G. J., Miller, C. A. (2005). Chemically induced destabilization of water-in-crude oil emulsions. *Industrial & Engineering Chemistry Research*, *44*(5), 1139-1149.

Peng, J., Liu, Q., Xu, Z., Masliyah, J. (2012). Novel magnetic demulsifier for water removal from diluted bitumen emulsion. *Energy & Fuels*, *26*(5), 2705-2710.

Pereira, J. F., Barber, P. S., Kelley, S. P., Berton, P., Rogers, R. D. (2017). Double salt ionic liquids based on 1-ethyl-3-methylimidazolium acetate and hydroxyl-functionalized ammonium acetates: strong effects of weak interactions. *Physical Chemistry Chemical Physics*, *19*(39), 26934-26943.

Pereira, M. M., Pedro, S. N., Gomes, J., Sintra, T. E., Ventura, S. P. M., Coutinho, J. A. P., Freire, M. G., Mohamadou, A. (2019). Synthesis and characterization of analogues of glycine-betaine ionic liquids and their use in the formation of aqueous biphasic systems. *Fluid Phase Equilibria*, *494*, 239-245.

Pernak, J., Rzemieniecki, T., Klejdysz, T., Qu, F., Rogers, R. D. (2020). Conversion of quinine derivatives into biologically active ionic liquids: advantages, multifunctionality and perspectives. *ACS Sustainable Chemistry & Engineering, 8,* 9263-9267.

Piccioli, M., Aanesen, S. V., Zhao, H., Dudek, M., Øye, G. (2020). Gas flotation of petroleum produced water: a review on status, fundamental aspects, and perspectives. *Energy & Fuels*, *34*(12), 15579-15592.

Pillai, P., Kumar, A., Mandal, A. (2018). Mechanistic studies of enhanced oil recovery by imidazolium-based ionic liquids as novel surfactants. *Journal of Industrial & Engineering Chemistry*, *63*, 262-274.

Prabowo, A. R., Bae, D. M. (2019). Environmental risk of maritime territory subjected to accidental phenomena: Correlation of oil spill and ship grounding in the Exxon Valdez's case. *Results in Engineering*, *4*, 100035.

Quijano, G., Couvert, A., Amrane, A., Darracq, G., Couriol, C., Le Cloirec, P., Paquin, L., Carrié, D. (2011). Toxicity and biodegradability of ionic liquids: new perspectives towards whole-cell biotechnological applications. *Chemical Engineering Journal*, *174*(1), 27-32.

Ramirez-Corredores, M. M. (2017). The science and technology of unconventional oils: finding refining opportunities. Academic press.

Ratti, R. (2014). Ionic liquids: synthesis and applications in catalysis. *Advances in Chemistry*, *2014*(3), 1-16.

Ravera, F., Dziza, K., Santini, E., Cristofolini, L., Liggieri, L. (2021). Emulsification and emulsion stability: The role of the interfacial properties. *Advances in Colloid and Interface Science*, *288*, 102344.

Rawlins, C. H. (2009). Flotation of fine oil droplets in petroleum production circuits. In *Recent Advances in Mineral Processing Plant Design*, 232-246, Society for Mining, Metallurgy & Exploration.

Raya, S. A., Saaid, I. M., Ahmed, A. A., Umar, A. A. (2020). A critical review of development and demulsification mechanisms of crude oil emulsion in the petroleum industry. *Journal of Petroleum Exploration and Production Technology*, *10*(4), 1711-1728.

Reddy, S. R., Fogler, H. S. (1981). Emulsion stability: determination from turbidity. *Journal of Colloid and Interface Science*, *79*(1), 101-104.

Ren, B., Kang, Y. (2018). Demulsification of oil-in-water (O/W) emulsion in bidirectional pulsed electric field. *Langmuir*, *34*(30), 8923-8931.

Romero, A., Santos, A., Tojo, J., Rodriguez, A. (2008). Toxicity and biodegradability of imidazolium ionic liquids. *Journal of Hazardous Materials*, *151*(1), 268-273.

Rongsayamanont, W., Tongcumpou, C., Phasukarratchai, N. (2020). Diesel-contaminated soil washing by mixed nonionic surfactant emulsion and seed germination test. *Water, Air, & Soil Pollution*, *231*(6), 1-10.

Rostami, H., Nikoo, A. M., Rajabzadeh, G., Niknia, N., Salehi, S. (2018). Development of cumin essential oil nanoemulsions and its emulsion filled hydrogels. *Food Bioscience*, *26*, 126-132.

Ruberg, E. J., Elliott, J. E., Williams, T. D. (2021). Review of petroleum toxicity and identifying common endpoints for future research on diluted bitumen toxicity in marine mammals. *Ecotoxicology*, *30*(4), 537-551.

Saad, M. A., Kamil, M., Abdurahman, N. H., Yunus, R. M., Awad, O. I. (2019). An overview of recent advances in state-of-the-art techniques in the demulsification of crude oil emulsions. *Processes*, *7*(7), 470.

Saien, J., Hashemi, S. (2018). Long chain imidazolium ionic liquid and magnetite nanoparticle interactions at the oil/water interface. *Journal of Petroleum Science and Engineering*, *160*, 363-371.

Saien, J., Kharazi, M. (2016). A comparative study on the interface behavior of different counter anion long chain imidazolium ionic liquids. *Journal of Molecular Liquids*, *220*, 136-141.

Saien, J., Kharazi, M., Asadabadi, S. (2015a). Adsorption behavior of long alkyl chain imidazolium ionic liquids at the n-butyl acetate+ water interface. *Journal of Molecular Liquids*, *212*, 58-62.

Saien, J., Kharazi, M., Asadabadi, S. (2015b). Adsorption behavior of short alkyl chain imidazolium ionic liquids at N-Butyl acetate+ water interface: experiments and modeling. *Iranian Journal of Chemical Engineering (IJChE)*, *12*(2), 59-74.

Sakthivel, S., Velusamy, S., Nair, V. C., Sharma, T., Sangwai, J. S. (2017). Interfacial tension of crude oil-water system with imidazolium and lactam-based ionic liquids and their evaluation for enhanced oil recovery under high saline environment. *Fuel*, *191*, 239-250.

Salager, J. L., Morgan, J. C., Schechter, R. S., Wade, W. H., Vasquez, E. (1979). Optimum formulation of surfactant/water/oil systems for minimum interfacial tension or phase behavior. *Society of Petroleum Engineers Journal*, *19*(02), 107-115.

Santos, D., da Rocha, E. C. L., Santos, R. L. M., Cancelas, A. J., Franceschi, E., Santos, A. F., Fortuny, M., Dariva, C. (2017). Demulsification of water-in-crude oil emulsions using single mode and multimode microwave irradiation. *Separation and Purification Technology*, *189*, 347-356.

Santos, M. M., & Branco, L. C. (2020). Ionic liquids and deep eutectic solvents for application in pharmaceutics. *Pharmaceutics*, *12*(10), 909.

Santos, R. L. M., Filho, E. B. M., Dourado, R. S., Santos, A. F., Borges, G. R., Dariva, C., Darvia, C., Santana, C. C., Franceschi, E., Santos, D. (2019). Study on the use of aprotic ionic liquids as potential additives for crude oil upgrading, emulsion inhibition, and demulsification. *Fluid Phase Equilibria*, *489*, 8-15.

Sartomo, A., Santoso, B., Muraza, O. (2020). Recent progress on mixing technology for water-emulsion fuel: A review. *Energy Conversion and Management*, *213*, 112817.

Sastry, N. V., Vaghela, N. M., Aswal, V. K. (2012). Effect of alkyl chain length and head group on surface active and aggregation behavior of ionic liquids in water. *Fluid Phase Equilibria*, *327*, 22-29.

Saththasivam, J., Loganathan, K., Sarp, S. (2016). An overview of oil–water separation using gas flotation systems. *Chemosphere*, *144*, 671-680.

Schaeffer, N., Conceição, J. H. F., Martins, M. A. R., Neves, M. C., Pérez-Sánchez, G., Gomes, J. R. B., Papaiconomou, N., Coutinho, J. A. P. (2020). Non-ionic hydrophobic eutectics–versatile solvents for tailored metal separation and valorisation. *Green Chemistry*, *22*(9), 2810-2820.

Sernaglia, M., Blanco, D., Battez, A. H., Viesca, J. L., González, R., Bartolomé, M. (2020). Two fatty acid anion-based ionic liquids-part I: Physicochemical properties and tribological behavior as neat lubricants. *Journal of Molecular Liquids*, *305*, 112827.

Shahavi, M. H., Hosseini, M., Jahanshahi, M., Meyer, R. L., Darzi, G. N. (2019). Evaluation of critical parameters for preparation of stable clove oil nanoemulsion. *Arabian Journal of Chemistry*, *12*(8), 3225-3230.

Shinoda, K. (1967). The correlation between the dissolution state of nonionic surfactant and the type of dispersion stabilized with the surfactant. *Journal of Colloid and Interface Science*, *24*(1), 4-9.

Shinoda, R., Uchimura, T. (2018). Evaluating the creaming of an emulsion via mass spectrometry and uv–vis spectrophotometry. *ACS Omega*, *3*(10), 13752-13756.

Shirota, H., Castner, E. W. (2005). Why are viscosities lower for ionic liquids with− $CH_2Si(CH_3)_3$ vs− $CH_2C(CH_3)_3$ substitutions on the imidazolium cations?. *The Journal of Physical* Chemistry *B*, *109*(46), 21576-21585.

Schmidt, F., Schönhoff, M. (2020). Solvate cation migration and ion correlations in solvate ionic liquids. *The Journal of Physical Chemistry B*, *124*(7), 1245-1252.

Shehzad, F., Hussein, I. A., Kamal, M. S., Ahmad, W., Sultan, A. S., Nasser, M. S. (2018). Polymeric surfactants and emerging alternatives used in the demulsification of produced water: A review. *Polymer Reviews*, *58*(1), 63-101.

Shokri, A., Fard, M. S. (2022). A critical review in electrocoagulation technology applied for oil removal in industrial wastewater. *Chemosphere*, *288*, 132355.

Silva, E. B., Santos, D., Alves, D. R. M., Barbosa, M. S., Guimarães, R. C. L., Ferreira, B. M. S., Guarnieri, R. A., Franceschi, E., Dariva, C., Santos, A. F., Fortuny, M. (2013). Demulsification of heavy crude oil emulsions using ionic liquids. *Energy & Fuels*, *27*(10), 6311-6315.

Silva, I. A., Almeida, F. C., Souza, T. C., Bezerra, K. G., Durval, I. J., Converti, A., Sarubbo, L. A. (2022). Oil spills: impacts and perspectives of treatment technologies with focus on the use of green surfactants. *Environmental Monitoring and Assessment*, *194*(3), 1-29.

Silva, L. P., Moya, C., Sousa, M., Santiago, R., Sintra, T. E., Carreira, A. R. F., Palomar, J., Coutinho, J. A. P., Carvalho, P. J. (2020). Encapsulated amino-acid-based ionic liquids for CO_2 capture. *European Journal of Inorganic Chemistry*, *2020*(33), 3158-3166.

Singh, S. K., Savoy, A. W. (2020). Ionic liquids synthesis and applications: An overview. *Journal of Molecular Liquids*, *297*, 112038.

Slater, C. S., Savelski, M. (2007). A method to characterize the greenness of solvents used in pharmaceutical manufacture. *Journal of Environmental Science and Health, Part A*, *42*(11), 1595-1605.

Sousa, A. M., Pereira, M. J., Matos, H. A. (2021). Oil-in-water and water-in-oil emulsions formation and demulsification. *Journal of Petroleum Science and Engineering*, 110041.

Stewart, M., Arnold, K. (2009). Produced water treating systems. In *Emulsions and Oil Treating Equipment*, 107−211, Elsevier.

Subramanian, D., Wu, K., Firoozabadi, A. (2015). Ionic liquids as viscosity modifiers for heavy and extra-heavy crude oils. *Fuel*, *143*, 519-526.

Sun, H., Wang, Q., Li, X., He, X. (2020). Novel polyether-polyquaternium copolymer as an effective reverse demulsifier for O/W emulsions: Demulsification performance and mechanism. *Fuel*, *263*, 116770.

Sun, P., Armstrong, D. W. (2010). Ionic liquids in analytical chemistry. *Analytica Chimica Acta*, 661(1), 1-16.

Szepiński, E., Smolarek, P., Milewska, M. J., Łuczak, J. (2020). Application of surface active amino acid ionic liquids as phase-transfer catalyst. *Journal of Molecular Liquids*, *303*, 112607.

Taha, A., Ahmed, E., Ismaiel, A., Ashokkumar, M., Xu, X., Pan, S., Hu, H. (2020). Ultrasonic emulsification: An overview on the preparation of different emulsifiers-stabilized emulsions. *Trends in Food Science & Technology*, *105*, 363-377.

Taleghani, N. D., Tyagi, M. (2017). Impacts of major offshore oil spill incidents on petroleum industry and regional economy. *Journal of Energy Resources Technology*, *139*(2).

Tawalbeh, M., Al Mojjly, A., Al-Othman, A., Hilal, N. (2018). Membrane separation as a pre-treatment process for oily saline water. *Desalination*, *447*, 182-202.

Techtmann, S. M., Zhuang, M., Campo, P., Holder, E., Elk, M., Hazen, T. C., Conmy, R., Santo Domingo, J. W. (2017). Corexit 9500 enhances oil biodegradation and changes active bacterial community structure of oil-enriched microcosms. *Applied and Environmental Microbiology*, *83*(10), e03462-16.

Thompson, D. G., Taylor, A. S., Graham, D. E. (1985). Emulsification and demulsification related to crude oil production. *Colloids and Surfaces*, *15*, 175-189.

Tian, Y., McGill, W. B., Whitcombe, T. W., Li, J. (2019). Ionic liquid-enhanced solvent extraction for oil recovery from oily sludge. *Energy & Fuels*, *33*(4), 3429-3438.

Tian, Y., Zhou, J., He, C., He, L., Li, X., Sui, H. (2022). The formation, stabilization and separation of oil–water emulsions: A review. *Processes*, *10*(4), 738.

Turguła, A., Stęsik, K., Materna, K., Klejdysz, T., Praczyk, T., Pernak, J. (2020). Third-generation ionic liquids with N-alkylated 1, 4-diazabicyclo [2.2.2] octane cations and pelargonate anions. *RSC Advances*, *10*(15), 8653-8663.

Usuki, T., Onda, S., Yoshizawa-Fujita, M., Rikukawa, M. (2017). Use of [C_4mim] Cl for efficient extraction of caffeoylquinic acids from sweet potato leaves. *Scientific Reports*, 7(1), 1-7.

Varjani, S., Joshi, R., Srivastava, V. K., Ngo, H. H., Guo, W. (2020). Treatment of wastewater from petroleum industry: current practices and perspectives. *Environmental Science and Pollution Research*, *27*(22), 27172-27180.

Walden, P. (1914). Molecular weights and electrical conductivity of several fused salts. *Bulletin de l'Academie Imperiale des Sciences de St.-Petersbourg*, *8*, 405-422.

Wang, D., Yang, D., Huang, C., Huang, Y., Yang, D., Zhang, H., Liu, Q., Tang, T., El-Din, M.G., Kemppi, T., Perdicakis, B., Zeng, H. (2021). Stabilization mechanism and chemical demulsification of water-in-oil and oil-in-water emulsions in petroleum industry: A review. *Fuel*, *286*, 119390.

Wang, H., Chen, M., Jin, C., Niu, B., Jiang, S., Li, X., Jiang, S. (2018). Antibacterial [2-(methacryloyloxy) ethyl] trimethylammonium chloride functionalized reduced graphene oxide/poly (ethylene-co-vinyl alcohol) multilayer barrier film for food packaging. *Journal of Agricultural and Food Chemistry*, *66*(3), 732-739.

Wang, L., Yang, J., He, X., Zhao, M., Cheng, D., Wang, A., Yin, G., Zhao, B., Liu, Y., Wang, W. (2020). Study on the surface properties and aggregation behavior of quaternary ammonium surfactants with amide bonds. *ACS Omega*, *5*(28), 17042-17050.

Wang, Z., Zhang, J., Lu, B., Li, Y., Liang, Y., Yuan, J., Zhao, M. Wang, B., Mai, C., Zhang, J. (2019). Novel bio-renewable matrinium-based ionic liquids derived from Chinese herb medicine: Synthesis, physicochemical properties and biological activity. *Journal of Molecular Liquids*, *296*, 111822.

Winsor, P. A. (1954). Solvent properties of amphiphilic compounds. Butterworths Scientific Publications.

Wong, S. F., Lim, J. S., Dol, S. S. (2015). Crude oil emulsion: A review on formation, *classification* and stability of water-in-oil emulsions. *Journal of Petroleum Science and Engineering*, *135*, 498-504.

Wu, J., Xu, Y., Dabros, T., Hamza, H. (2004). Development of a method for measurement of relative solubility of nonionic surfactants. *Colloids and Surfaces A: Physicochemical and Engineering Aspects*, *232*(2-3), 229-237.

Wu, J., Xu, Y., Dabros, T., Hamza, H. (2003). Effect of demulsifier properties on *destabilization* of water-in-oil emulsion. *Energy & Fuels*, *17*(6), 1554-1559.

Yahya, M. S., Sangapalaarachchi, D. T., Lau, E. V. (2019). Effects of carbon chain length of *imidazolium*-based ionic liquid in the interactions between heavy crude oil and sand particles for enhanced oil recovery. *Journal of Molecular Liquids*, *274*, 285-292.

Yan, S., He, G., Ye, D., Guo, Y., Fang, W. (2020). Amphiphilic hyperbranched polyethyleneimine for highly efficient oil–water separation. *Journal of Materials Chemistry A*, *8*(5), 2412-2423.

Yang, Z., Duan, M., Li, Y., Chen, Q., Fang, S., Liu, X. (2021). An in situ displacement method to evaluate demulsification performance of demulsifiers. *Journal of Dispersion Science and Technology*, *42*(5), 686-692.

Yao, C., Hou, Y., Sun, Y., Wu, W., Ren, S., Liu, H. (2020). Extraction of aromatics from aliphatics using a hydrophobic dicationic ionic liquid adjusted with small-content water. *Separation and Purification Technology*, *236*, 116287.

Yonguep, E., Chowdhury, M. (2021). Optimization of the demulsification response surface methodology. *South African Journal of Chemical Engineering*, *36*(1), 105-117.

Yonguep, E., Fabrice, K. K., Katende, J. K., Chowdhury, M. (2022). Formation, stabilization and chemical demulsification of crude oil-in-water emulsions: A review. *Petroleum Research*.

Yuan, S., Wang, Y., Wang, X., Wang, Y., Liu, S., Duan, M., Fang, S. (2022). Efficient demulsification of cationic polyacrylate for oil-in-water emulsion: Synergistic effect of adsorption bridging and interfacial film breaking. *Colloids and Surfaces A: Physicochemical and Engineering Aspects*, *640*, 128393.

Yudina, N. V., Nebogina, N. A., Prozorova, I. V. (2021). Composition of the resin-asphaltene components in the interfacial layers of water-in-oil emulsions. *Petroleum Chemistry*, *61*(5), 568-575.

Zahid, A., Sandersen, S. B., Stenby, E. H., Von Solms, N., Shapiro, A. (2011). Advanced waterflooding in chalk reservoirs: Understanding of underlying mechanisms. *Colloids and Surfaces A: Physicochemical and Engineering Aspects*, *389*(1-3), 281-290.

Zembyla, M., Murray, B. S., Sarkar, A. (2020). Water-in-oil emulsions stabilized by surfactants, biopolymers and/or particles: A review. *Trends in Food Science & Technology*, *104*, 49-59.

Zhang, L., He, G., Ye, D., Zhan, N., Guo, Y., Fang, W. (2016). Methacrylated hyperbranched polyglycerol as a high-efficiency demulsifier for oil-in-water emulsions. *Energy & Fuels*, *30*(11), 9939-9946.

Zhang, L., Wei, L., Shi, L., Dai, X., Guo, S., Jia, X., Liu, C. (2022). Synthesis and characterization of a novel reticulated multi-branched fluorinated polyether demulsifier for w/o emulsion demulsification. *Journal of Polymer Research*, *29*(5), 1-12.

Zhang, L., Ying, H., Yan, S., Zhan, N., Guo, Y., Fang, W. (2018a). Hyperbranched poly (amido amine) as an effective demulsifier for oil-in-water emulsions of microdroplets. *Fuel*, *211*, 197-205.

Zhang, L., Ying, H., Yan, S., Zhan, N., Guo, Y., Fang, W. (2018b). Hyperbranched poly (amido amine) demulsifiers with ethylenediamine/1, 3-propanediamine as an initiator for oil-in-water emulsions with microdroplets. *Fuel*, *226*, 381-388.

Zhang, P., Wang, H., Liu, X., Shi, X., Zhang, J., Yang, G., Sun, K., Wang, J. (2014). The dynamic interfacial adsorption and demulsification behaviors of novel amphiphilic dendrimers. *Colloids and Surfaces A: Physicochemical and Engineering Aspects*, *443*, 473-480.

Zhang, S., Sun, N., He, X., Lu, X., Zhang, X. (2006). Physical properties of ionic liquids: database and evaluation. *Journal of Physical and Chemical Reference Data*, *35*(4), 1475-1517.

Zhang, Z., Kang, N., Zhou, J., Li, X., He, L., Sui, H. (2019). Novel synthesis of choline-based amino acid ionic liquids and their applications for separating asphalt from carbonate rocks. *Nanomaterials*, *9*(4), 504.

Zhao, H. (2003). Current studies on some physical properties of ionic liquids. *Physics and Chemistry of Liquids*, *41*(6), 545-557.

Zhao, H., Baker, G. A. (2015). Oxidative desulfurization of fuels using ionic liquids: A review. *Frontiers of Chemical Science and Engineering*, *9*(3), 262-279.

Zhao, Y., Ji, X., Wu, L., Tian, J., Zhang, C. (2021). Preparation of demulsifying functional membrane and its application in separation of emulsified oil. *Separation and Purification Technology*, *276*, 119299.

Zhou, J., Sui, H., Jia, Z., Yang, Z., He, L., Li, X. (2018). Recovery and purification of ionic liquids from solutions: a review. *RSC Advances*, *8*(57), 32832-32864.

Zhou, L., Zhang, J., Yin, Y., Zhang, W., Yang, Y. (2021). Effects of ultrasound-assisted emulsification on the emulsifying and rheological properties of myofibrillar protein stabilized pork fat emulsions. *Foods*, *10*(6), 1201.

Zolfaghari, R., Abdullah, L. C., Biak, D. R., Radiman, S. (2018). Cationic Surfactants for Demulsification of Produced Water from Alkaline–Surfactant–Polymer Flooding. *Energy & Fuels*, *33*(1), 115-126.

Zolfaghari, R., Fakhru'l-Razi, A., Abdullah, L. C., Elnashaie, S. S., Pendashteh, A. (2016). Demulsification techniques of water-in-oil and oil-in-water emulsions in petroleum industry. *Separation and Purification Technology*, *170*, 377-407.

APPENDIX A

Table A1: ANOVA for response surface quadratic model for O/W emulsion turbidity difference.

Source	Sum of Squares	DF[1]	Mean Square	F-value	P-value	Significance
Model	5576.35	14	398.31	16.98	<0.0001	*
X_1-Amplitude	133.69	1	133.69	5.70	0.0316	*
X_2-Sonication time	342.95	1	342.95	14.62	0.0019	*
X_3-Water salinity	1184.22	1	1184.22	50.47	<0.0001	*
X_4-pH of water	463.66	1	463.66	19.76	0.0006	*
X_1X_2	487.45	1	487.45	20.77	0.0004	*
X_1X_3	224.07	1	224.07	9.55	0.0080	*
X_1X_4	88.25	1	88.25	3.76	0.0729	
X_2X_3	94.84	1	94.84	4.04	0.0641	
X_2X_4	3.46	1	3.46	0.1474	0.7068	
X_3X_4	39.30	1	39.30	1.68	0.2165	
X_1^2	52.84	1	52.84	2.25	0.1557	
X_2^2	1145.14	1	1145.14	48.81	<0.0001	*
X_3^2	849.14	1	849.14	36.19	<0.0001	*
X_4^2	675.46	1	675.46	28.79	<0.0001	*
Residual	328.49	14	23.46			
Lack of Fit	307.38	8	38.42	10.92	0.0046	
Pure Error	21.11	6	3.52			
Cor Total	5904.84	28				

[1] degree of freedom, * Significant (P-values < 0.05)

Table A2: Model summary statistics for the generated quadratic model by RSM.

Parameter	Value	Parameter	Value
Std. Dev.	4.84	R^2	0.94
Mean	18.95	Adjusted R^2	0.88
CV	25.56	Predicted R^2	0.69
		Adequate precision	14.9067

APPENDIX B

Table B1: ANOVA for response surface quadratic model of demulsification by DSS.

Source	Sum of squares	DF[1]	Mean square	F-value	P-value
Model	7884.14	6	1314.02	12.40	0.0001
X_1-DSS concentration	3690.12	1	3690.12	34.83	<0.0001
X_2-Oil concentration	578.40	1	578.40	5.46	0.0361
X_3-Shaking time	293.65	1	293.65	2.77	0.1199
X_1X_2	639.03	1	639.03	6.03	0.0289
X_2X_3	497.70	1	497.70	4.70	0.0494
X_1^2	2185.24	1	2185.24	20.63	0.0006
Residual	1377.35	13	105.95		
Lack of fit	1355.59	8	169.45	38.94	0.0004
Pure error	21.76	5	4.35		
Cor total	9261.49	19			

[1] degree of freedom

Table B2: Model summary statistics for the generated quadratic model of demulsification by DSS.

Parameter	Value	Parameter	Value
Std. Dev.	10.29	R^2	0.8513
Mean	88.54	Adjusted R^2	0.7826
COV %	11.63	Predicted R^2	0.4197
-	-	Adeq Precision	13.3589

APPENDIX C

Table C1: ANOVA for response surface quadratic model for demulsification by ionic liquids.

Source	Sum of Squares	DF[1]	Mean Square	F-value	P-value	
Model	348.66	11	31.70	8.03	<0.0001	significant
X_1-ionic liquid concentration	21.35	1	21.35	5.41	0.0301	
X_2-Settling time	108.09	1	108.09	27.40	<0.0001	
X_3-Ionic liquid type	141.88	2	70.94	17.98	<0.0001	
X_1X_2	3.00	1	3.00	0.7604	0.3931	
X_1X_3	5.06	2	2.53	0.6411	0.5367	
X_2X_3	1.82	2	0.9118	0.2311	0.7957	
X_1^2	0.9127	1	0.9127	0.2313	0.6355	
X_2^2	56.43	1	56.43	14.30	0.0011	
Residual	82.85	21	3.95			
Lack of Fit	58.19	15	3.88	0.9436	0.5722	not significant
Pure Error	24.67	6	4.11			
Cor Total	431.52	32				

[1] degree of freedom

Table C2: Model summary statistics for the generated quadratic model.

Parameter	Value	Parameter	Value
Std. Dev.	1.99	R^2	0.80
Mean	89.79	Adjusted R^2	0.70
COV %	2.21	Predicted R^2	0.50
-	-	Adeq Precision	11.49